UCHL1 IN THE MAMMALIAN NERVOUS SYSTEM

APPROVED BY SUPERVISORY COMMITTEE

_____

_____

_____

To Nellie

UCHL1 IN THE MAMMALIAN NERVOUS SYSTEM

by

KALISA GALINA MYERS

THESIS

Presented to the Faculty of the Graduate School of Biomedical Sciences

The University of Texas Southwestern Medical Center at Dallas

In Partial Fulfillment of the Requirements

For the Degree of

MASTER OF SCIENCE

The University of Texas Southwestern Medical Center at Dallas

Dallas, Texas

August, 2008

UCHL1 IN THE MAMMALIAN NERVOUS SYSTEM

KALISA GALINA MYERS, M.S.

The University of Texas Southwestern Medical Center at Dallas, 2008

WEICHUN LIN, Ph.D.

UCHL1, or Ubiquitin Carboxy Terminal Hydrolase L1, is a de-ubiquitinating enzyme (DUB) thought to be involved in ubiquitin recycling. Beyond this, its natural function is almost wholly unknown. Mice lacking this enzyme exhibit a severe and rapidly progressing neurodegenerative phenotype. Using one of these mouse models, in which a lacz-neo construct is cloned in under the UCHL1 promoter, we have studied the gross progression of phenotype of these mice, characterized the expression pattern of UCHLO1 in brain, spinal cord, and lumbar dorsal root ganglia, described degeneration of muscle spindles, and established a timecourse of degeneration of neuromuscular junctions. Presented in this thesis is the culmination of these studies.

TABLE OF CONTENTS

Abstract	v
Table of contents	vi
List of figures	vii
List of tables	viii
List of appendices	ix
List of abbreviations	x
Introduction	1
Chapter 1	3
Chapter 2	7
Chapter 3	11
Chapter 4	17
Summary	22
Works Cited	23
Appendix	25
Figures	31

LIST OF FIGURES

Figure 1. UCHL1 phenotype progression schematic
Figure 2. Phenotype representative photographs
Figure 3. UCHL1 survival curve
Figure 4. Somatosensory cortex expression
Figure 5. Motor cortex expression
Figure 6. Gracile nucleus expression
Figure 7. Adult spinal cord expression
Figure 8. Embryonic spinal cord expression
Figure 9. Lumbar dorsal root ganglia expression
Figure 10. UCHL1 expression atlas
Figure 11. UCHL1 expression in hippocampus, dentate gyrus
Figure 12. Hippocampus, dentate gyrus, twin stained slides
Figure 13. Full, Partial, Vacant endplates
Figure 14. Group 1 (43-48 days) endplate photos
Figure 15. Group 2 (63-67 days) endplate photos
Figure 16. Group 3 (92-99 days) endplate photos
Figure 17. Group 4 (157-174 days) endplate photos
Figure 18. Full endplate graph
Figure 19. Partial endplate graph
Figure 20. Vacant endplate graph
Figure 21. Group 1 (43-48 days) spindle photos
Figure 22. Group 2 (63-67 days) spindle photos
Figure 23. Group 3 (92-99 days) spindle photos
Figure 24. Group 4 (157-174 days) spindle photos

LIST OF TABLES

Table 1. UCHL1 expression in key areas of interest
Table 2. Total endplate counts for UCHL1-/- EDL's
Table 3. Total endplate counts for UCHL1+/+ and +/- EDL's
Table 4. Spindle counts using H&E method

LIST OF APPENDICES

Appendix 1: Raw data for EDL endplate counts

LIST OF ABBREVIATIONS

UCHL1	Ubiquitin Carboxy Terminal Hydrolase L1, subject of this thesis
Gad	Gracile Axonal Dystrophy, the first UCHL1 knockout mouse
PGP9.5	Protein Gene Product 9.5, how UCHL1 was originally isolated
DRG	Dorsal Root Gangion
UCHL1-/-	$UCHL1^{tm1Dgen}$/ $UCHL1^{tm1Dgen}$ mice (used in this study)
EDL	Extensor Digitorum Longus muscle (used in this study)
PFA	Paraformaldehyde
PBS	Phosphate-Buffered Saline
NMJ	Neuromuscular Junction
AG	Anterior Gracilis muscle (discussed in this study)

Introduction

Gracile Axonal Dystrophy mice, the discovery of UCHL1, and purpose of this thesis

The *gad* (gracile axonal dystrophy) mouse was originally discovered as a spontaneous mutant and named for the characteristic dystrophic axons found in its gracile tracts[1]. The mutated gene turned out to be the gene for Ubiquitin-Carboxy Terminal Hydrolase 1, or UCHL1 [2]. This protein, previously called PGP 9.5 [3], was originally discovered in extracts of whole human brain [4] and found to be neuron-specific [5-7]. UCHL1 is a de-ubiquitinating enzyme, and as such, is thought to be important for maintaining healthy cellular ubiquitin levels. All cells, including neurons, have numerous de-ubiquitinating enzymes, and so it is a little surprising that loss of this one causes the amount of devastation that it does in the *gad* mice.

Gad mice, though born apparently healthy, exhibit a strikingly severe and rapidly progressing gross neurodegenerative phenotype, starting with spastic motion of hindlimbs upon tail suspension at 30 days of age, total hindlimb paralysis by 80 days of age, and premature death at 6 months of age. Incontinence, hunchback, tremor, and protrusion of the penis in males are all apparent at the time of death in *gad* mice. These symptoms are thought to be closely correlated with the pathologies found in the gracile nucleus and fasciculi of affected mice, since dystrophic axons become more apparent as symptoms worsen [1]. Dystrophic axons in the cervical gracile fascicles become obvious at the onset of hindlimb paralysis, and the axons “die back” caudally towards the thoracic and lumbar regions of the gracile tracts, and finally towards the lumbar dorsal root ganglia, which shows a significant decrease in cell area [8], [9].

Thus UCHL1 is vital for the maintenance of at least one major sensory tract.

Noting the damage to the lumbar DRG’s, [8], Oda et al [10] undertook a study of muscle spindles of *gad* mice as young as 10 days old. It was found that in contrast to healthy mice, *gad* mice fail to complete normal development of their muscle spindles, instead exhibiting a “dying-back” type degeneration in which the Ia afferents degenerate in a distal-proximal direction. At P15, both normal and *gad* mice have completed the initial development of the annulospiral endings. However, while the spindles of normal mice continue to enlarge, the spindles of *gad* mice rapidly degenerate, with abnormal spindle innervation apparent by P20, and near-total degeneration apparent by P30 [10].

Thus UCHL1 is vital for the health and possibly the development of muscle spindles.

Curious about the state of motor axons in the *gad* mouse, Miura et al[11] undertook a study of motor endplates of *gad* mice ranging from 40-120 days of age. Noting that the axons of *gad* mice tended to “die back” in a distal-proximal direction, this group utilized the anterior gracilis muscle, which is innervated both proximally and distally by the same axon. True to the previously observed pattern, vacant endplates at the distal end of the muscle could be observed by 60 days of age, and progressing towards the proximal end as age increased and the nerve continued to die back.

Thus UCHL1 is vital for maintaining innervation of neuromuscular junctions.

Clearly UCHL1 is necessary for the survival of both motor and sensory axons. The Ia afferents coiling around the muscle spindle[10], the axons of motor neurons innervating muscle endplates[11], ascending axons of sensory neurons in the dorsal horn of the spinal cord and the gracile fascicles[1, 8] all show pathological changes in the *gad* mice. Why does lack of UCHL1, a “mere” de-ubiquitinating enzyme, result in such striking degeneration of all these different nerves over a period of just a few months? What is UCHL1 doing that is so vitally important to their survival? Elucidation of the mechanism of degeneration in *any* of these areas may be of enormous importance in understanding the natural role of UCHL1 in the mammalian nervous system, which in turn is necessary for explaining the numerous links that exist between UCHL1 and human neurodegenerative diseases [12-15].

Chapter 1: Observations of phenotype and generation of a survival curve for the UCHL1^{tm1Dgen}/ UCHL1^{tm1Dgen} (UCHL1-/-) mice

1.1 Introduction

Gad mice die at 6 months of age [1]. Since UCHL1-/- mice are missing the same gene, it is reasonable to expect that they will show a similar lifespan. However, *gad* mice and UCHL1-/- mice are, and should be treated, as two different strains of mouse. It follows that the phenotypic progression and survival curve may be different between the two strains, and no published survival curve is available for these mice. The purpose of this chapter is to report qualitative observations on the phenotype of the UCHL1-/- mice from symptom onset to death, and results of our survival curve.

It should be noted that behavioral tests done by Deltagen reveal that UCHL1-/- mice exhibit at least 3 significant phenotypes. First, they exhibit decreased time immobile in a tail suspension test. Second, they fall off of a rotarod faster than wildtype. Third, they exhibit increased time to show response (paw licking) on a hotplate, indicating an altered nociceptive threshold. However, no timecourse on the appearance of these symptoms is available.

1.2 Materials and Methods

1.2.1.Animals

UCHL1 mice were obtained from the MMRRC, and are freely available to any non-profit investigator. Current availability of mice and pricing information can be found by following this link: http://www.mmrrc.org/strains/11642/011642.html

UCHL1^{tm1Dgen}/ UCHL1^{tm1Dgen} mice were originally generated by Deltagen, Inc as a targeted mutation of the UCHL1 gene and later donated to the NIH. Chimeras in which a *lacz/neo* construct was cloned in under the UCHL1 promoter were generated using ES cells. UCHL1^{tm1Dgen}/UCHL1 heterozygotes were produced by crossing the progeny of the chimeras with C57BL/6 mice, and UCHL1^{tm1Dgen}/ UCHL1^{tm1Dgen} homozygotes were generated by mating the heterozygotes with each other.

The *lacz/neo* construct sequence, PCR confirmations, and summaries of behavioral phenotypes are freely available from the company, and can be found by following this link: http://www.informatics.jax.org/external/ko/deltagen/1320.html.

1.2.2. Qualitative Observations on phenotype progression

Qualitative observations of UCHL1-/- mice were made over a period of approximately 8 months, starting from the time of weaning to time of death, dissection, or euthanasia. Mutant and healthy (i.e.; wt or heterozygous littermates) mice were observed in their cages daily to several times a week to observe gait and other gross physical characteristics, such as hunchback and tremor. After weaning, mice were also suspended

by their tail daily to several times a week, until the appearance of noticeable spastic motion of their hindlimbs and footclasp. When any of these physical characteristics was noticed, it was dated and recorded on the cage cards. When the mutants succumbed or were euthanized due to symptoms, the cage cards were collected and the data summarized. In addition, for those mice surviving past 4 months, notes made by the ARC veterinary technicians were also used to confirm progression of paralysis and increasing severity of phenotype. Judgment about when to euthanize the older mice was based on the technicians' notes and communication with the lab.

1.2.3 Survival Curve

To determine if the UCHL1-/- mice have a normal lifespan, 15 mutants and 15 wildtype or heterozygous littermates were set aside for the generation of a survival curve. Mutants were only counted in the survival curve if they died in their cages or were euthanized on advice from an ARC veterinary technician. Those mice that were euthanized exhibited no complications other than those apparently brought on by the mutation. Wildtype and heterozygous littermates that outlived their homozygous mutant siblings were used for subsequent dissection and/or breeding, but were kept alive while the mutants were still viable.

1.3 Results

1.3.1 Observations on progression of phenotype

Figure 1 shows a schematic summarizing onset and progression of phenotype observed in the UCHL1-/- mutants. The majority of mutants cannot be readily distinguished from their wildtype and heterozygous littermates until they are close to 2 months of age. The exception is a small number of mutants that die between 4-5 weeks of age; this has happened in 2 litters of mice, and account for 4/15 of the survival curve deaths. By 2 months, when the mutants are picked up by the tail, they all exhibit clasping and spastic motion of their hindlimbs (Figure 2 A-D). This spasticity increases in severity as the mice age. In addition, mutants begin to exhibit a whole-body tremor. Between 2 and 3 months of age, the phenotype becomes even more obvious.

By 3.0 months of age, the mutant mice are easily distinguished from their healthy littermates. Hunchback is apparent and sometimes pronounced. They begin to have trouble with their step cycle, often holding a hindlimb up for a prolonged period before setting it back down, resulting in a clumsy, hopping gait (fig. 3d). Their tremor worsens. However, the mutants can ambulate enough to easily reach food and water. The spastic motion and clasping observed in the hindlimbs upon tail suspension is dramatically increased. All these symptoms increase in severity between 3 and 4 months.

By 4.0 months of age, UCHL1-/- mice have obvious trouble ambulating. The hindlimbs become partially paralyzed, causing them trouble reaching food and water. Muscle atrophy is apparent. When the mutants do ambulate, they have a jerky, clumsy swing and

step cycle. Clonus in the forelimbs is occasionally observed upon tail suspension. They tend to move in circles, leaning into one side as they do so. 4.0 month old UCHL1-/- mice will tend to move much less overall than their littermates, and can often be found slouching in a hunched position with their hindlimbs awkwardly splayed out under them (Figure 2, E,F). Floor-feeding is sometimes initiated either by myself or the ARC veterinary technicians. Kyphoscoliosis, tremor, and spastic motion of hindlimbs is even more pronounced. All these symptoms increase in severity between 4 and 5 months of age, except for the apparent loss of balance- this simply progresses into full-blown hindlimb paralysis.

By 5.0 months of age, UCHL1-/- mice must be floor-fed, as their hindlimb paralysis is severe enough to completely prevent them from reaching food and water. EDL muscles freshly dissected from a 5.0 month old mutant will twitch spontaneously for at least 3 hours. Kyphoscoliosis and hindlimb spasticity is very pronounced, as is hindlimb muscle atrophy. The mice can move their hindlimbs if provoked, but usually drag them. Tremor is pronounced. All these symptoms increase in severity between 5 and 6 months of age, as the mice enter the final stages of their illness.

6.0 month old UCHL1-/- exhibit total hindlimb paralysis and severe muscle atrophy. The mice cannot move their legs. The legs often appear scissored (crossed over each other), and are dragged behind the mice. In addition, clonus can be readily observed in the forelimbs. The hindlimbs are never flaccid, in contrast, they appear to be in constant spasm. The tremor continues to get worse. Males sometimes exhibit an exposed penis. Mutants may die at this stage, but many are able to survive with constant floor-feeding.

7.0 and 8.0 month old UCHL1-/- mice are almost completely paralyzed. (Fig 2, G,H) They have obvious trouble even moving to moistened food and water on the floor of the cage. They can still move their bodies around with their forelimbs, but have great difficulty doing so. At this point, it becomes inhumane to allow the mutants to progress any further, as they become unable to eat and drink normally. Mice that survived to this stage were euthanized, dissected, and included in the survival curve.

1.3.2. Survival curve

4 of the 15 mutants set aside for the survival curve study died very early, between 4 and 5 weeks of age. 3 of the 4 early deaths occurred in the same litter and were thought to be a result of poor lactation. However, there were no wt or heterozygous deaths in this litter. 1 of the 4 early deaths occurred within a different litter, supporting the idea that these early deaths, while rare, are a result of the mutation. Additionally, these 4 mutants all exhibited symptoms at the time of their death that are usually seen later, such as clumsy gait, tremor, and weight loss. 1/15 mutants died at 16 weeks of age, and was the only mutant who did not look exceptionally ill at the time of death. The remaining mutants (8/15) lived to at least 30 weeks of age. 1 mutant died naturally at 30 weeks of age, and the remaining mutants were euthanized between 32 and 36 weeks of age because the symptoms were so severe. Results of the survival curve are shown in figure 3, along with

representative photographs of UCHL1+/+ and UCHL1-/- littermates at 1.5 and 3.0 months of age.

1.4 Conclusions

UCHL1-/- mice were found to exhibit all the same symptoms seen in *gad* mice, only with a later onset time. Although most UCHL1-/- mice lived past 30 weeks of age, their condition, like that of the *gad* mice, was very poor by 6 months of age. They most likely would have died at this time if it had not been for the exceptional quality of care they were provided in the ARC. From the results of the survival curve, it appears that the lifespan of the UCHL1-/- mice is 30 weeks of age, less than a third of the lifespan of a normal mouse. It should also be noted that the relatively small *n* of UCHL1-/- mice presented in the survival curve here (15) results in an over-emphasis of deaths at the 4-5 week timepoint. These early deaths were actually quite rare.

Chapter 2: The Expression Pattern of UCHL1 in Mammalian Brain and Spinal Cord

2.1 Introduction

The classic pathology described in *gad* mice is dystrophic axon stumps found in the gracile nucleus of the medulla [1]. Subsequent studies document additional pathology in the sensory system [8, 9], including the gracile tracts of the spinal cord dorsal horn, and in the cell bodies of the lumbar dorsal root ganglia. Based on the pathologies documented here in *gad* mice, it is reasonable to suspect that the dorsal column-medial lemniscus system is particularly susceptible to the results of this mutation (why?).

Within this sensory system (which is responsible for the transduction of fine touch, vibration, and conscious proprioception), the first neuron be one of a number of sensory endings- miessner's corpuscles, muscle spindles, merkels discs, ruffinian corpuscles, pascinian corpuscles, or even hair follicle receptors. All of these axons' cell body is the DRG. The "CNS end" of the DRG travels through the dorsal horns of the spinal cord, becoming part of the gracile tract (or cuneate tract, if the sensory information is entering above T6). These tracts travel all the way up to the gracile nucleus of the medulla, where they finally synapse with the second-order neurons there. The axons of these neurons dessucate and become part of the medial lemniscus, which travels through the brainstem to synapse on 3rd order neurons in the VPL nucleus of the thalamus. These neurons in turn synapse onto neurons in the primary somatosensory cortex.

This is actually pretty informative, because pathology in *gad* mice has been documented in several components of this system: The DRG, which shows reduced cell area [9], the peripheral projections of the DRG in the muscle spindle [10], and the central projections of the DRG in the gracile tracts and medulla [1, 8, 9]. In addition, the motor system in *gad* mice seems to fall apart too, with documented age-dependent degeneration of motor endplates [11]. The spastic paralysis of the hindlimbs seen in *gad* and UCHL1-/- mice is reminiscent of an upper-motor neuron disorder. Thus the descending motor commands coming from the primary motor cortex could be degenerating too.

Based on this information, of particular interest in this study was the evaluation of UCHL1 expression in the primary motor and somatosensory cortex, gracile nucleus of the medulla, dorsal and ventral horns of the spinal cord, and lumbar dorsal root ganglia. Although the *lacz* construct makes information about the subcellular localization of UCHL1 potentially unreliable, it does make possible an accurate study of those cell types which express UCHL1. In addition, we took the opportunity to study the UCHL1 expression pattern throughout the brain and spinal cord.

2.2 Materials and Methods

2.2.1 Animals

For the expression study in brain and spinal cord, 6 adult UCHL1 heterozygous mice ranging from ages 2 months to 4 months were selected on the basis of their current

availability. 3 mice were perfused for collection of fixed tissues, while fresh tissues were collected from the other 3. 1 fresh heterozygous UCHL1 E18.5 embryo was also collected for the spinal cord expression study.

2.2.2. Tissue collection

The following tissues were collected from all mice: Brain, spinal cord, lumbar DRG's, and sciatic nerves, thigh, gastrocnemius, soleus, tibia, EDL, lumbric, and trianularis sterni muscles, and footpad skin.

For fixed tissues:
For collection of fixed tissues, mice were put under isoflurane anesthesia and perfused first with 20mL ice-cold PBS, followed by 20mL ice-cold freshly prepared 4%PFA. Tissues were then dissected out and post-fixed overnight in 4% PFA at 4^{o}C. The following morning tissues were washed 3X30min in 1XPBS, 1X60min in 1XPBS+0.1M glycine, 1X15min in 1XPBS, and placed in 1XPBS+30%sucrose at 4^{o}C overnight or until tissues sank. They were then mounted in OCT on dry ice and kept at -80^{o}C.

For fresh tissues:
For collection of fresh tissues, mice were euthanized by isoflurane overdose, or anasthatized by isoflurane and euthanized by cervical dislocation. Tissues were quickly collected, directly mounted in OCT, and stored at -80^{o}C.

2.2.3. Preparation and staining of tissues

30um frozen coronal or saggital brain sections and transverse spinal cord sections were prepared and mounted on slides in sets of 10. Frozen embryonic spinal cord sections were collected at 50um. 1 slide from each set was then stained with freshly prepared x-gal solution, and incubated either overnight at room temperature, or for 3 hours at 37^{o}C. All incubations were done in the dark. After incubation in x-gal solution, slides were mounted with 50ul 2.5%PVA, and dried at room temperature for 2 hours to overnight. Additionally, twin sets of slides were stained with cresyl violet (Nissl stain), for specific comparison with the x-gal stained slides.

2.2.4. Evaluation of expression pattern

Initial evaluation of UCHL1 expression pattern was done by examination of x-gal stained slides under a stereomicroscope. Representative images of all brain and spinal cord levels were gathered. Further evaluation was done under a light microscope, using 10X and 40X objectives to closer observe and document the expression pattern in those tissues of particular interest. In addition, tissues showing especially intense stain were also photographed. Finally, twin slides stained with Nissl were prepared and used for comparative staining of those regions of interest, as well as those areas which stained heavily.

2.3 Results

2.3.1. UCHL1 expression in specific areas of interest

Table 1. UCHL1 expression levels in areas of particular interest

Area of interest	Expression level
1^{o} somatosensory cortex	++
1^{o} motor cortex	++
lumbar dorsal root ganglia	+++
gracile nucleus of medulla	-
spinal cord dorsal horn	+++
spinal cord ventral horn	++

UCHL1 was found to have high expression in both primary somatosensory (figure 4) and primary motor cortex (figure 5). However, this level of expression was seen in all levels of cortex, except the cerebellar cortex, which showed more modest and diffuse staining. Little to no staining, however, was seen in the gracile nucleus of the medulla. This result was surprising, and possibly erroneous. As mentioned in the materials and methods section of this chapter, 3/6 mice studied were killed by cervical dislocation, which made recovery of the junction between the cervical spinal cord and brainstem (i.e. the region containing the caudal medulla) difficult. Thus the gracile nucleus of the medulla was only thoroughly evaluated in 3 of the 6 mice used in the expression study. Saggital sections prepared from 1 of these mice did in fact show a small amount of staining in the gracile nucleus (figure 6).

Strong staining was observed in the spinal cord dorsal horns in thoracic and lumbar levels, but was absent in upper cervical levels (figure 7). Motor neurons of the ventral horn also stained throughout the spinal cord, however, their staining was not as consistently intense as those sensory neurons in the dorsal horn.

Overall the staining in adult spinal cord was less than that in brain, with relatively little gray matter besides the dorsal and ventral horns staining. Scattered staining, which may be interneurons, was consistently observed. To see if the same trend would hold true in embryonic spinal cord, a heterozygous UCHL1 embryo at E18.5 was sectioned and stained. Surprisingly, embryonic spinal cord showed a much more uniform pattern of expression, with strong staining still seen in the dorsal and ventral horns (figure 8). This result was consistent with a trend which presented itself during the course of this study: younger tissue stained better, indicating that UCHL1 may be differentially expressed as a function of age.

The strongest staining found of all these areas of interest, however, was by far the cell body of the lumbar DRG (figure 9) Interestingly, only neuronal staining was seen, with

glia totally devoid of blue color. This is consistent with earlier studies of UCHL1 expression, in which glia was found not to react with PGP9.5 antibody.

2.3.2. UCHL1 expression in other brain areas

Figure 10 shows an atlas of UCHL1 throughout representative areas of the brain. From this figure it is apparent that UCHL1 is highly expressed throughout the brain. Expression is not completely uniform, however, and some areas of the brain were found to stain more intensely than others. All levels of cortex stained intensely, with the exception of the cerebellar cortex, which exhibited a lighter stain. Expression was particularly high in the mitral and glomeruli cell layers of the olfactory bulb, all cell layers of the accessory olfactory bulb, and throughout the anterior olfactory nuclei. The hippocampus and dentate gyrus were found to stain with a level of intensity rivaled only by that seen in the cell body of the DRG (figure 11). When compared with twin Nissl sections, it was found that all cell types of the hippocampus and dentate gyrus express UCHL1 (figure 12). Recent work done with UCHL1 inhibitors in mouse hippocampal slices show that LTP is abolished when UCHL1 is inhibited, and recovered when the inhibition is removed. In addition, UCHL1 can rescue the loss of LTP in mouse hippocampal slices induced by amyloid beta-peptide [16]. Other studies have shown that UCHL1 is necessary for LTP in Aplysia[17]. Thus a high level of expression here is interesting. Other areas of brain showing particularly high UCHL1 expression included the amygdala, piriform cortex, and the inferior olivary nuclei.

2.4 Conclusions

In summary, brain regions showing the strongest levels of UCHL1 expression were cortex (all levels except in the cerebellum), hippocampus, dentate gyrus, accessory olfactory bulb, anterior olfactory nuclei, inferior olivary nuclei, and amygdala. UCHL1 expression was not observed in the white matter of the brain, or in glia. UCHL1 expression was surprisingly not seen in the gracile nucleus of the medulla, however, this particular finding could be a result of technical error.

Chapter 3: Degeneration of endplates in the EDL muscles of UCHL1-/- mice

3.1 Introduction

The neuromuscular junction, where motor nerves terminate upon the pretzel-shaped clusters of acetylcholine receptors, is one of the most classic and beautiful examples of a synapse. It is also of particular interest in this study, because it too degenerates in *gad* mice[11]. The goal of this chapter is to describe the timecourse of NMJ degeneration in the Extensor Digitorum Longus (EDL) muscle of UCHL1-/- mice, a long thin muscle which controls the movement of the toes. The EDL muscle was chosen for study for the following reasons: First, it is relatively small, making it possible to evaluate all the endplates within it, second, because spindle degeneration in this muscle has already been characterized in *gad* mice[10], and third, because it was possible to coordinate simultaneous electrophysiological studies of the muscle with Fujun Chen, a postdoctoral fellow in the lab. EDL muscle is also often evaluated alongside the soleus muscle, which is its slow-twitch counterpart. Soleus muscles were not evaluated in this study. However, electrophysiological data were collected from them, and the methods described here provide the basis for extending this study to the soleus muscle.

Motor endplate denervation has been established in *gad* mice by Miura et al, who studied endplates on the Anterior Gracilis (AG) muscle [11]. This muscle has two distinct endplate zones, one innervated proximally, the other innervated distally, by the same axon. This study showed that distal endplates were more susceptible to degeneration in *gad* mice, while proximal endplates were spared for a longer time. However, all endplates were found to degenerate eventually, as the motor axon continued to die back. This study is important and frequently cited throughout this chapter for several reasons. First, it establishes the importance of UCHL1 in maintaining a healthy synapse. Second, it illustrates the sensitivity of longer axons to the degeneration that results from lack of this enzyme. Third, the rapid pattern of endplate denervation was almost perfectly reproduced in this study. Taken together with the data presented here, a good rationale is now provided for using the NMJ as a model that can be used to uncover the mechanism(s), the reason(s), the answer(s), to why UCHL1 would be so vital to the survival of so many different components of a mammalian nervous system.

3.2 Materials and Methods

3.2.1. Animals and dissection

33 mice, ages 43- 174 days, were used in this study. Mice were divided into 4 age groups: 43-48 days old, 63-67 days old, 92-99 days old, and 166-174 days old. Each group had a minimum of 3 mutants and 3 wt or het age matched or littermate controls. Thus n was at least 3 for each age group. A one-tailed t-test was used for statistical analysis.

Mice were killed by cervical dislocation, followed by immediate removal of either EDL or both EDL and soleus muscles for electrophysiological recordings (Fujun Chen). Meanwhile, brain, spinal cord, DRG's, sciatic nerves, thigh, tibia, lumbric,

gastrocnemius, and trainularis sterni muscles were freshly dissected out and mounted in OCT, and stored at -80^{o}C for future use.

3.2.2. Preparation and staining of slides

After recordings were completed, the EDL and soleus muscles were fixed overnight at 4^{o}C in 2% PFA. The following morning the tissues were promptly washed 3X30 min in 1X PBS, 1X60 min in 1XPBS+0.1M glycine, 1X15 min in 1X PBS, and rocked overnight at 4^{o}C in 1XPBS+30% sucrose or until tissues sank. When tissues sank in sucrose, they were separately mounted in OCT. An entire EDL cut into 30um saggital sections usually fit onto 1 set of 4 slides, so that the entire set of slides (i.e., the entire EDL muscle), was evaluated for each mouse in the endplate study.

After tissue had been sectioned and dried, slides were washed 3X5 min in 1X PBS, 1X5 min in 1XPBS+0.1 M glycine, 1X5 min in 1X PBS, and incubated 45-60 min in antibody dilution buffer (1%BSA +0.3% triton). Antibody dilution buffer was removed, and replaced with primary antibody: anti-syntaxin I379, a polyclonal antibody produced in rabbit, and a generous gift from the Sudhof lab. Slides were incubated in 1^{o} antibody overnight, covered, at room temperature. The following morning, 1^{o} antibody was removed and saved for re-use.

After removal of 1^{o} antibody, slides were incubated 30 min in 1:5000 tx-red conjugated bungarotoxin to label the endplates.

After removal of bungarotoxin, slides were washed 3X10 min in 1XPBS+0.05% triton, and incubated in 2^{o}antibody (1:600 FITC-conjucated anti-rabbit), for 60 minutes if fresh, and for 90 minutes if re-used.

After removal of 2^{o} antibody, slides were again washed 3X10 min in 1XPBS +0.05% triton, 1X10 min in 1XPBS, rinsed in MQH_2O, and mounted quickly with vectorshield. After a brief 15-min drying, the slides were covered up and numbered, and all evaluation was done in blind.

3.2.3. Evaluation of slides

For each muscle section, each and every endplate was observed under a 20X objective. Endplates were found with bungarotoxin, then the fluorescence microscope switched to FITC to judge the innervation pattern. 3 different cell counters were used: 1 for full endplates, 1 for partial endplates, and 1 for vacant endplates. Representative photographs of each are shown in figure 13. A full endplate was defined as having FITC totally covering the bgt. That is, if the FITC and bgt matched exactly, the endplate was counted as fully innervated. A partial endplate was defined as having FITC covering some, but not all, areas of bgt staining. If there were no bgt-labelled areas co-stained with FITC on an endplate, that endplate was counted as totally denervated, or vacant. Every single endplate on every single section of every single slide was evaluated in this manner. When

all 4 slides had been evaluated, total numbers of full, partial, and vacant endplates were added up, and these are the totals presented here.

3.3 Results

Total counts for all mutants are shown below in table 2, and healthy wildtype or heterozygous mice in tables 2 and 3. Graphical representations of the totals of full, partial, and vacant endplates counted over the 4 age groups are shown in figures 18-20.

Table 2. Total endplate counts for all UCHL1-/- EDL's

UCHL1-/- mouse	days old	#full	#partial	#vacant
4456	43	1493	129	26
4453	46	1643	191	32
4458	48	1353	264	78
4597	48	1361	342	147
4599	63	805	185	96
4600	65	1345	375	227
4732	67	1012	435	169
4308	84	1075	540	212
3839	85	1059	457	267
4596	95	945	315	175
4595	95	1132	428	168
4607	99	838	327	153
4058	168	287	262	1001
4043	173	442	397	1260
4045	174	544	310	753

Table 3. Total endplate counts for all UCHL1+/+ and +/- EDL's

UCHL1 +/+ or +/- mouse	days old	#full	#partial	#vacant
3700	46	1952	80	26
4452	47	984	19	14
4610	47	1783	15	1
3583	48	1241	46	40
4608	49	1828	8	1
4611	50	1769	19	3
4609	53	1854	19	9
4142	57	1116	79	19
4140	58	1811	93	36
3562	92	1256	78	28
4603	94	1633	4	0
4593	96	1757	19	3
4057	157	1732	2	6
4044	166	1869	.5	0
4046	168	1808	3	2

In the youngest age group studied, significant damage to the health of the endplates was already apparent (figure 14). Although many more full endplates were visible in this age group than in the older cohorts, there was a significant($p \leq .01$) increase in the number of partially innervated endplates in the mutants when compared to WT or heterozygous mice. There was no significant difference, however, in the number of vacant endplates. This finding is consistent with Miura et al [11], who found many full endplates in the AG muscle of 40-day old *gad* mice, and no vacant endplates.

It is also interesting to note that the number of both partial and vacant endplates within this cohort increases with age (table 2). In the 43-day old EDL, 129 partial endplates and 26 vacant endplates were found, while at 48 days (less than a week later), the number of partial endplates was twice as high. The number of vacant endplates showed a similar increase, with at least three times as many vacant endplates found at 48 days than at 43 days. While a higher *n* for each one of these ages would be needed to determine the exact nature of the changes within such a short period of time, these results are consistent with observed phenotype (obvious spastic leg movements are often noticed between 50 and 60 days of age), and with the observed rapid and dramatic progressive nature of the phenotype.

Kikuchi et al [9] report finding spheroids in the gracile nucleus as early as 40 days of age, although only a few mice of this age group were studied (no exact *n* is given). Mukoyama et al [8] report finding no abnormalities in spinal cord or medulla in 50-day old *gad* mice. Oda et al [10], however, report that at 40 days of age, *gad* mice stop gaining weight at the same rate as their healthy littermates. Finally, Miura et al [11] report that endplates are normal at 40 days, but show noticeable degeneration by 60 days.

These results are highly consistent with Miura et al [11], who report 2% denervation of proximal endplates in the AG muscle by 40 days of age. In the 43-day old mouse studied here, 1.6% denervation was found. Miura et al also report 11% denervation (i.e, vacant endplates) at 64 days, while the 63-day old mouse studied here shows 9.6%. Thus the degeneration of endplates in the EDL muscle of the UCHL1-/- mouse appears to follow a similar pattern of degeneration seen in those endplates at the proximal zone of the AG muscle in *gad* mice. Between 40 and 50 days, it appears that the motor axons are “pulling back” in ernest, producing a large number of endplates that, while not completely vacated, may not be fully functional either, consistent with the timing of onset of phenotype in many of these mice.

In the 63-67 day old age group, a dramatic increase in the number of vacant endplates is observed, consistent with reported percentages of endplate denervation in the proximal endplate zone of the AG muscle of 60-day-old *gad* mice. The EDL muscles of 63-67 day old mice have significantly less fully innervated endplates, significantly more partially innervated endplates, and a number of completely vacated endplates that is significantly higher than the control. Although the statistical significance of the difference between the number of partial endplates counted in mutant vs heterozygous or WT is lower ($p=.012$) in this age group than in the 92-99 day old age group (where $p=.0015$), the actual

denervation appears to be taking place between 40 and 60 days of age. The number of partial endplates tallied over this short timecourse shows a larger increase, while at later timepoints it appears to plateau. Thus the apparent increase in significance at the older timepoint is due to lower variation between the samples.

Again this morphology is consistent with the outward appearance of phenotype. Whereas mice younger than 50 days of age often appear healthy, 60-day old UHCL1 mutants are easily distinguished from their WT and het littermates. Obvious spasticity can be seen in the hindlimbs upon tail suspension, and, as mice approach 2.5 months of age, changes in gait are very obvious. Thus these results are consistent both with literature on the *gad* mice [11], and with observations of gross phenotype described in the previous chapter. Representative photographs of the appearance of endplates in this group is shown in figure 15.

Within the 92-99 day old cohort, degeneration of endplates in the EDL muscles of UCHL1-/- mice appears to continue in ernest. Within this age group, there is a significant decrease in the number of full endplates, as well as a significant increase in the number of both partial and vacant endplates. Representative photographs of endplates within this age group is shown in figure 16.

However, were this a crime scene, the perpetrators would have already fled the country. That is, there is no longer a regular climb in the number of partial and vacant endplates with each passing day, rather, the degeneration appears to have slowed.

The gap in the number of partial and vacant endplates found between 43 and 67 days of age are much larger than that found between 67 and 99 days. This “crash and plateau” pattern is also observed by Miura et al, who shows, in the distal endplate zone, 3% denervation at 40 days of age, vs 90% denervation at 81 days of age. Thus while denervation continues in older mice, the rate at which the denervation occurs is much less than that observed in the earlier timepoints.

An additional phenotype was also observed in this age group: many endplates were found to be either fully or partially occupied with what looked like regenerating nerve (fig 16). These nerve endings, however, did not appear to follow the highly detailed contours of the endplate as would be expected of healthy nerve. Instead, these nerves appeared spindly, weak, diffuse and disorganized, often covering a much larger area than the endplate itself, while failing to reach nearby vacant endplates. Occasionally these thin nerves were found to roughly follow the major contours of the endplate, but never exactly, and always with extraneous nerve branches not in contact with endplate. Additionally, many of these nerves appeared to be degenerating themselves, with large bright “blobs” picked up by the syntaxin antibody present at their terminal endings.

Regenerating axons are well documented in both the endplates [11] and spindles [10] of *gad* mice. The appearance of these axons documented here are strikingly similar to those described by Miura et al, who also observed the “knoblike” endings. The timecourse of

their appearance is also consistent with Miura et al documenting their appearance at 80 days of age.
UCHL1-/- mice in the 157-174 day old age group exhibit total spastic hindlimb paralysis, and the morphology of their endplates in the EDL muscles reflect it. The number of vacant and partial endplates in this age group is now similar to the number of healthy endplates found in their WT and het littermates. There is a highly significant difference (P=.00008) in the number of full endplates counted between KO's in this cohort and healthy controls. The number of vacant endplates in this age group far exceeds that found in the 92-99 day old age group. Large groups of completely vacant endplates are visible, and whole sections of muscle are often observed without a single healthy endplate. The regenerating axons are gone, leaving literally nothing behind but dying endplates in their wake. Representative photographs of endplates from this age group are shown in figure 17.

3.4 Conclusions

Endplates degenerate in an age-dependent manner in EDL muscles of UCHL1-/- mice, and this degeneration is rapid over the first 60 postnatal days. The motor axons appear to regenerate but ultimately fail. Consistent with the phenotype of total hindlimb paralysis by 5 months, UCHL1-/- in the 157-174 day old age group have almost no full endplates left in their EDL muscles.

Chapter 4: Degeneration of muscle spindles in the EDL muscles of UCHL1-/- mice

4.1. Introduction

The role of the muscle spindle in the mammalian nervous system is very different from that of the neuromuscular junction, and its structure and innervation pattern reflect this difference. Most muscle fibers are extrafusal muscle fibers. However, deep in the "belly" of every muscle lie several fusiform-shaped structures- wide in the middle, and tapered at the ends. This structure is encapsulated with collagen, and within this capsule, are so-called *intrafusal* muscle fibers- those fibers within the fusiform structure. The innervation pattern of the intrafusal muscle fibers is different from that of extrafusal muscle fibers. The capsule, the intrafusal muscle fibers within it, and the special innervating neurons together make up the structure known as the muscle spindle. It is this structure that provides information about how far a muscle is stretched out, and the rate at which it is being stretched. Thus sensory nerves innervate the intrafusal fibers, with the exception of the specialized gamma motor neurons which innervate the ends. 1 large primary sensory axon, called the Ia afferent, coils around the center of all the intrafusal fibers, and additional secondary sensory axons coil around those intrafusal fibers which detect muscle length. There are usually several such distinctively innervated intrafusal muscle fibers within the capsule structure, making the muscle spindle both a beautiful and easily recognizable structure. The cell body of the Ia afferent is actually the cell body of the dorsal root ganglion, which can make several synapses in the spinal cord.

Muscle spindles play a role in regulating gait. As described in Chapter 1, The UchL1 mutants exhibit a very awkward gait, and in particular, a prolonged transition into and sometimes out of, swing phase. Degeneration of muscle spindles has also been described to occur very early in *gad* mice[10]. Also, the posture, gait, hindlimb motions, and splaying of feet observed in UCHL1-/- mice bears striking resemblance to knockout mice lacking Erbb2, which fail to develop functional muscle spindles [18], [19]. Thus an understanding of muscle spindle degeneration in the UCHL1-/- mice may go a long way in explaining its phenotype.

4.2. Materials and Methods

Muscle spindles, which also label very nicely with the syntaxin I379 antibody, were evaluated for morphology alongside the endplates on the slides whose preparation and staining is described in the materials and methods of the previous chapter.

Since counting spindles in saggital sections can easily lead to an underestimation (if a few sections are lost on the cryostat), or an overestimation (if the same spindle is counted more than once), a separate method was used to quantify spindles. Frozen 14um transverse sections through the "belly", i.e., the middle portion, were prepared on sets of 4 slides. The slides were then stained with Hematoxylin and Eosin. Spindles were identified by their distinctive appearance in cross-section, in which the bag and chain fibers encircled by the thick capsule can be easily seen. 10 UCHL1+/+ or +/- EDL's, and

4 UCHL1-/- EDL's over all four age groups were evaluated in this way, and are listed in Table 4.

4.3. Results

Unlike the degeneration of endplates observed in the UCHL1-/- mice, evidence of spindle degeneration was found in all age groups studied. Spindle counts gathered via the H&E cross-section method are shown below in Table 4. The number of spindles counted was unchanged between mutant and wildtype EDL's, and also did not appear to vary with age in either group.

Table 4. Spindles counted using cross-sections

sample ID	genotype	days of age	#spindles
4593	+/-	96	17
3562	+/+	92	19
4596	-/-	95	17
4603	+/+	94	18
4046	+/+	168	17
4599	-/-	63	19
4607	-/-	99	13
4721	+/+	65	17
4720	+/+	63	13
4719	+/+	64	14
4608	+/-	49	19
4611	+/+	50	13
4609	+/-	53	20
4058	-/-	168	18

4.3.1. Group 1 (43-48 days old)

In the 43-48 day old cohort, muscle spindles did not appear normal (figure 21). Even in this younger age group, in which numbers of fully innervated endplates were not significantly different from healthy controls, it was immediately obvious that something was wrong with the spindles. At first glance, they simply appeared to be carelessly sectioned, overstained, or both. Closer examination, however, made it obvious that the apparently "messy" appearance of the spindles was not artifact, but phenotype. Spindles of even the older age groups do not ever appear this way.

Within this age group, all mutant spindles exhibited the following characteristics:

1) They were small. In healthy samples, at least 1 very large, and very long, muscle spindle was found in the belly of the muscle, and often 2, arranged in tandem (a finding previously reported in murine EDL muscles). Spindles of this size and arrangement were not seen in this age group, however. Instead, only very small spindles were found.

2) They contained aggregates of some sort, which reacted with the synt antibody. These aggregates often had a spheroid, bloblike appearance, and were located throughout the spindle.

3) The fine structure of many of their afferent coils was lost. Whereas normal spindles show “tight” coils, separated by small but easily distinguishable spaces, many afferent coils of mutant spindles showed a much more disorganized pattern, with afferents running into each other such that in some places, the distinctive coiling pattern was completely abolished.

4). There were fewer coils. Afferent coils were actually found in most of the spindles, however, there appeared to be fewer of them than in WT or het spindles. The coils were wider and diffuse in appearance, and the spaces between those coils appeared to be larger, almost as if the mutant mice had failed to “fill them in” during postnatal development.

4.3.2. Group 2 (63-67 days old)

The muscle spindles of mutants in the 63-67 day old cohort did not show any improvement (figure 22). Instead, most of the abnormalities present in the youngest age group were also present here. Within this age group, the following abnormalities of the muscle spindle were observed:

1) The majority of spindles found were much smaller than those seen in het or wt EDL muscles. However, a few large spindles were also seen, indicating that they may have been overlooked in the previous age group.

2) The fine structure of the afferent coils was missing, accompanied by spheroid aggregates (easily seen in figure 22E).

3) Fine, disorganized nerves with knoblike endings were seen in several spindles within this age group (22D). These fine, spindly nerves did not appear to form coils, however. For the most part, they were found “hovering” over and around the spindles, forming numerous unproductive fine branches which ran into and around each other, with no indication of a particular direction. These fine sproutings also had bright “knoblike” endings, such that at first glance, on of these ill-destined disorganized mat of nerves sometimes looked like an aggregate themselves, or even artifact. However, they were never observed in wildtype or heterozygous spindles.

4) Again, afferent coils were readily visible in most of the spindles, but they did not show the same fine structure so characteristic of a healthy spindle. The coils were wide, diffuse, and often either touching each other or exhibiting wide gaps between themselves. Thus wherever afferent coils were seen, they had an eerie “almost normal” appearance, which, when compared with healthy samples, were obviously anything but. A few spindles began to show very poor staining (22F).

4.3.3. Group 3

Characteristics of mutant spindles examined within the 92-99 day old age group (figure 23) were as follows.

1) The spheroid aggregates are still found in close proximity to the intrafusal fibers, and sometimes can be seen sticking to each other (23D and E).

2) While most spindles in this age group still have the struggling coils, many spindles can also be seen which have large areas of intrafusal fiber which appear completely vacant. The loss of fine structure of the already abnormal coils is even more apparent. Coils may appear “faded” , as if they are understained (22F).

3) Fine, regenerating axon sprouts can still be seen (23D), but are not as prominent and “overgrown” as those seen in the 63-67 day old age group.

4.3.4 Group 4

Somewhat surprisingly, this age group offers the best look at all of the morphological abnormalities seen throughout the course of the entire study (Figure 24). In fact, the majority of spindles in this age group were found to exhibit every abnormality found in all the other age groups.

1) The spheroid bloblike aggregates are still highly visible in close proximity to the intrafusal fibers.

2) The fine, spindly, regenerating axons can be seen in all the mutant spindles, but unlike those seen in the 63-67 day old age group,many of these actually appear to have hit their mark, appearing in very close proximity or even on, the intrafusal fibers (24 E, arrowhead). Although they are vastly disorganized in comparison to healthy Ia afferents, they are vastly less so than those regenerating axons seen in the 63-67 day old group.

3) Fat diffuse afferent coils can be seen running into each other and obscuring the familiar coil pattern (24D, arrowhead).

4) Some spindles are found within this age group that are completely devoid of nerve, and can only be recognized by their prominent capsule (24F).

4.4. Conclusions

Conclusions drawn from this study are as follows.
1) Morphological abnormalities are apparent in all age groups studied, indicating that spindle degeneration begins earlier than 43 days of age.
2) Embryonic development of muscle spindles is probably normal, since Ia afferent coils are seen in all age groups studied

3) Postnatal development of muscle spindles may not be normal, since the afferent coils observed in the mutant tissue appeared farther apart than in age-matched and littermate controls. This is also the phenotype seen in *gad* mice [10]. However, these distances were not quantitatively measured in this study.
4) There is regenerating activity occurring, since finely sprouting axons are observed with regularity in 3 of the 4 age groups studied.

Summary and Future Research

UCHL1 is a de-ubiquitinating enzyme which is one of the many small enzymes thought to be important for maintaining healthy levels of cellular ubiquitin. Lack of this enzyme, as modeled by the *gad* mouse, results in devastation of both sensory and motor axons, leading to spastic paralysis and death. The natural function of UCHL1, other than its identification as a de-ubiquitinating enzyme, is completely unknown. It is highly conserved, however, and a particular polymorphism in human UCHL1 (S18Y), is linked to lower susceptibility to sporadic Alzheimer's disease, as well as a later onset time in Huntington's disease and decreased incidence of Parkinson's disease. A different polymorphism (I93M), is linked with an increased risk of Parkinson's disease. But perhaps the most convincing evidence of this enzyme's importance is in the UCHL1-/- mouse, who exhibits a profound and widespread neurodegenerative phenotype.

Based on previous work done with *gad* mice, and on the data presented here, it stands to reason that the next logical step in this project is to investigate the role of UCHL1 in axon transport. This and other studies have shown that the spindle is the earliest described component of the nervous system to degenerate in the UCHL1-/- mouse. Furthermore, from the work of Miura et al, it appears that the length of the axon is a critical factor in how quickly it degenerates in UCHL1-/- mice. Distal nerves degenerating first is nothing new. Sensory nerves often have a long way to travel, which makes for a long structure to maintain. A sciatic nerve ligation experiment would provide the answer to whether or not UCHL1-/- mice are defective in axon transport.

The work described in this thesis is as follows. First, a survival curve for the UCHL1-/- mouse has been generated, along with a detailed description of the outward phenotypic appearance of these mutants over the course of their short lifetime. Second, the expression pattern of UCHL1 in brain and spinal cord of these mice is described. Third, a timecourse of endplate degeneration spanning the age group between 43 and 174 days is presented. Fourth, morphological evidence for muscle spindle degeneration within these age groups is also given. Thus a good foundation has been laid to uncover the mechanisms by which lack of UCHL1 causes neurodegeneration.

Works Cited

1. Yamazaki, K., et al., *Gracile axonal dystrophy (GAD), a new neurological mutant in the mouse.* Proc Soc Exp Biol Med, 1988. **187**(2): p. 209-15.
2. Saigoh, K., et al., *Intragenic deletion in the gene encoding ubiquitin carboxy-terminal hydrolase in gad mice.* Nat Genet, 1999. **23**(1): p. 47-51.
3. Wilkinson, K.D., et al., *The neuron-specific protein PGP 9.5 is a ubiquitin carboxyl-terminal hydrolase.* Science, 1989. **246**(4930): p. 670-3.
4. Doran, J.F., et al., *Isolation of PGP 9.5, a new human neurone-specific protein detected by high-resolution two-dimensional electrophoresis.* J Neurochem, 1983. **40**(6): p. 1542-7.
5. Thompson, R.J., et al., *PGP 9.5--a new marker for vertebrate neurons and neuroendocrine cells.* Brain Res, 1983. **278**(1-2): p. 224-8.
6. Day, I.N. and R.J. Thompson, *Molecular cloning of cDNA coding for human PGP 9.5 protein. A novel cytoplasmic marker for neurones and neuroendocrine cells.* FEBS Lett, 1987. **210**(2): p. 157-60.
7. Wilson, P.O., et al., *The immunolocalization of protein gene product 9.5 using rabbit polyclonal and mouse monoclonal antibodies.* Br J Exp Pathol, 1988. **69**(1): p. 91-104.
8. Mukoyama, M., et al., *Neuropathology of gracile axonal dystrophy (GAD) mouse. An animal model of central distal axonopathy in primary sensory neurons.* Acta Neuropathol (Berl), 1989. **79**(3): p. 294-9.
9. Kikuchi, T., et al., *Axonal degeneration of ascending sensory neurons in gracile axonal dystrophy mutant mouse.* Acta Neuropathol (Berl), 1990. **80**(2): p. 145-51.
10. Oda, K., et al., *Dying back type axonal degeneration of sensory nerve terminals in muscle spindles of the gracile axonal dystrophy (GAD) mutant mouse.* Neuropathol Appl Neurobiol, 1992. **18**(3): p. 265-81.
11. Miura, H., et al., *Progressive degeneration of motor nerve terminals in GAD mutant mouse with hereditary sensory axonopathy.* Neuropathol Appl Neurobiol, 1993. **19**(1): p. 41-51.
12. Liu, Y., et al., *The UCH-L1 gene encodes two opposing enzymatic activities that affect alpha-synuclein degradation and Parkinson's disease susceptibility.* Cell, 2002. **111**(2): p. 209-18.
13. Naze, P., et al., *Mutation analysis and association studies of the ubiquitin carboxy-terminal hydrolase L1 gene in Huntington's disease.* Neurosci Lett, 2002. **328**(1): p. 1-4.
14. Xue, S. and J. Jia, *Genetic association between Ubiquitin Carboxy-terminal Hydrolase-L1 gene S18Y polymorphism and sporadic Alzheimer's disease in a Chinese Han population.* Brain Res, 2006. **1087**(1): p. 28-32.
15. Carmine Belin, A., et al., *S18Y in ubiquitin carboxy-terminal hydrolase L1 (UCH-L1) associated with decreased risk of Parkinson's disease in Sweden.* Parkinsonism Relat Disord, 2007.
16. Gong, B., et al., *Ubiquitin hydrolase Uch-L1 rescues beta-amyloid-induced decreases in synaptic function and contextual memory.* Cell, 2006. **126**(4): p. 775-88.

17. Hegde, A.N., et al., *Ubiquitin C-terminal hydrolase is an immediate-early gene essential for long-term facilitation in Aplysia.* Cell, 1997. **89**(1): p. 115-26.
18. Leu, M., et al., *Erbb2 regulates neuromuscular synapse formation and is essential for muscle spindle development.* Development, 2003. **130**(11): p. 2291-301.
19. Andrechek, E.R., et al., *ErbB2 is required for muscle spindle and myoblast cell survival.* Mol Cell Biol, 2002. **22**(13): p. 4714-22.

APPENDIX: Endplate counts raw data

Date	slide#blind	slide ID	sample ID	genotype	age(days)	#full	#partial	#vacant	#spindles	
4/3/2008	1		3700	UchL1+/+	46	403	22	14	9	
2/5/2008	1 and 3		3700	UchL1+/+	46	508	21	10	9	
4/12/2008	4	1b	3700	UchL1+/+	46	441	37	2	12	
	not blind	1a,2a	3700	UchL1+/+	46	600	0	0	9	
						1952	**80**	**26**	**39**	sum
2/5/2008	6 and 11		4140	UchL1+/+Ubr+	58	570	8	6	6	
4/11/2008	3	1b	4140	UchL1+/+Ubr+	58	233	38	13	4	
4/11/2008	9	2b	4140	UchL1+/+Ubr+	58	87	23	6	5	
4/12/2008	1	1d	4140	UchL1+/+Ubr+	58	227	21	11	5	
4/12/2008	3	2d	4140	UchL1+/+Ubr+	58	68	3	0	3	
	not blind	1a,2a	4140	UchL1+/+Ubr+	58	626	0	0	7	
						1811	**93**	**36**	**30**	sum
4/12/2008	6	1d	4142	UchL1+/-UbR-	57	155	18	7	1	
4/12/2008	7	1c	4142	UchL1+/-UbR-	57	96	9	3	1	
4/12/2008	8	2d	4142	UchL1+/-UbR-	57	169	19	2	4	
4/12/2008	9	2c	4142	UchL1+/-UbR-	57	170	33	7	5	
	not blind	1a,2a	4142	UchL1+/-UbR-	57	526	0	0	13	
						1116	**79**	**19**	**24**	sum
2/5/2008	9 and 10(2nd)		4452	UchL1+/-UbR-	47	571	6	2	6	2 edl's
	not blind 2nd		4452	UchL1+/-UbR-	47	480	0	0	6	
4/3/2008	2		4452	UchL1+/-UbR-	47	27	0	1	0	
4/3/2008	6		4452	UchL1+/-UbR-	47	156	24	20	0	
4/3/2008	10(1st)		4452	UchL1+/-UbR-	47	n/a	n/a	n/a	9	
	not blind 1st		4452	UchL1+/-UbR-	47	544	0	0	12	
4/3/2008	10(2nd)		4452	UchL1+/-UbR-	47	n/a	n/a	n/a	10	
4/12/2008	3	2b	4452	UchL1+/-UbR-	47	n/a	n/a	n/a	n/a	
4/12/2008	7	1b	4452	UchL1+/-UbR-	47	149	3	3	0	
4/12/2008	2	3c	4452	UchL1+/-UbR-	47	21	2	1	0	
4/12/2008	5	3b	4452	UchL1+/-UbR-	47	20	3	1	0	
						1968	**38**	**28**	**43**	sum
						984	**19**	**14**	**21.5**	sum/2
4/3/2008	3		3583	UchL1+/-	48	404	44	40	7	
4/12/2008	9	1c	3583	UchL1+/-	48	327	2	0	4	
	not blind		3583	UchL1+/-	48	510	0	0	7	
						1241	**46**	**40**	**18**	sum

4/3/2008	4		4456	UchL1-/-UbR-	43	135	10	2	0	
4/3/2008	9		4456	UchL1-/-UbR+	43	283	43	4	7	
2/5/2008	2 and 12		4456	UchL1-/-UbR+	43	413	11	1	2	
4/11/2008	2	2b	4456	UchL1-/-UbR+	43	228	17	3	7	
4/11/2008	5	2a	4456	UchL1-/-UbR+	43	271	31	12	13	
4/12/2008	4	1d	4456	UchL1-/-UbR+	43	66	6	3	0	
4/12/2008	10	1b	4456	UchL1-/-UbR+	43	97	11	1	0	
						1493	**129**	**26**	**29**	sum
4/3/2008	5		4453	UchL1-/-UbR-	46	218	36	6	3	
4/3/2008	7		4453	UchL1-/-UbR-	46	219	47	10	7	
2/5/2008	4 and 8		4453	UchL1-/-UbR-	46	544	17	4	7	
4/12/2008	1	1b	4453	UchL1-/-UbR-	46	132	30	2	6	
4/12/2008	2	1a	4453	UchL1-/-UbR-	46	163	36	5	7	
4/12/2008	5	2a	4453	UchL1-/-UbR-	46	216	15	2	2	
4/12/2008	6	2b	4453	UchL1-/-UbR-	46	151	10	3	2	
						1643	**191**	**32**	**34**	sum
4/3/2008	8		4458	UchL1-/-UbR+	48	316	111	32	17	
2/5/2008	5 and 7		4458	UchL1-/-UbR+	48	513	74	20	4	
4/12/2008	8	2b	4458	UchL1-/-UbR+	48	282	38	7	8	
4/12/2008	10	2a	4458	UchL1-/-UbR+	48	242	41	19	9	
						1353	**264**	**78**	**38**	sum
2/27/2008	2 and 9		4046	UchL1+/+	168	554	3	2	4	
5/15/2008	5	1b EDL	4046	UchL1+/+	168	432	0	0	4	
5/15/2008	2	2b EDL	4046	UchL1+/+	168	6	0	0	0	
5/16/2008	7	1d EDL	4046	UchL1+/+	168	399	0	0	4	
5/16/2008	10	1c EDL	4046	UchL1+/+	168	417	0	0	3	
						1808	**3**	**2**	**15**	sum

2/27/2008	3,6, and 10		4044	UchL1+/-	166	628	1	0	10	
5/15/2008	10	1b EDL	4044	UchL1+/-	166	331	0	0	6	
5/15/2008	8	2b EDL	4044	UchL1+/-	166	753	0	0	15	
5/16/2008	1	1d EDL	4044	UchL1+/-	166	341	0	0	3	
5/16/2008	6	1c EDL	4044	UchL1+/-	166	331	0	0	1	
5/16/2008	1	2d EDL	4044	UchL1+/-	166	721	0	0	4	
5/16/2008	4	2c EDL	4044	UchL1+/-	166	633	0	0	1	
						3738	**1**	**0**	**40**	sum
						1869	**0.5**	**0**	**20**	sum/2
2/27/2008	8		4057	UchL1+/+	157	499	2	6	2	
5/15/2008	4	1d EDL	4057	UchL1+/+	157	466	0	0	4	
5/16/2008	3	1c EDL	4057	UchL1+/+	157	395	0	0	7	
5/16/2008	6	1b EDL	4057	UchL1+/+	157	372	0	0	1	
						1732	**2**	**6**	**14**	sum
2/27/2008	1,5,and7		4043	UchL1-/-	173	251	150	312	3	
5/15/2008	9	3b EDL	4043	UchL1-/-	173	9	9	35	4	
5/15/2008	6	2b EDL	4043	UchL1-/-	173	60	77	215	2	
5/16/2008	2	2d EDL	4043	UchL1-/-	173	55	79	304	8	
5/16/2008	8	2c EDL	4043	UchL1-/-	173	64	76	360	4	
5/16/2008	3	3c EDL	4043	UchL1-/-	173	3	6	34	1	
						442	**397**	**1260**	**22**	sum
2/27/2008	4		4058	UchL1-/-	168	106	101	260	3	
5/15/2008	7	1b EDL	4058	UchL1-/-	168	64	71	178	2	
5/16/2008	4	1c EDL	4058	UchL1-/-	168	96	52	321	3	
5/16/2008	7	1d EDL	4058	UchL1-/-	168	21	38	242	0	
						287	**262**	**1001**	**8**	sum
2/27/2008	11 and 12		4045	UchL1-/-	174	205	79	165	3	
5/15/2008	3	1c EDL	4045	UchL1-/-	174	99	51	56	4	
5/15/2008	1	2c EDL	4045	UchL1-/-	174	50	51	104	4	
5/16/2008	5	1d EDL	4045	UchL1-/-	174	81	38	61	1	
5/16/2008	9	1b EDL	4045	UchL1-/-	174	65	41	111	3	
5/16/2008	2	2d EDL	4045	UchL1-/-	174	33	30	123	2	
5/16/2008	8	2b EDL	4045	UchL1-/-	174	11	20	133	1	
						544	**310**	**753**	**18**	sum

3/14/2008		4609	UchL1+/-	53	585	2	2	12	
4/25/2008	6 1b EDL	4609	UchL1+/-	53	423	8	1	6	
4/25/2008	9 1d EDL	4609	UchL1+/-	53	426	8	6	5	
4/17/2008	9 1c EDL	4609	UchL1+/-	53	420	1	0	7	
					1854	**19**	**9**	**30**	sum
3/14/2008		4610	UchL1+/-	47	486	7	1	10	
4/17/2008	2 1c EDL	4610	UchL1+/-	47	459	4	0	9	
4/25/2008	5 1b EDL	4610	UchL1+/-	47	373	0	0	3	
4/17/2008	6 1d EDL	4610	UchL1+/-	47	465	4	0	4	
					1783	**15**	**1**	**26**	sum
3/14/2008		4611	UchL1+/+	50	463	6	1	3	
4/25/2008	2 1d EDL	4611	UchL1+/+	50	409	7	0	1	
4/25/2008	8 1b EDL	4611	UchL1+/+	50	417	2	1	1	
4/17/2008	4 1c EDL	4611	UchL1+/+	50	480	4	1	3	
					1769	**19**	**3**	**8**	sum
3/14/2008		4608	UchL1+/-	49	492	3	0	10	
4/29/2008	6 1d EDL	4608	UchL1+/-	49	444	1	1	9	
4/25/2008	7 1b EDL	4608	UchL1+/-	49	435	3	0	5	
4/17/2008	8 1c EDL	4608	UchL1+/-	49	457	1	0	9	
					1828	**8**	**1**	**33**	sum
3/14/2008		4600	UchL1-/-	65	305	156	101	3	
4/17/2008	3 1c EDL	4600	UchL1-/-	65	304	86	47	5	
4/25/2008	3 1d EDL	4600	UchL1-/-	65	362	47	33	8	
4/17/2008	10 1b EDL	4600	UchL1-/-	65	374	86	46	6	
					1345	**375**	**227**	**22**	sum
3/14/2008		4599	UchL1-/-	63	228	119	78	4	
4/25/2008	1 1d EDL	4599	UchL1-/-	63	207	18	4	3	
4/17/2008	5 1c EDL	4599	UchL1-/-	63	196	29	9	3	
4/17/2008	7 1b EDL	4599	UchL1-/-	63	174	19	5	2	
					805	**185**	**96**	**12**	sum

3/14/2008			4597	UchL1-/-	48	334	167	61	7	
4/17/2008	1	1c EDL	4597	UchL1-/-	48	341	70	34	5	
4/25/2008	4	1b EDL	4597	UchL1-/-	48	361	33	27	6	
4/25/2008	10	1d EDL	4597	UchL1-/-	48	325	72	25	9	
						1361	**342**	**147**	**27**	sum
4/11/2008	4	1a	4596	UchL1-/-	95	113	126	68	7	
4/16/2008	9	1b EDL	4596	UchL1-/-	95	298	49	37	3	
5/9/2008	2	1d EDL	4596	UchL1-/-	95	250	98	58	7	
5/7/2008	3	1c EDL	4596	UchL1-/-	95	284	42	12	4	
						945	**315**	**175**	**21**	
4/16/2008	2	1a EDL	4308	UchL1-/-	84	239	56	17	2	
4/29/2008	2	2b EDL	4308	UchL1-/-	84	76	28	21	2	
4/29/2008	5	2d EDL	4308	UchL1-/-	84	60	19	8	0	
4/29/2008	7	1d EDL	4308	UchL1-/-	84	222	124	44	3	
4/29/2008	8	1c EDL	4308	UchL1-/-	84	184	116	53	7	
4/29/2008	9	1b EDL	4308	UchL1-/-	84	155	147	36	10	
4/29/2008	12	2c EDL	4308	UchL1-/-	84	40	19	28	1	
4/29/2008	14	2a EDL	4308	UchL1-/-	84	99	31	5	2	
						1075	**540**	**212**	**27**	sum
4/16/2008	3	1a EDL	4607	UchL1-/-	99	329	84	29	5	
5/9/2008	1	1d EDL	4607	UchL1-/-	99	281	112	60	8	
5/9/2008	2	1b EDL	4607	UchL1-/-	99	228	131	64	4	
5/7/2008	6	1c EDL	4607	UchL1-/-	99	this slide was unreadable				
						838	**327**	**153**	**17**	sum
4/16/2008	4	1a EDL	4593	UchL1+/-	96	449	11	2	2	
5/9/2008	6	1b EDL	4593	UchL1+/-	96	422	0	0	2	
5/9/2008	5	1d EDL	4593	UchL1+/-	96	466	2	0	5	
5/7/2008	9	1c EDL	4593	UchL1+/-	96	420	6	1	4	
						1757	**19**	**3**	**13**	sum
4/16/2008	5	1a EDL	4603	UchL1+/+	94	293	3	0	4	
5/9/2008	9	1b EDL	4603	UchL1+/+	94	352	0	0	4	
5/9/2008	9	1d EDL	4603	UchL1+/+	94	516	0	0	4	
5/7/2008	5	1c EDL	4603	UchL1+/+	94	472	1	0	2	
						1633	**4**	**0**	**14**	sum

4/16/2008	6	1a EDL	3839	UchL1-/-	85	323	127	52	6
4/29/2008	4	1b EDL	3839	UchL1-/-	85	270	100	52	3
4/29/2008	10	1d EDL	3839	UchL1-/-	85	218	134	100	4
4/29/2008	11	1c EDL	3839	UchL1-/-	85	248	96	63	2
						1059	**457**	**267**	**15** sum
4/16/2008	7	1a EDL	4595	UchL1-/-	95	324	100	25	2
5/9/2008	4	1c EDL	4595	UchL1-/-	95	255	147	59	5
5/9/2008	10	1d EDL	4595	UchL1-/-	95	281	79	41	5
5/7/2008	7	1b EDL	4595	UchL1-/-	95	272	102	43	5
						1132	**428**	**168**	**17** sum
4/16/2008	8	1a EDL	3562	UchL1+/+	92	350	9	0	3
4/29/2008	1	1c EDL	3562	UchL1+/+	92	298	38	9	3
4/29/2008	3	1d EDL	3562	UchL1+/+	92	255	27	17	5
4/29/2008	13	1b EDL	3562	UchL1+/+	92	353	4	2	3
						1256	**78**	**28**	**14** sum
5/9/2008	1	1d EDL	4721	UchL1+/+	65	444	0	0	4
5/9/2008	4	1a EDL	4721	UchL1+/+	65	433	0	0	8
5/9/2008	7	1b EDL	4721	UchL1+/+	65	417	1	0	7
5/7/2008	8	1c EDL	4721	UchL1+/+	65	298	4	2	4
						1592	**5**	**2**	**23** sum
5/9/2008	3	1a EDL	4732	UchL1-/-	67	217	118	38	3
5/9/2008	6	1d EDL	4732	UchL1-/-	67	270	113	39	6
5/7/2008	4	1b EDL	4732	UchL1-/-	67	245	102	53	7
5/7/2008	10	1c EDL	4732	UchL1-/-	67	280	102	39	13
						1012	**435**	**169**	**29** sum
5/9/2008	5	1a EDL	4719	UchL1+/+	64	465	0	0	5
5/9/2008	10	1b EDL	4719	UchL1+/+	64	338	0	0	5
5/9/2008	8	1d EDL	4719	UchL1+/+	64	503	0	0	3
5/7/2008	2	1c EDL	4719	UchL1+/+	64	417	3	0	1
						1723	**3**	**0**	**14** sum
5/9/2008	7	1a EDL	4720	UchL1+/+	63	342	0	0	1
5/9/2008	8	1b EDL	4720	UchL1+/+	63	388	0	0	3
5/9/2008	3	1d EDL	4720	UchL1+/+	63	431	0	0	7
5/7/2008	1	1c EDL	4720	UchL1+/+	63	365	2	10	5
						1526	**2**	**10**	**16** sum

Figure 1: Schematic of UCHL1 phenotype progression. *n*=15 UCHL1-/- mice included in the survival curve. Mice were observed from weaning to untimely death.

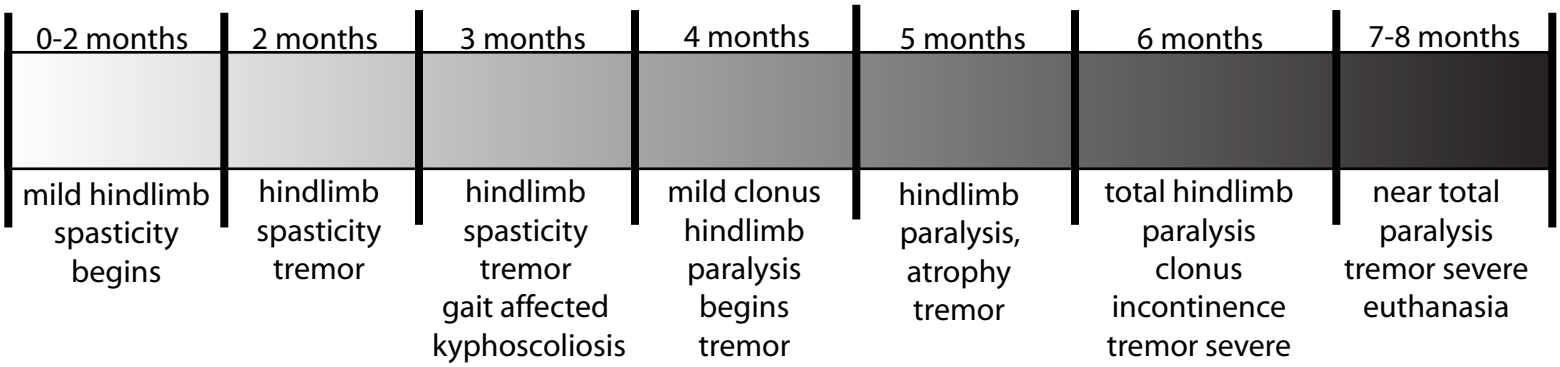
0-2 months
2 months
3 months
4 months
5 months
6 months
7-8 months
mild hindlimb spasticity begins
hindlimb spasticity tremor
hindlimb spasticity tremor gait affected kyphoscoliosis
mild clonus hindlimb paralysis begins tremor
hindlimb paralysis, atrophy tremor
total hindlimb paralysis clonus incontinence tremor severe
near total paralysis tremor severe euthanasia

Figure 2: Representative photographs of outward appearance of phenotype of UCHL1-/- mice.
A) 50-day old mutant exhibiting footclasp and onset of hindlimb spasticity.
B,C) 119-day old mutant showing typical spastic movements of hindlimbs.
D) 248-day old mutant exhibiting spastic hindlimb movements and clasping of forelimbs
E,F) 140-day old mutant exhibiting typical slouching posture with hindlimbs splayed clumsily underneath the body
G,H) 248-day old mutant, the same mutant shown in E and F, showing total spastic paralysis, shortly before euthanasia.

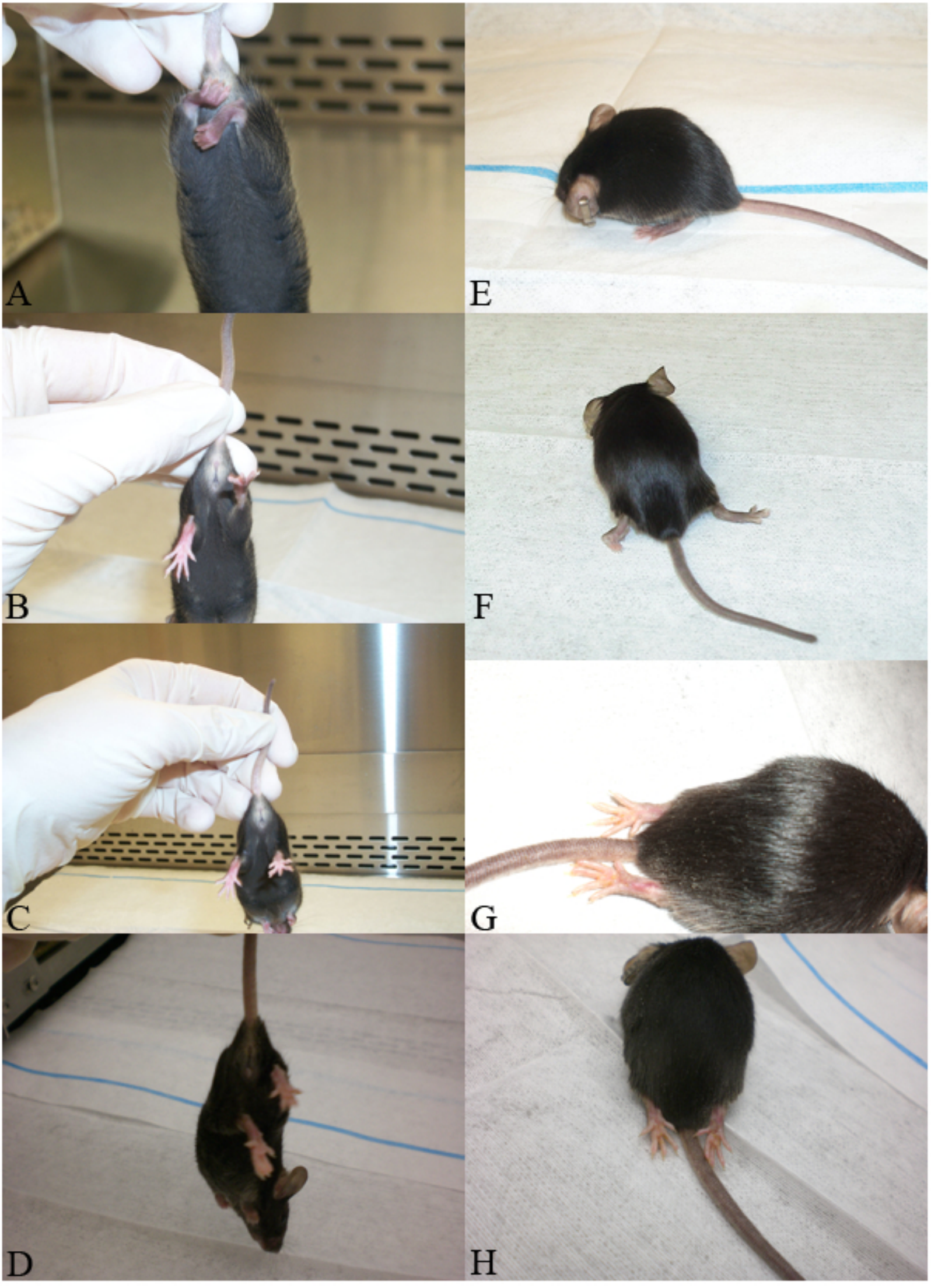
A
B
C
D
E
F
G
H

Figure 3: UCHL1 survival curve and representative photos of 1.5 month and 3.0 month old UCHL1+/+ and UCHL1-/- littermates.
A) 1.5 month old UCHL1 +/+ mouse, showing good posture
B) 1.5 month old UCHL1-/- littermate, showing good posture and lack of paralysis.
C) 3.0 month old UCHL1+/+ mouse, showing a healthy movement and posture
D) 3.0 month old UCHL1-/- mouse, showing beginning of problems with ambulation (note the feet splayed out in the back as the mouse "hops").
E) UCHL1 survival curve, *n*=15 UCHL1-/- mice, and 15 UCHL1+/+ or +/- littermates.

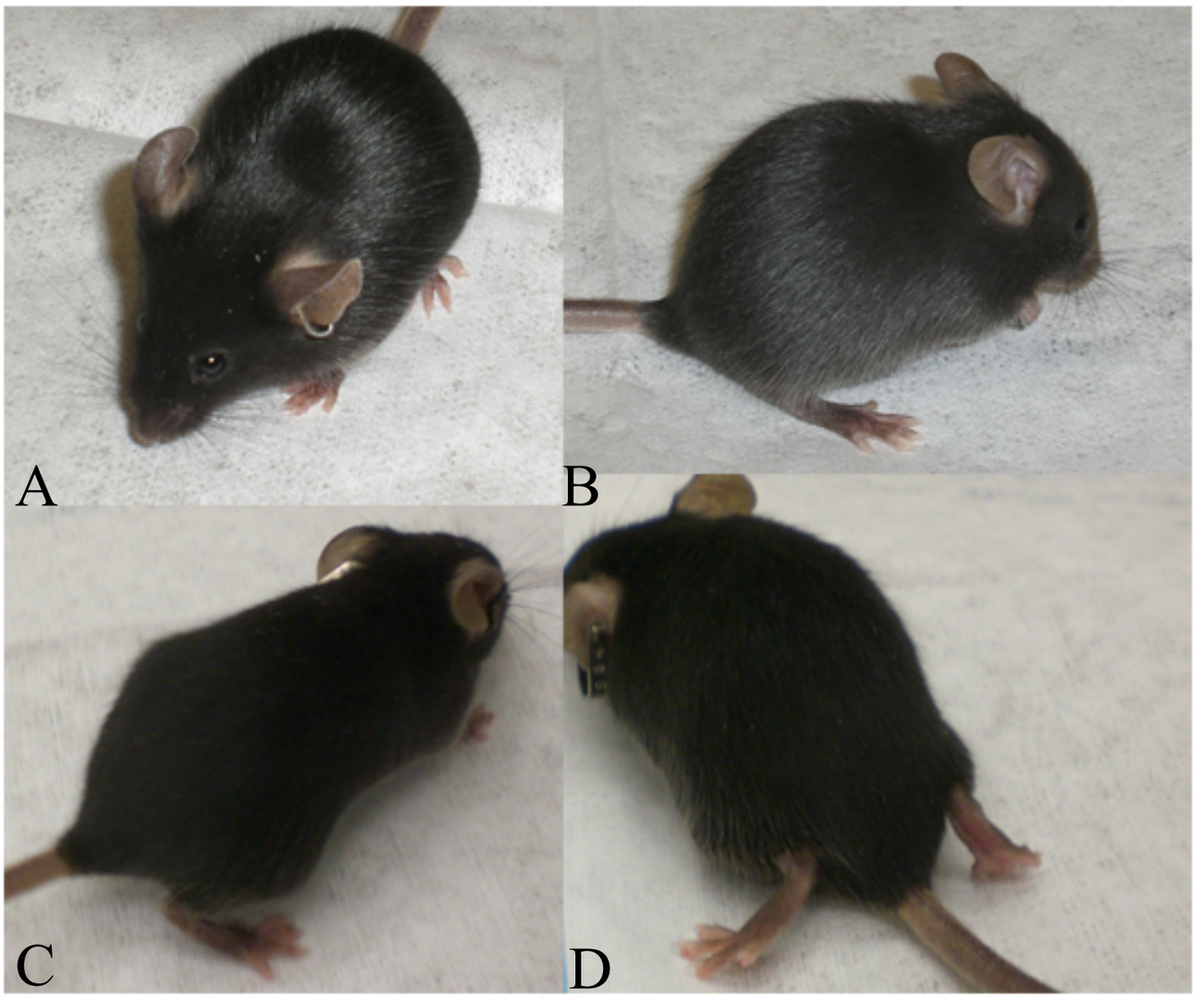
A
B
C
D

E

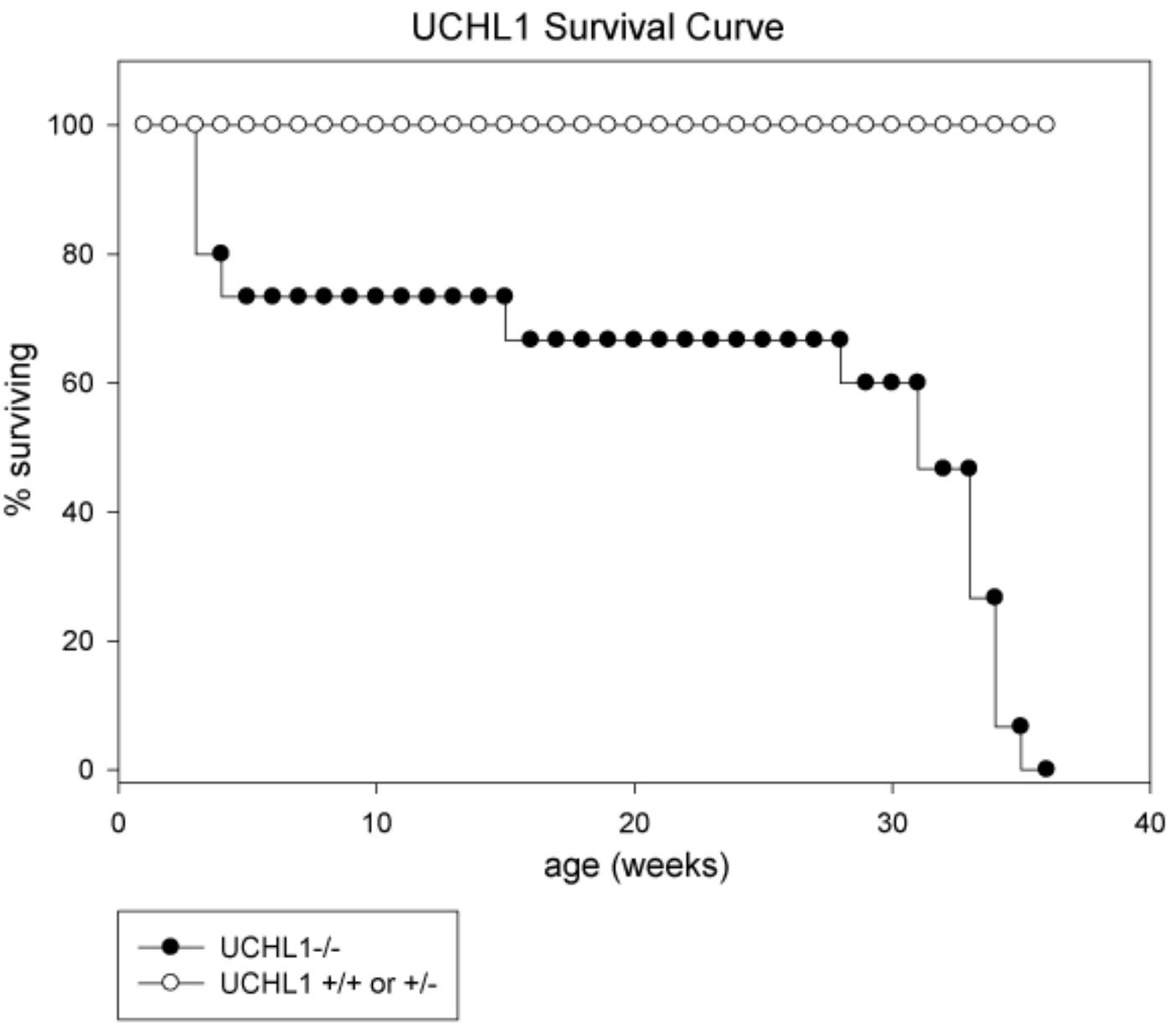
UCHL1 Survival Curve
100
80
60
40
20
0
% surviving
0
10
20
30
40
age (weeks)
UCHL1-/-
UCHL1 +/+ or +/-

Figure 4: UCHL1 expression pattern in primary somatosensory cortex.
A,B) Nissl stain and X-gal stained twin slides
C) Additional photography of the same region in a different mouse.

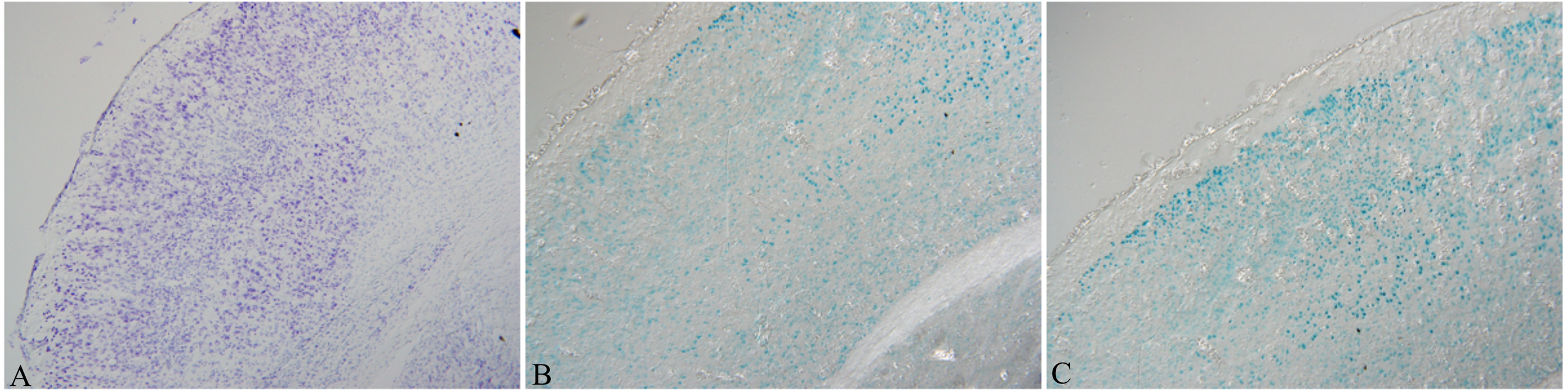
A
B
C

Figure 5: UCHL1 expression pattern in primary motor cortex.
A,B) Nissl and X-gal twin slides showing matching expression pattern.
C,D) Representative slides from 2 additional mice stained with X-gal.

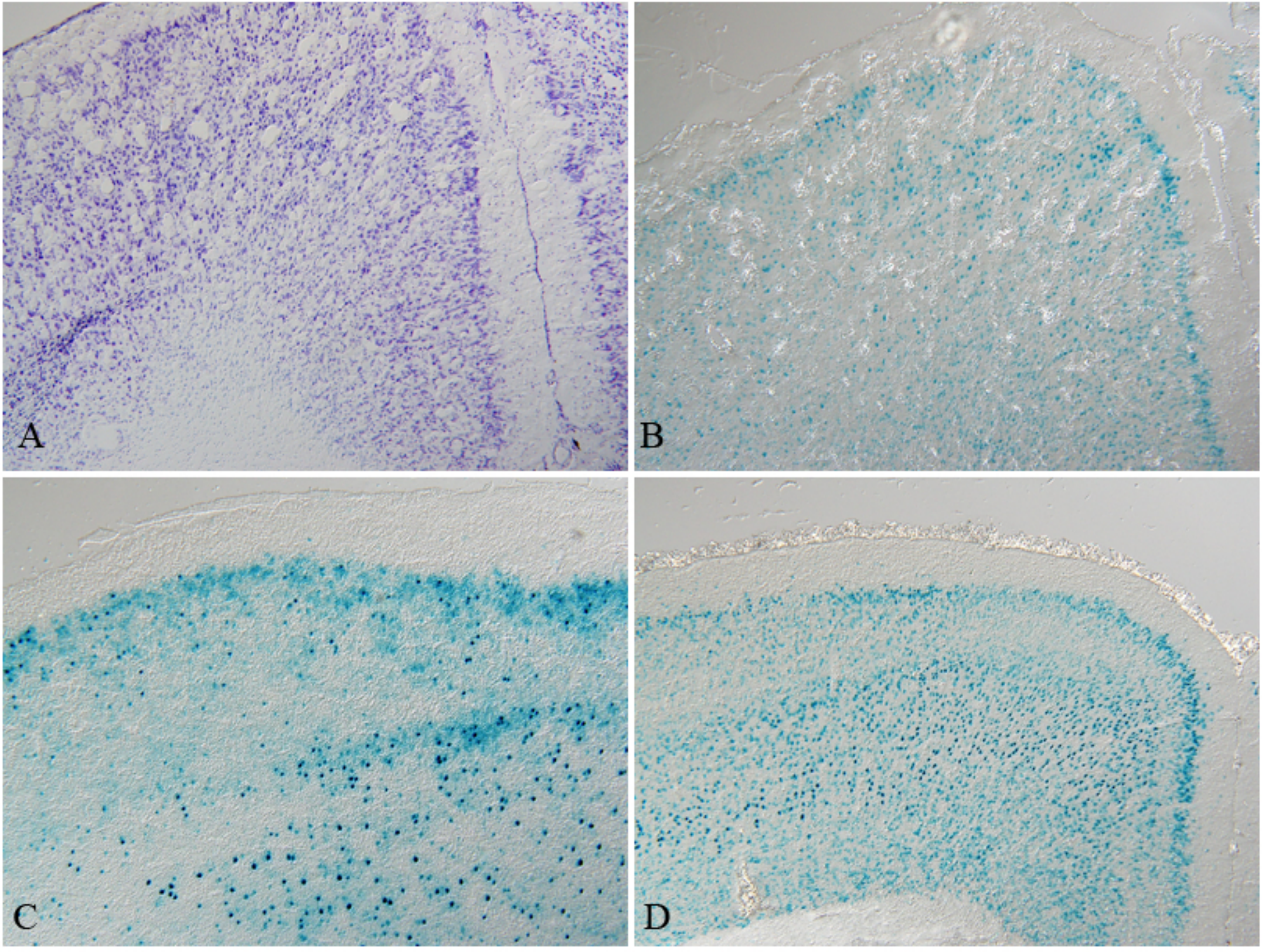
A
B
C
D

Figure 6: UCHL1 expression in the gracile nucleus of the medulla.
A,B) Nissl and X-gal twin slides. Of the 6 mice evaluated, this is the only sample that stained.

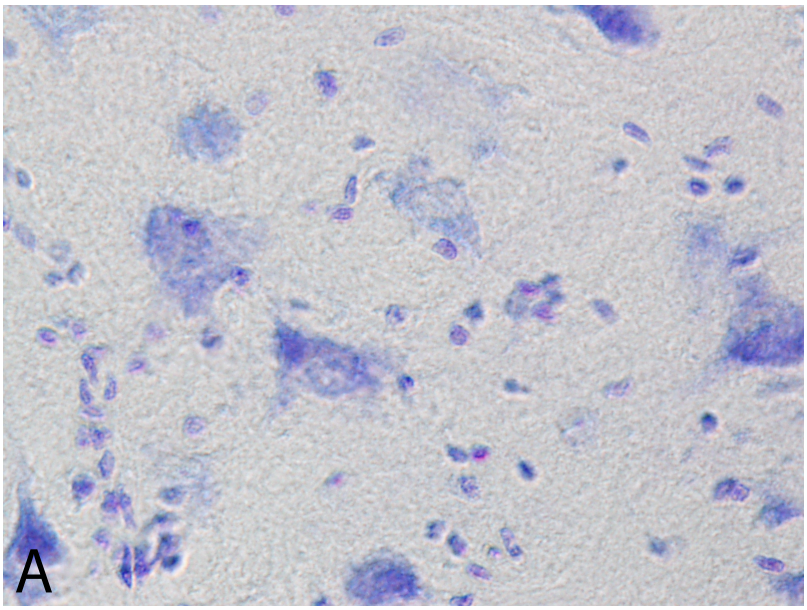
A

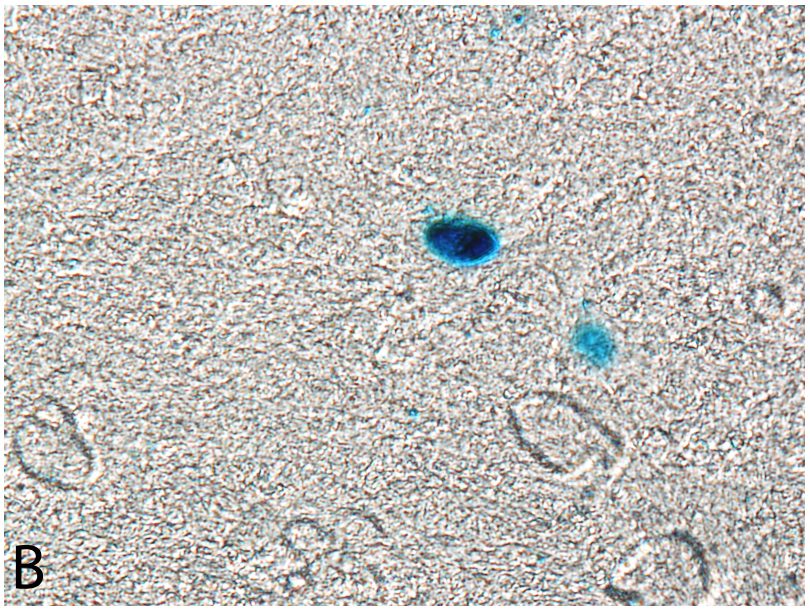
B

Figure 7: UCHL1 expression pattern in adult spinal cord.
A,B) UCHL1 expression pattern in cervical spinal cord, showing little UCHL1 expression, even in the dorsal horns.
C,D) UCHL1 expression in thoracic spinal cord, showing high UCHL1 expression in the dorsal horns, and in motor neurons of the ventral horn.
E,F): UCHL1 expression in lumbar spinal cord, showing UCHL1 expression in the dorsal and ventral horns. Additional staining may be interneurons.

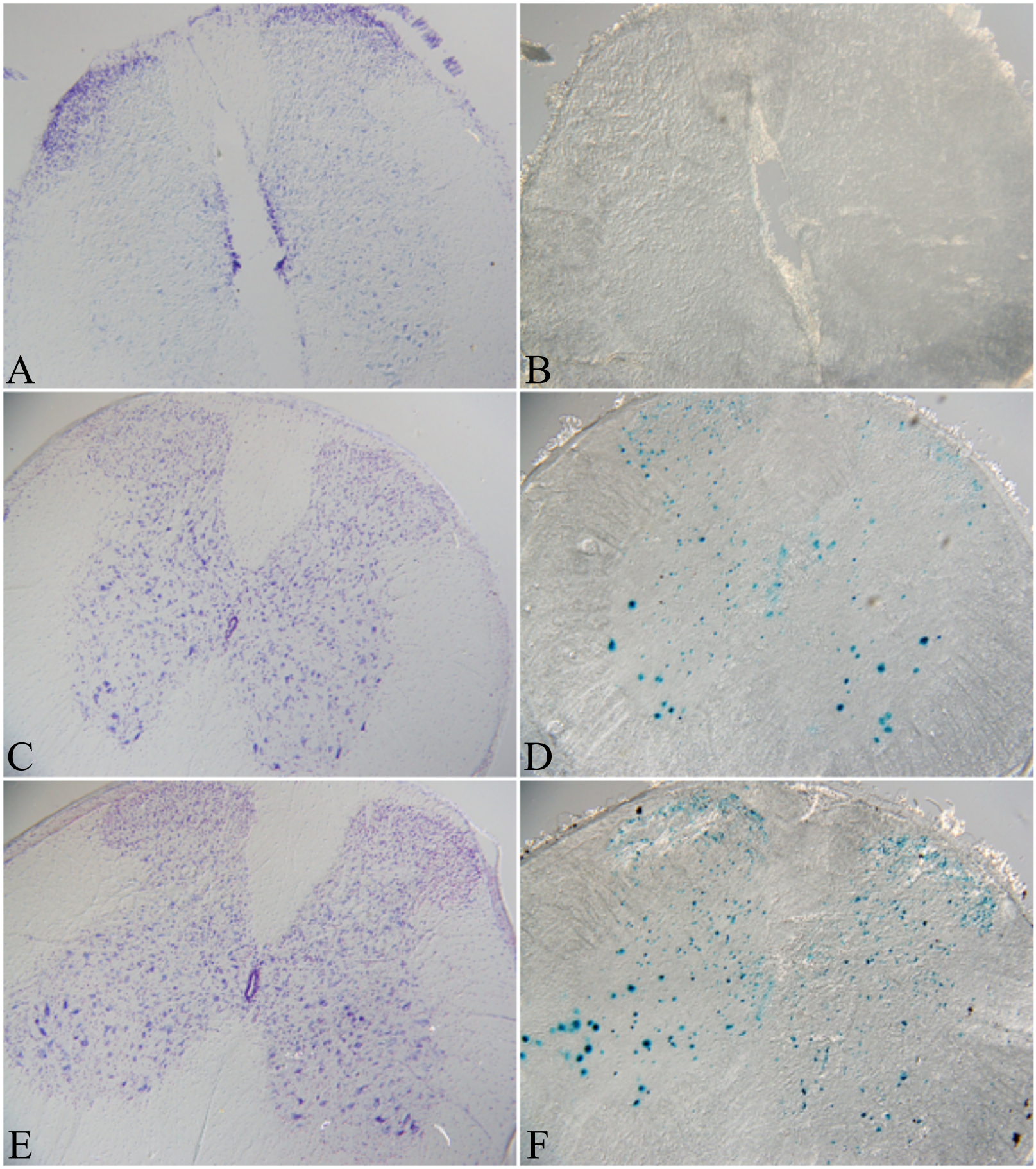
A
B
C
D
E
F

Figure 8: UCHL1 expression in embryonic spinal cord is much more uniform than that seen in adults. Nissl and X-gal stained twin slides are side by side.
A,B): Cervical spinal cord showing much stronger UCHL1 expression than in adult samples, but also shows reduced staining in the dorsal horns of this level.
C,D): Thoracic spinal cord showing strong UCHL1 expression, especially in the motor neurons of the ventral horn.
E-H): Lumbar spinal cord sections also show uniform UCHL1 expression.

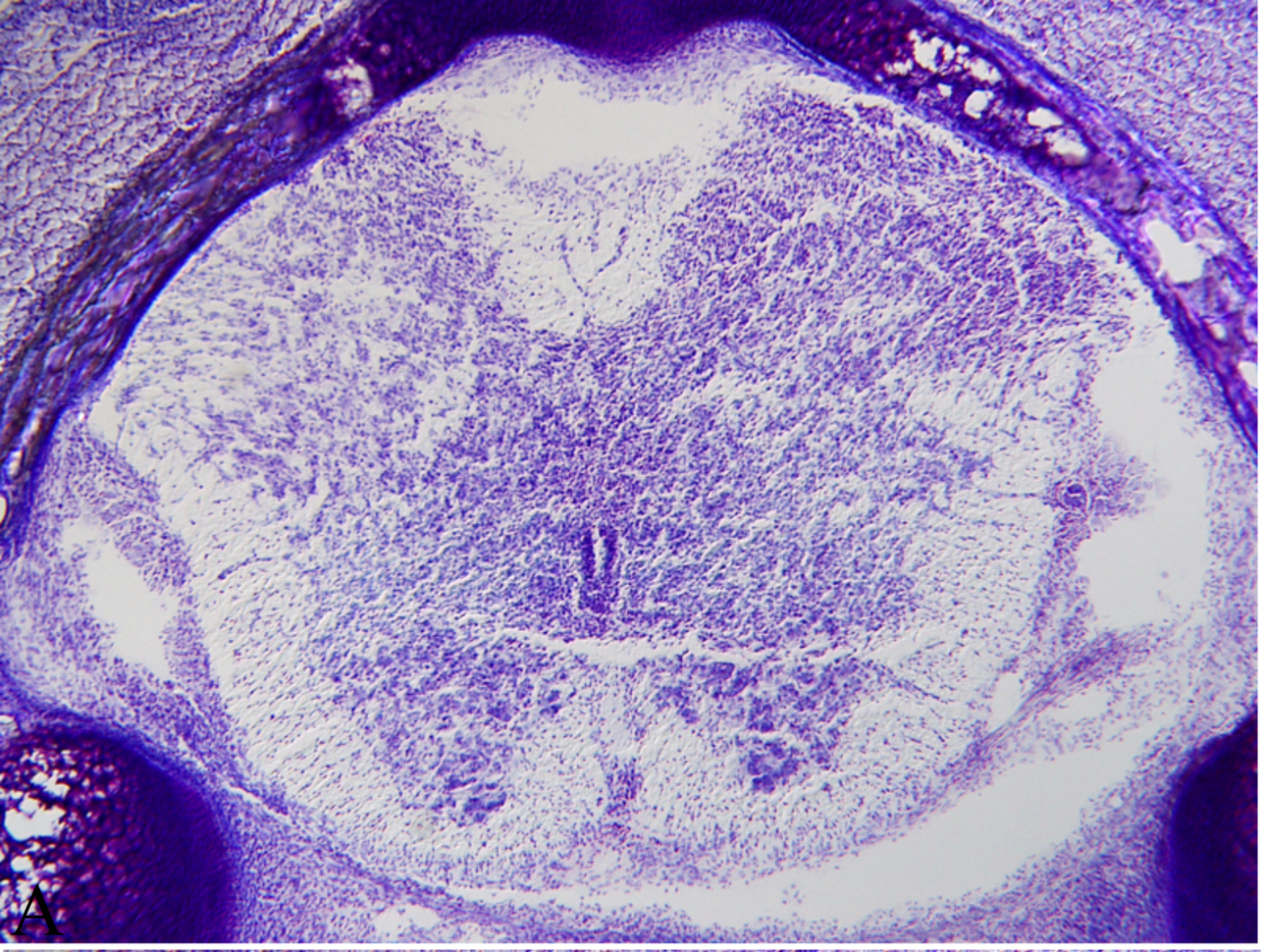
A

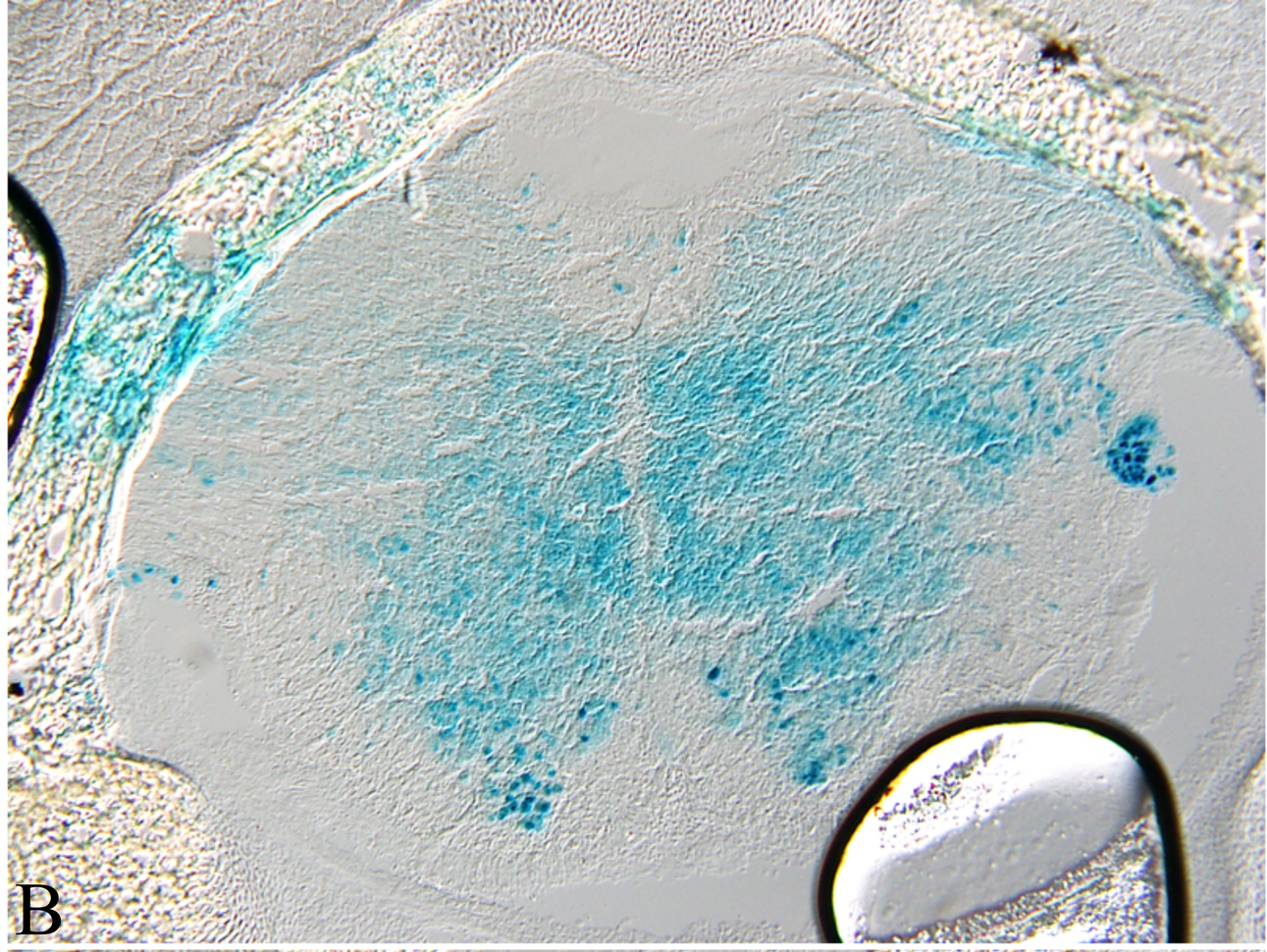
B

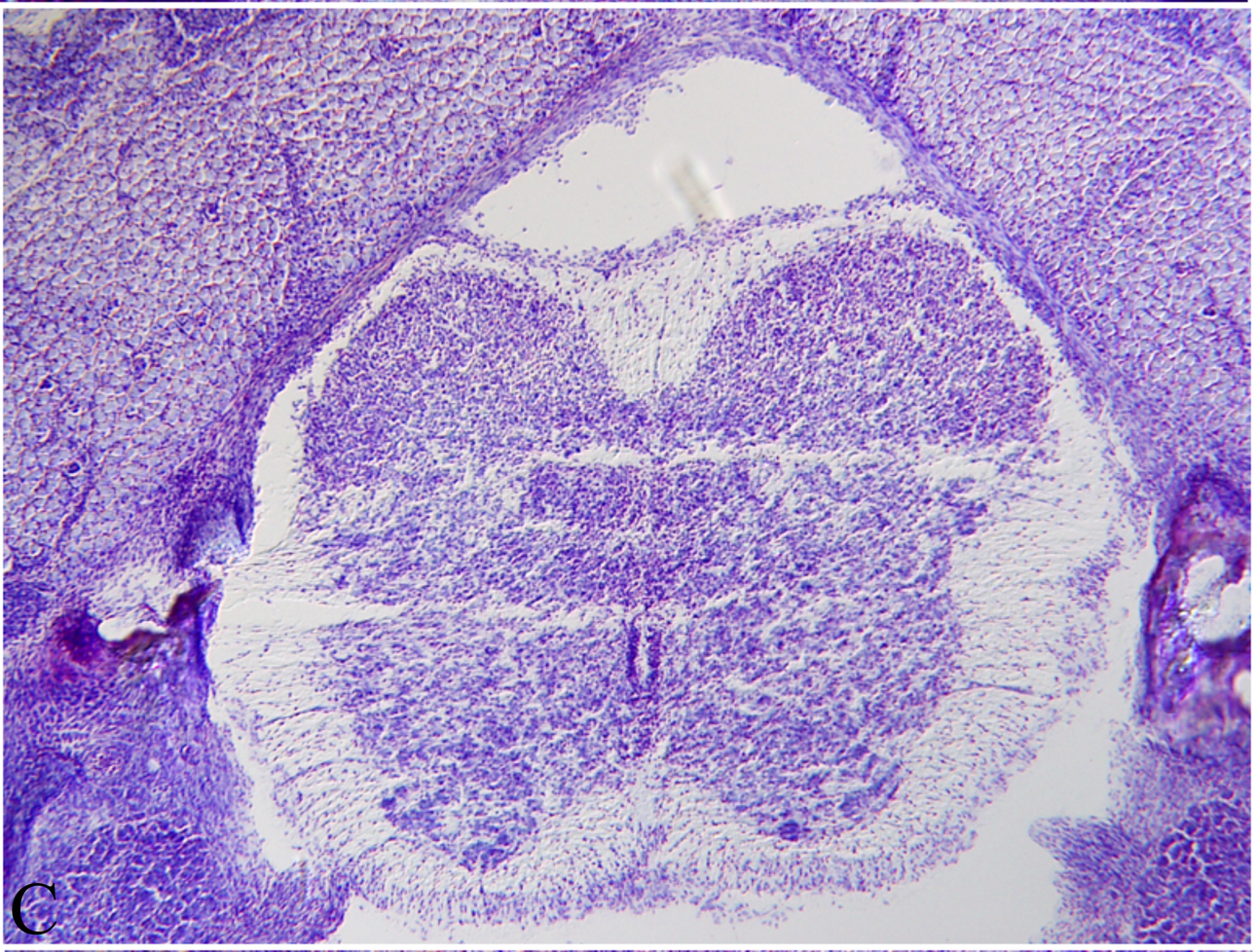
C

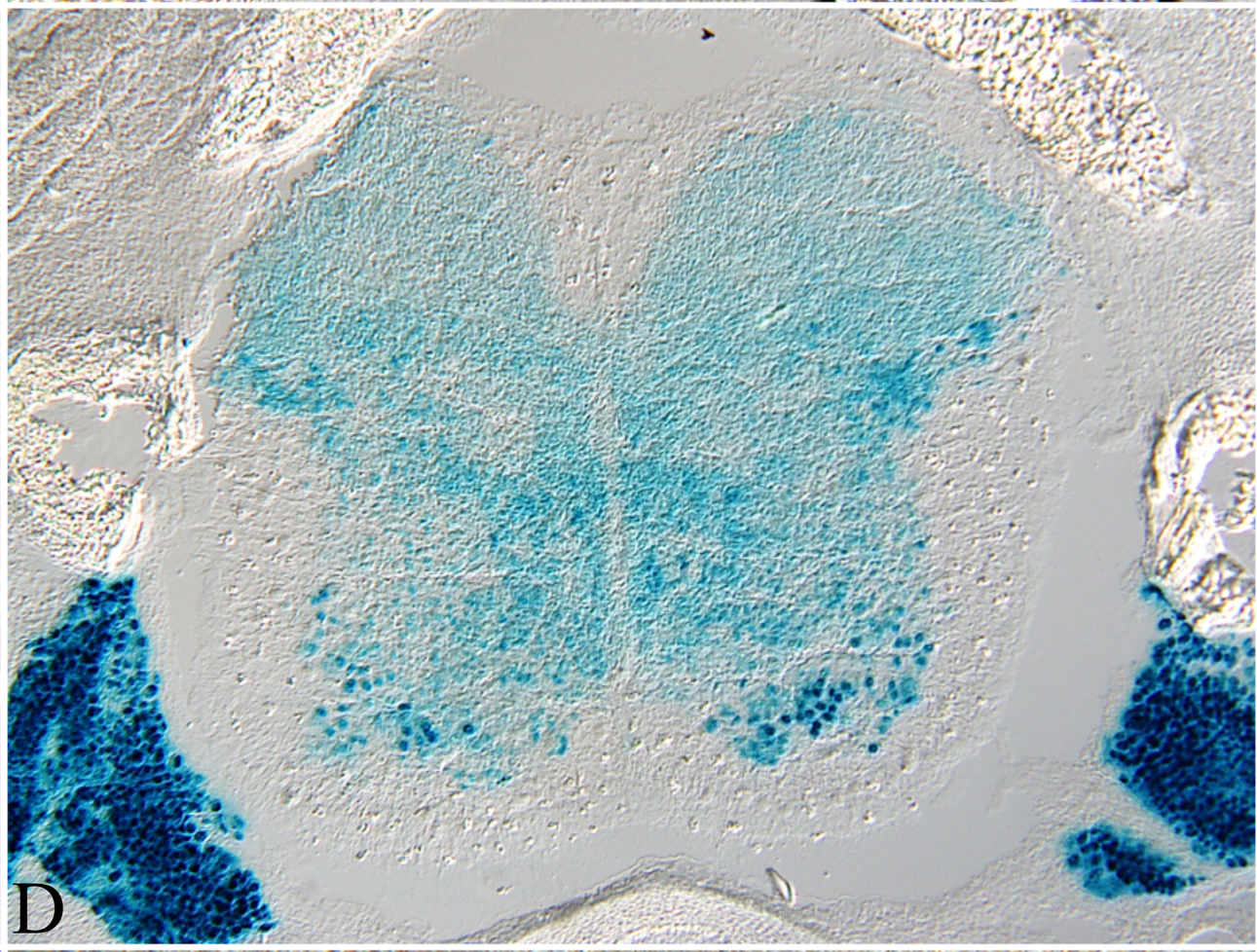
D

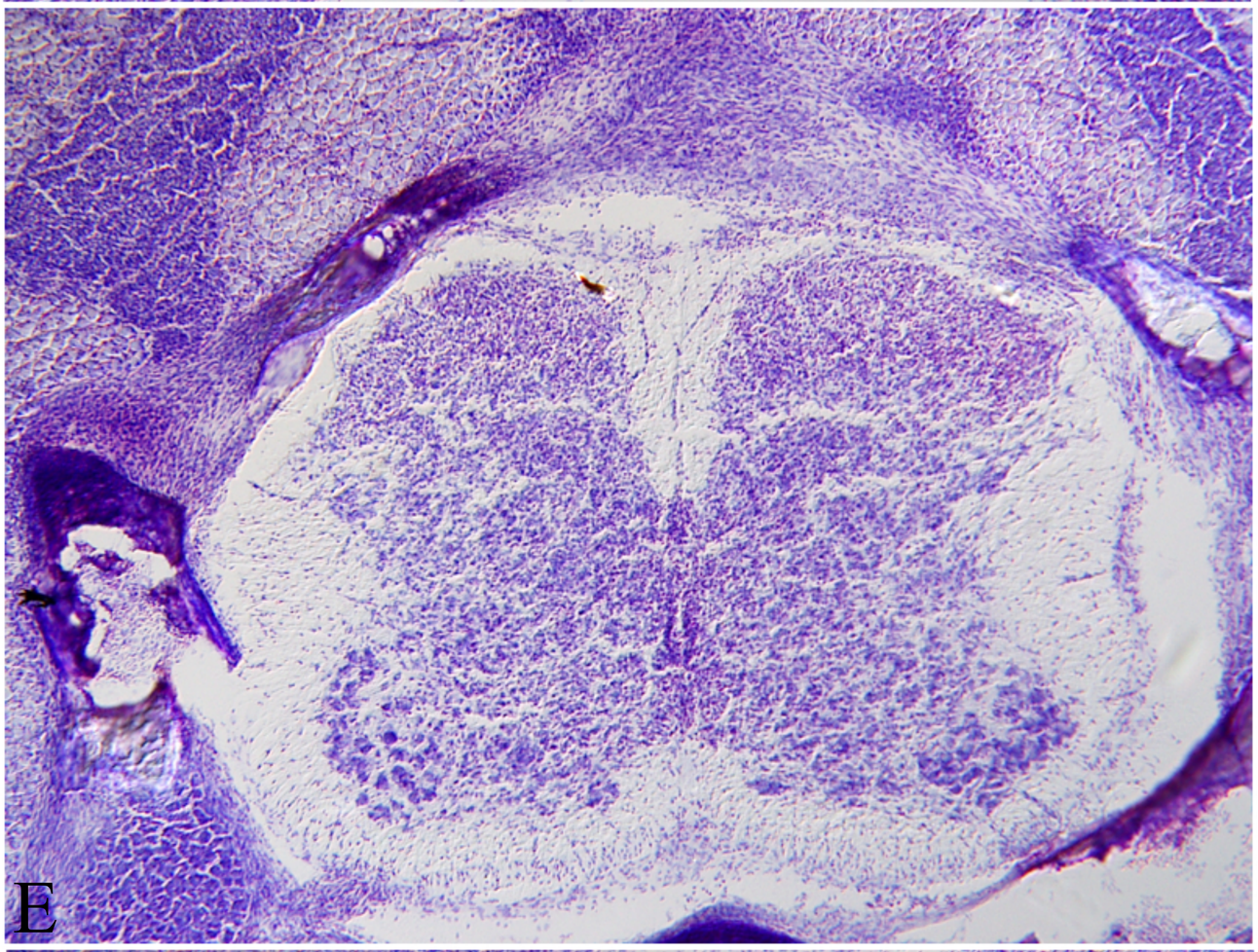
E

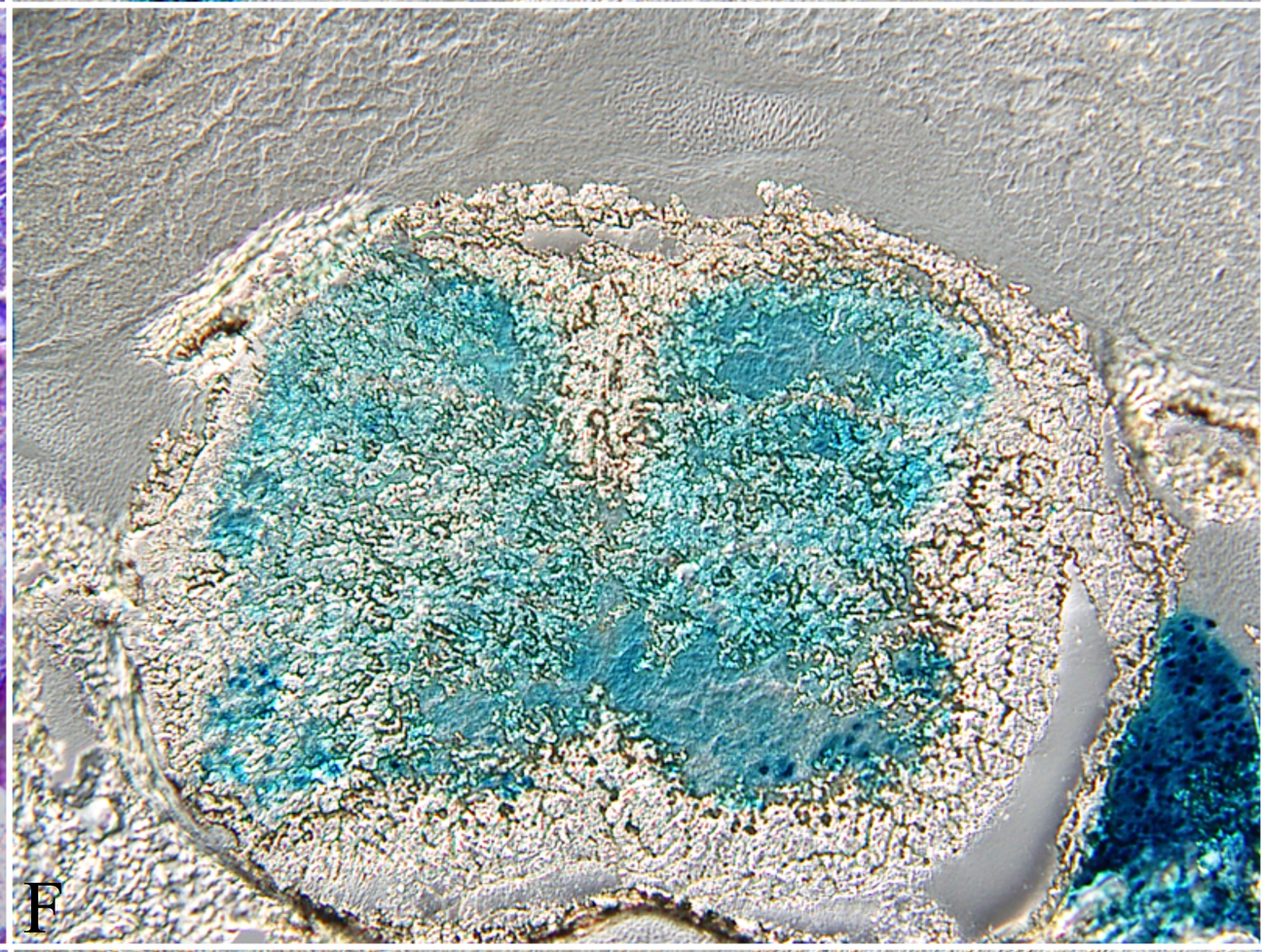
F

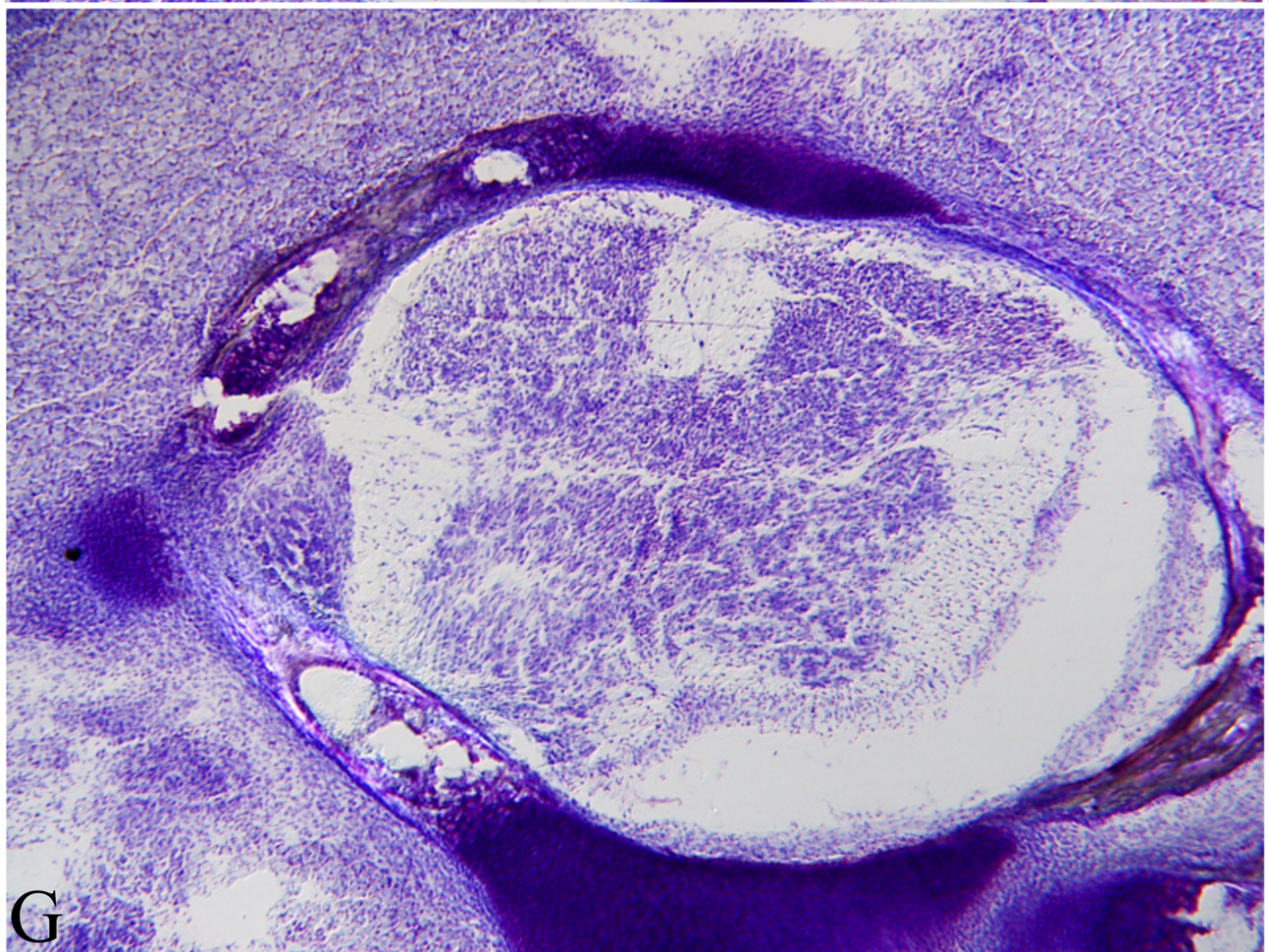
G

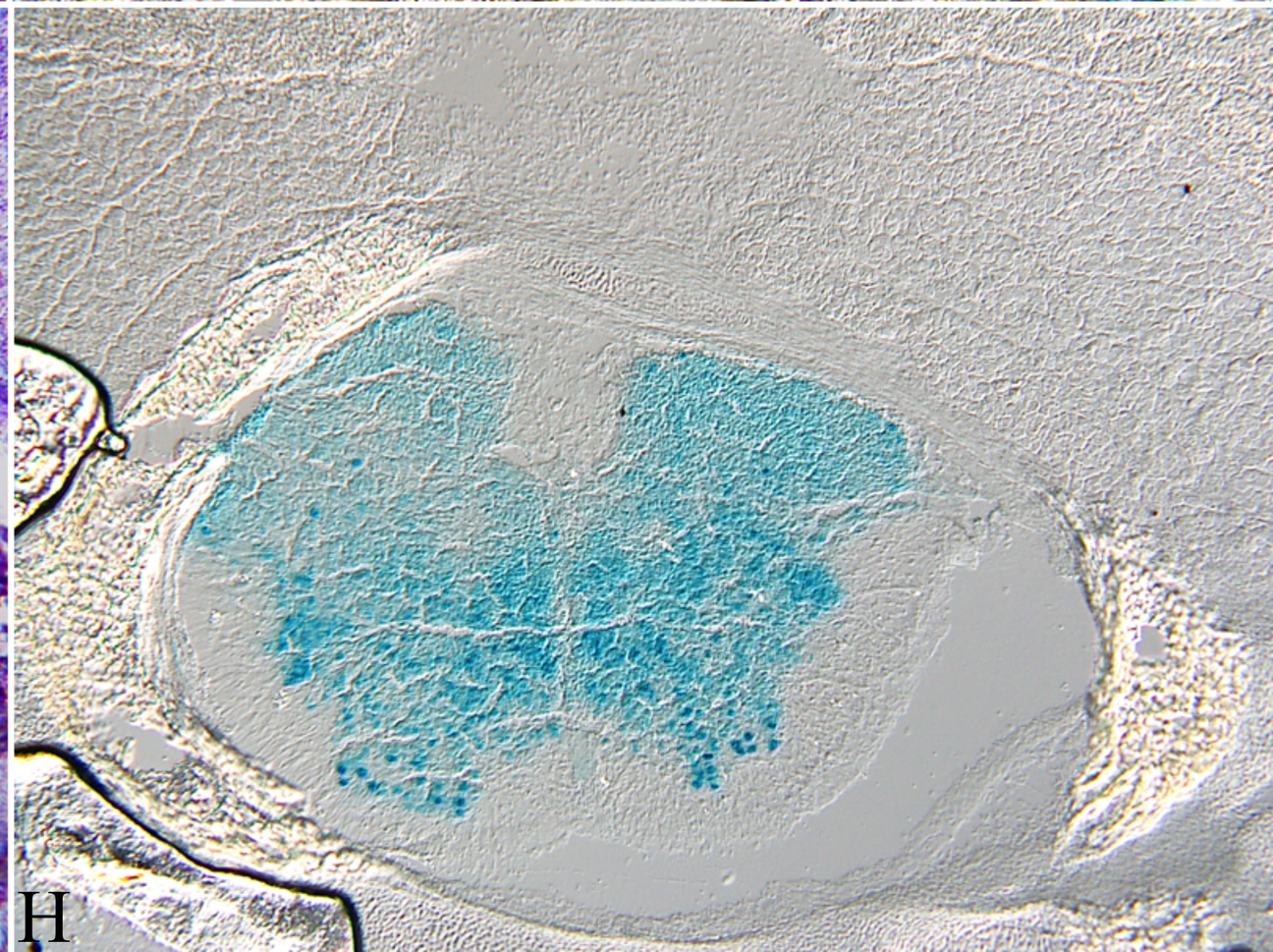
H

Figure 9: UCHL1 shows very high expression in the lumbar dorsal root ganglia. Nissl and X-gal stained twins are shown side by side.
A-D): Representative images showing strong nuclear staining in the cell bodies of lumbar dorsal root ganglia, with no staining seen in glia

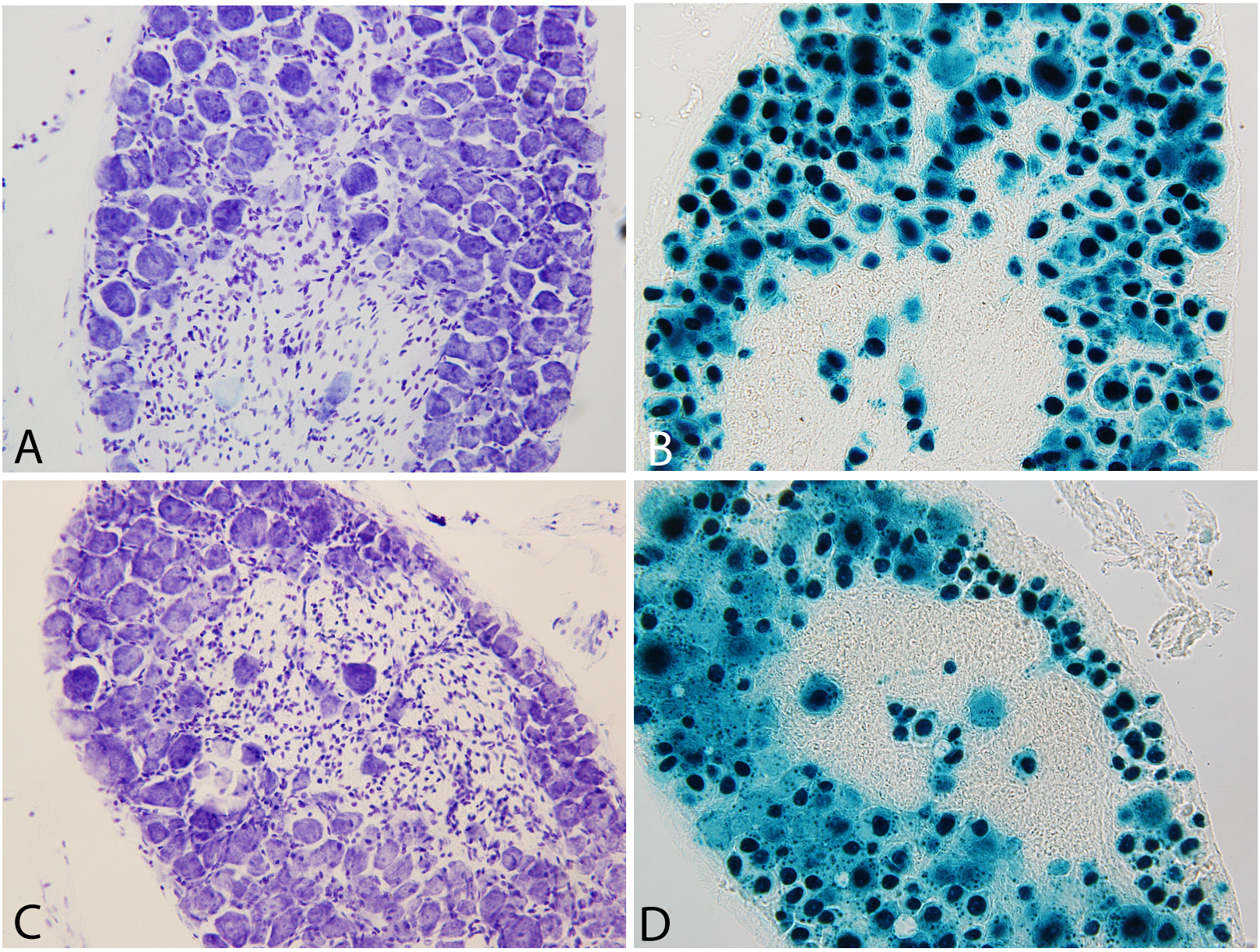
A
B
C
D

Figure 10: UCHL1 expression atlas.
Representative images of various brain levels, from olfactory bulb to caudal cerebellum are shown here. Expression was found to be particularly high in all levels of cortex, olfactory bulb, and hippocampus.

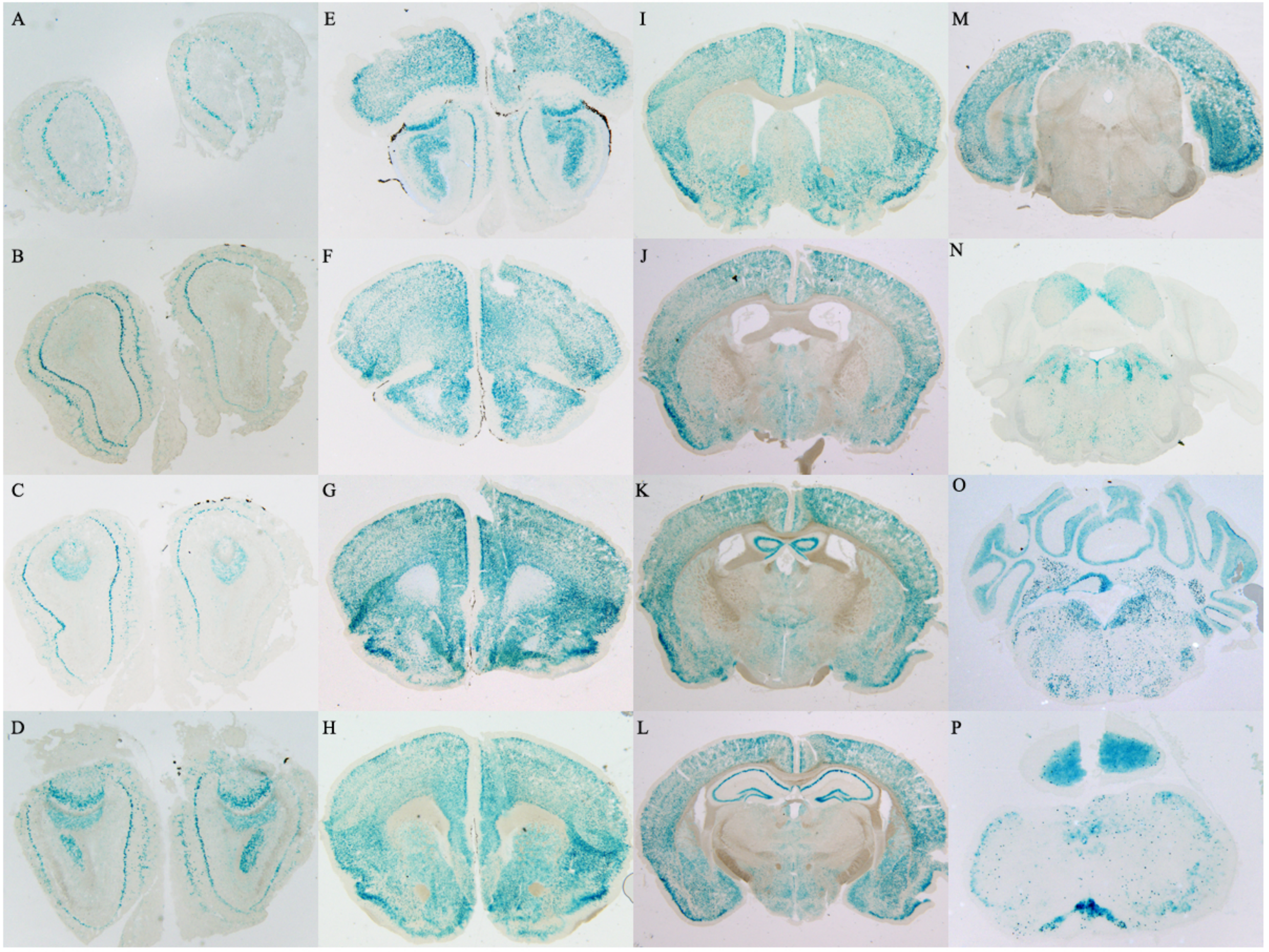
A
B
C
D
E
F
G
H
I
J
K
L
M
N
O
P

Figure 11: UCHL1 expression in the hippocampus and dentate gyrus.
A-C): UCHL1 expression in CA1, CA2, and CA3
D): UCHL1 is strongly expressed at the hippocampal formation.
E): UCHL1 is expressed in all cell types at the CA1-CA2 transition.
F): UCHL1 expression at the pyramidal cell layer.

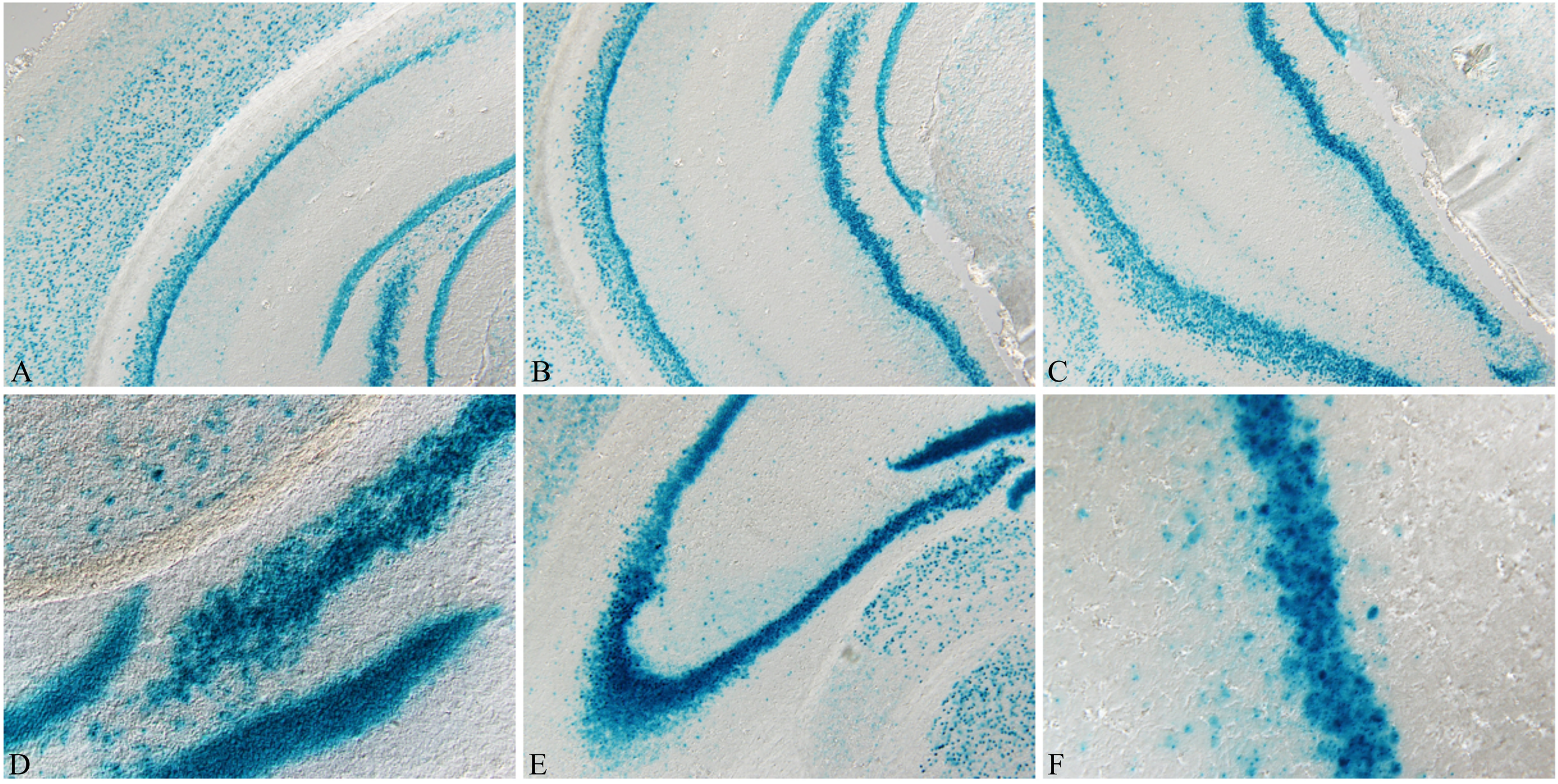
A
B
C
D
E
F

Figure 12: UCHL1 expression at all levels of hippocampus. Nissl and X-gal twin slides are shown side by side.

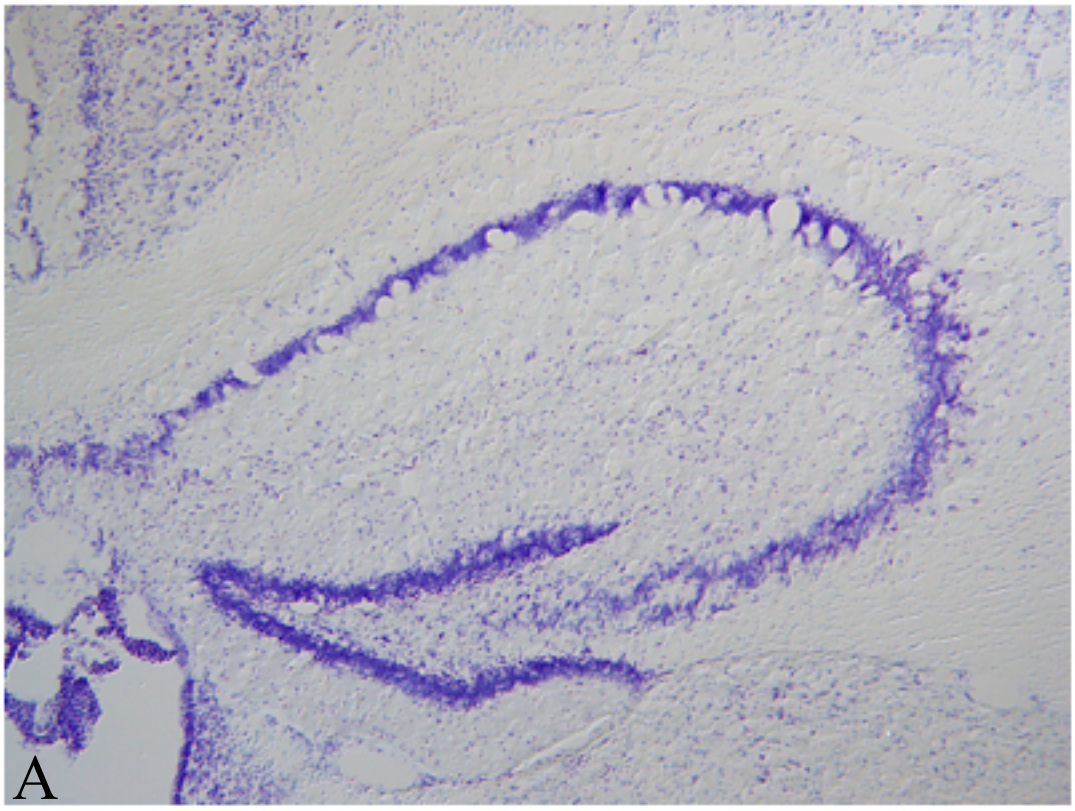
A

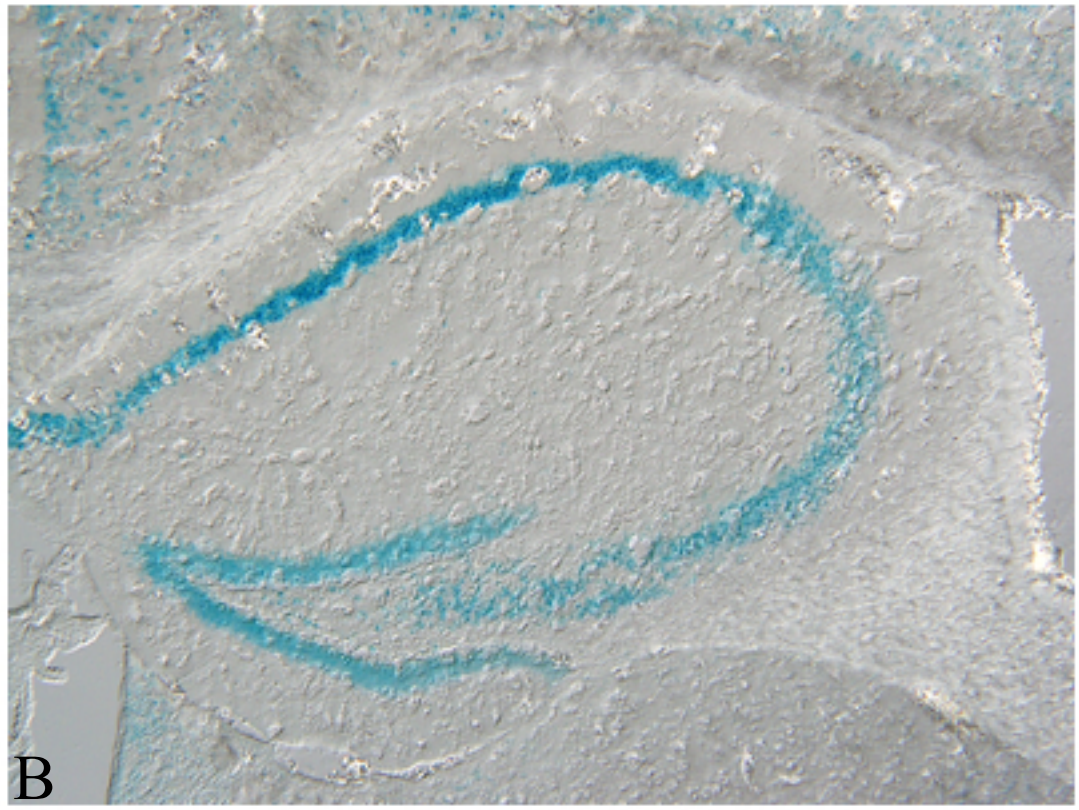
B

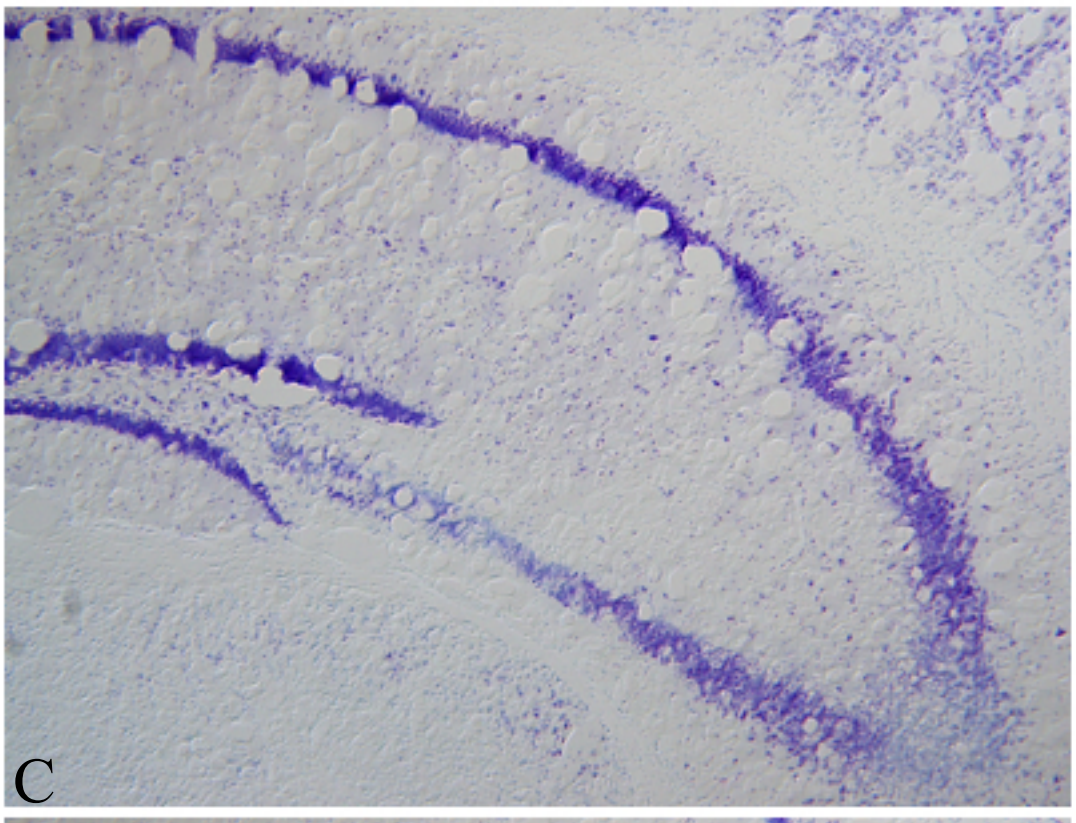
C

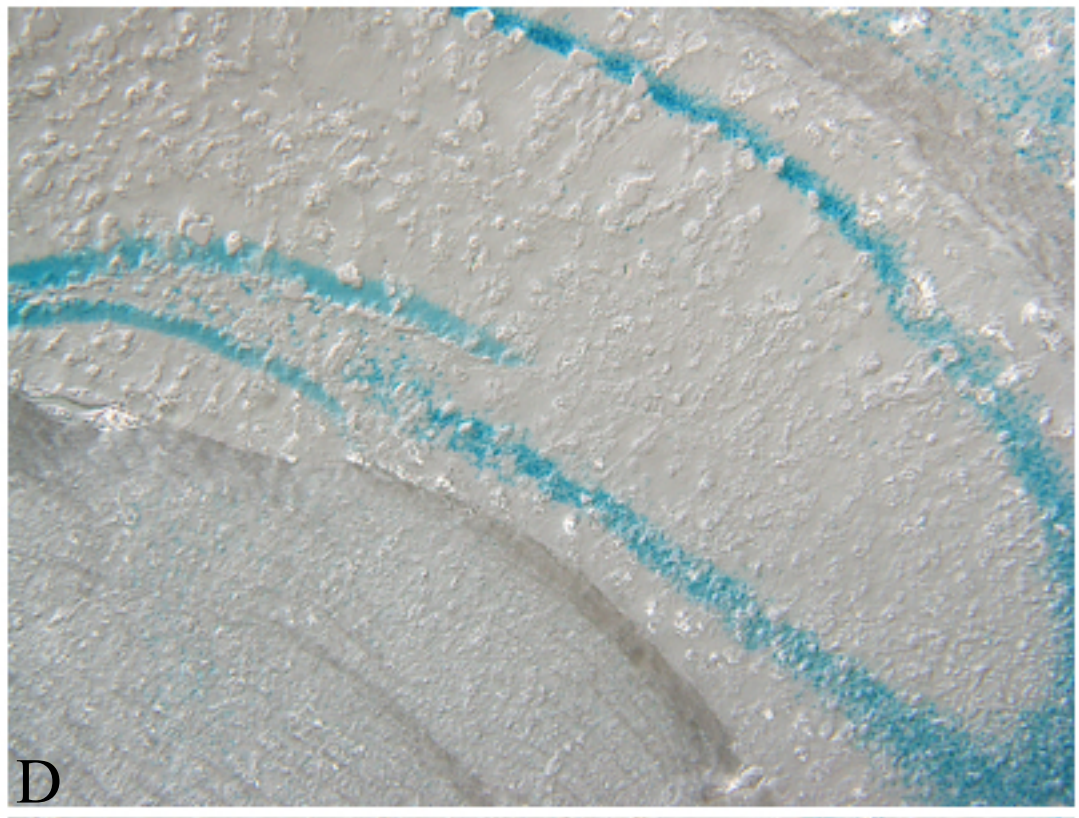
D

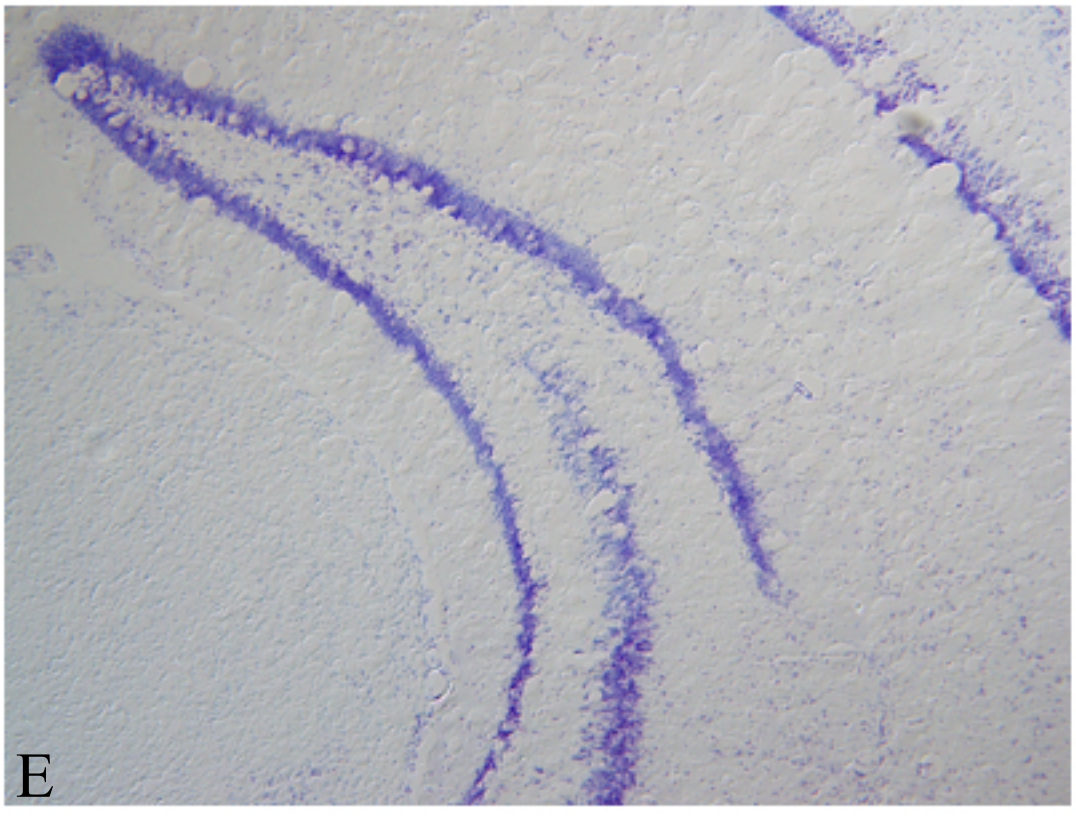
E

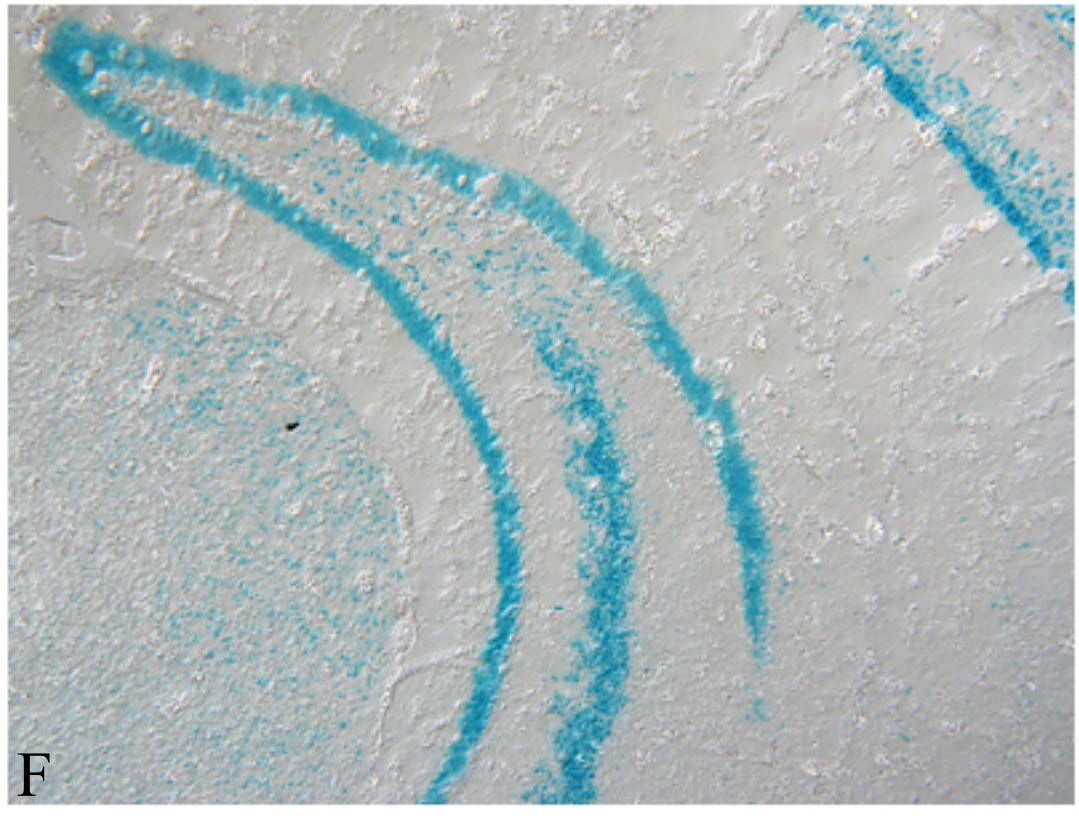
F

Figure 13: Representative images of full, partial, and vacant endplates. Muscle is double-stained with bungarotoxin (bgt,for endplates) and syntaxin (synt,for nerve), with bungarotoxin labeling on the left, and syntaxin labeling on the right.
A,B): A full endplate. Bgt and synt staining colocalize nicely.
C,D): A partial endplate. Synt staining does not completely cover the area stained with bgt.
E,F): A vacant endplate. Only dying nerve is left to react with the syntaxin antibody. Syntaxin staining on the endplate is almost completely gone.

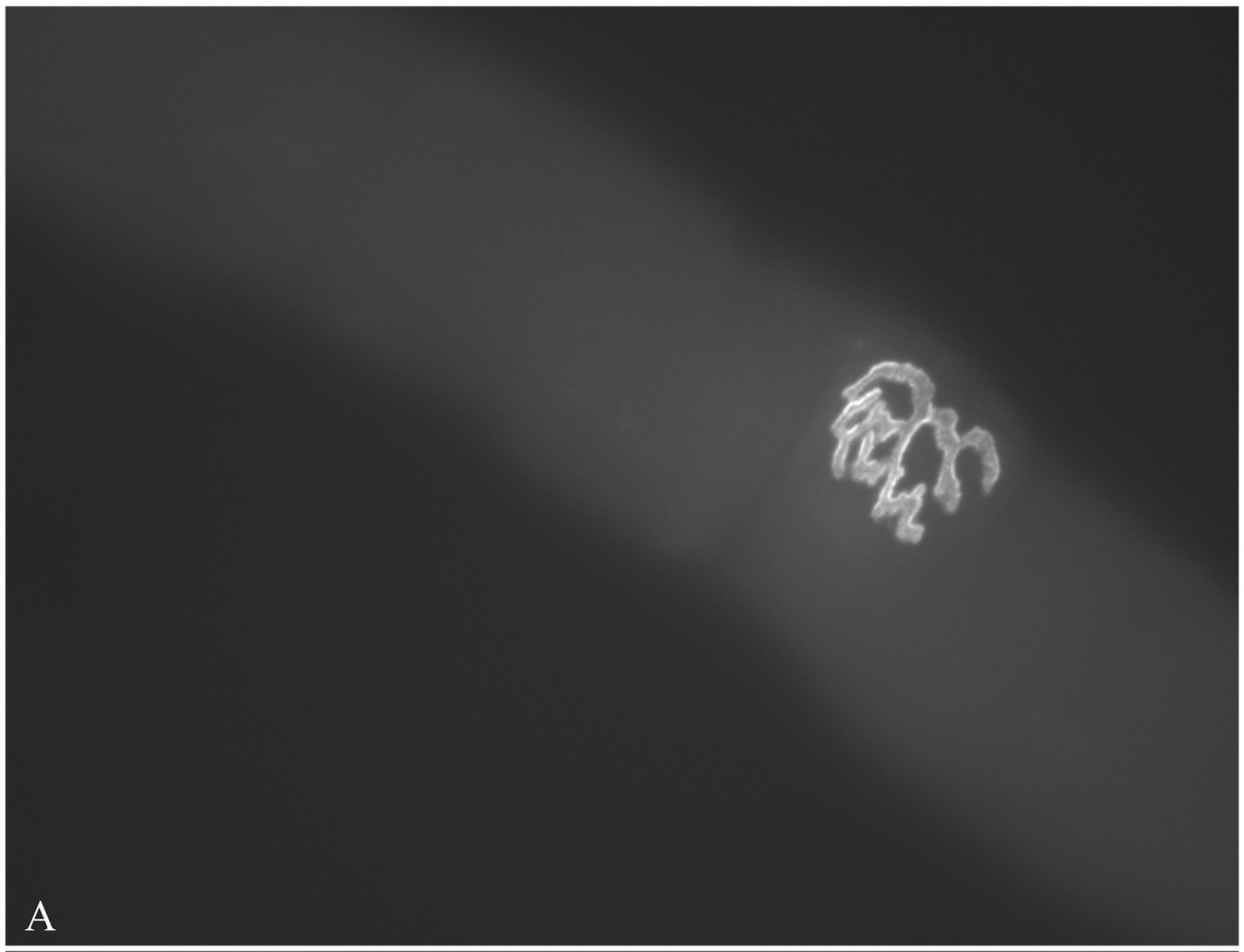
A

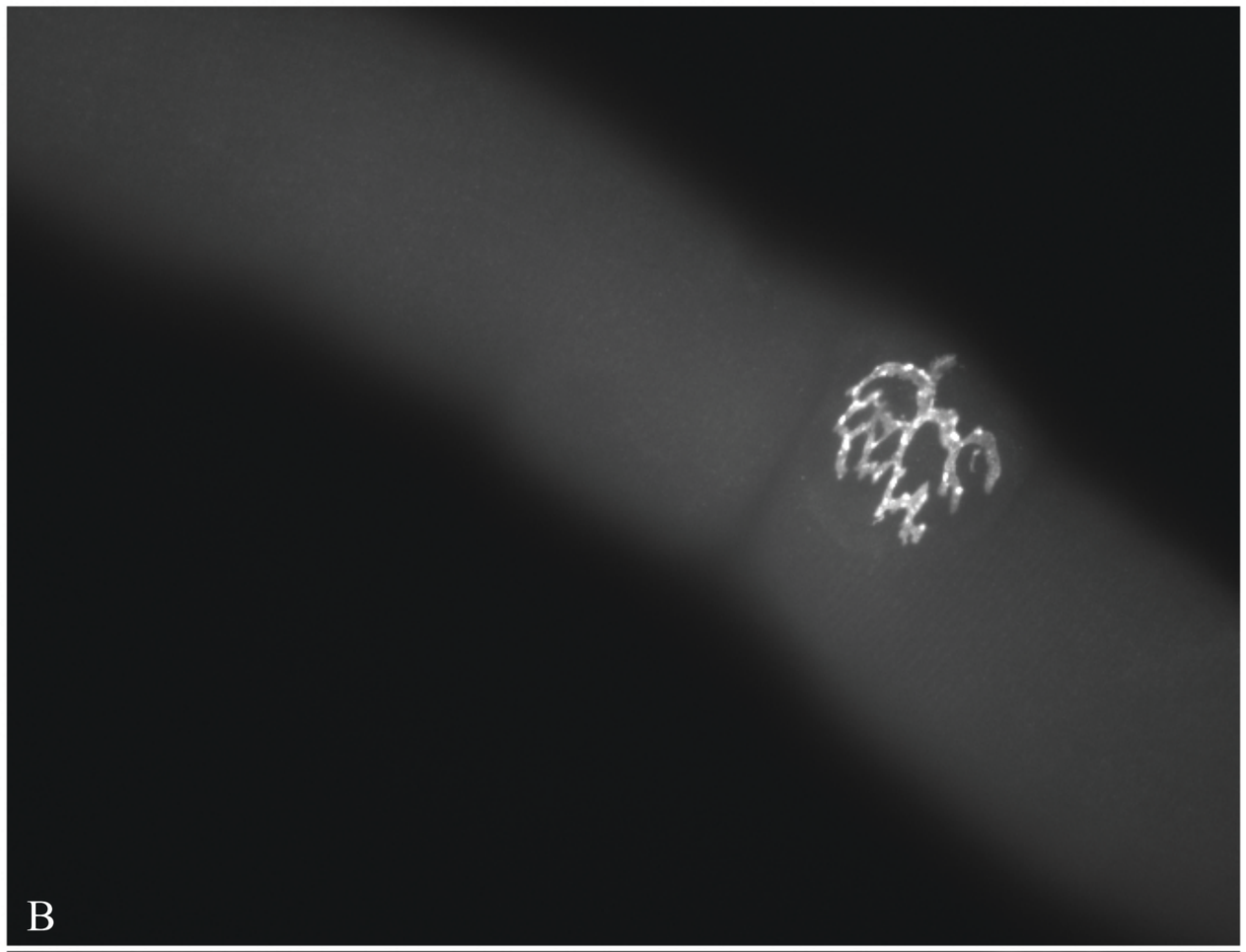
B

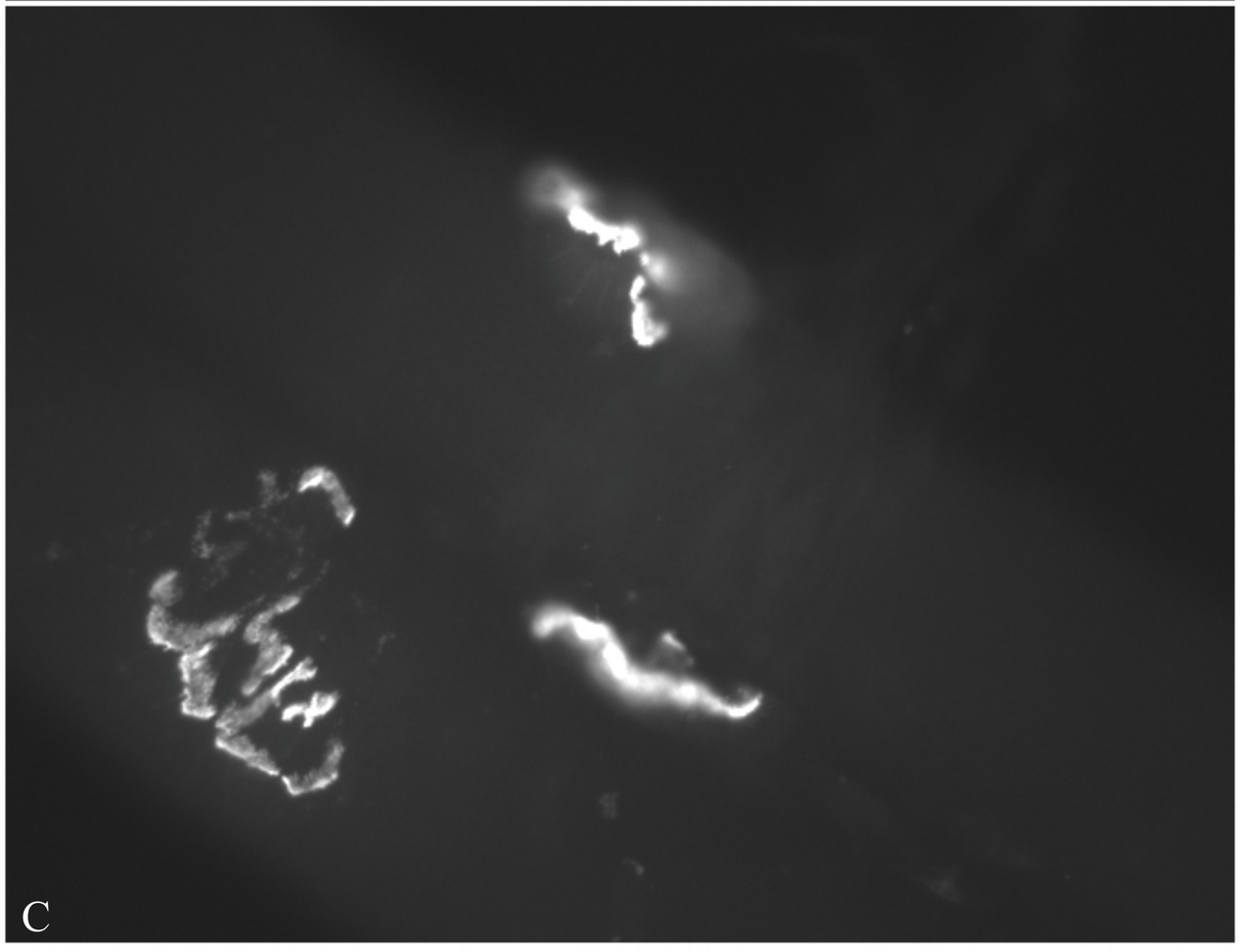
C

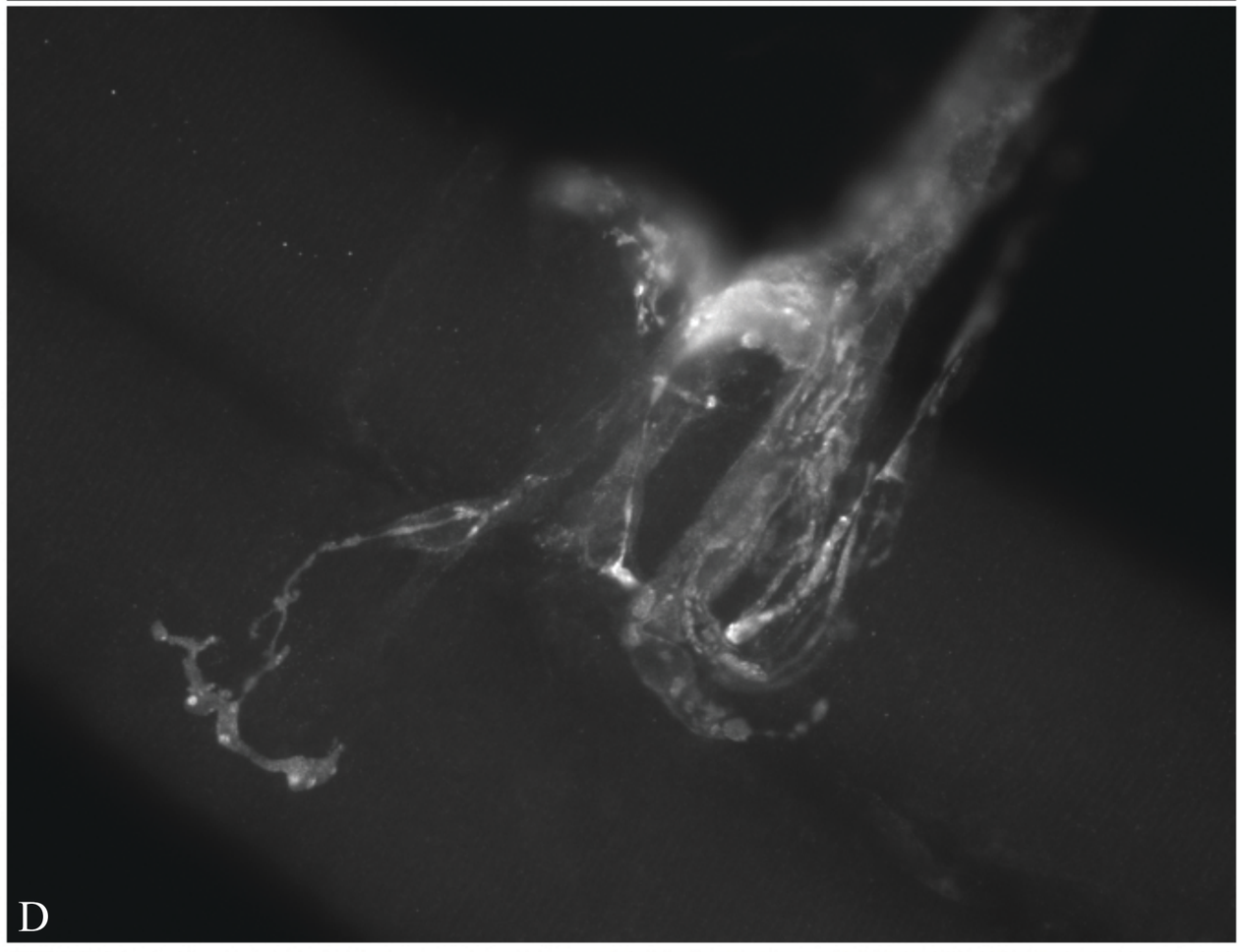
D

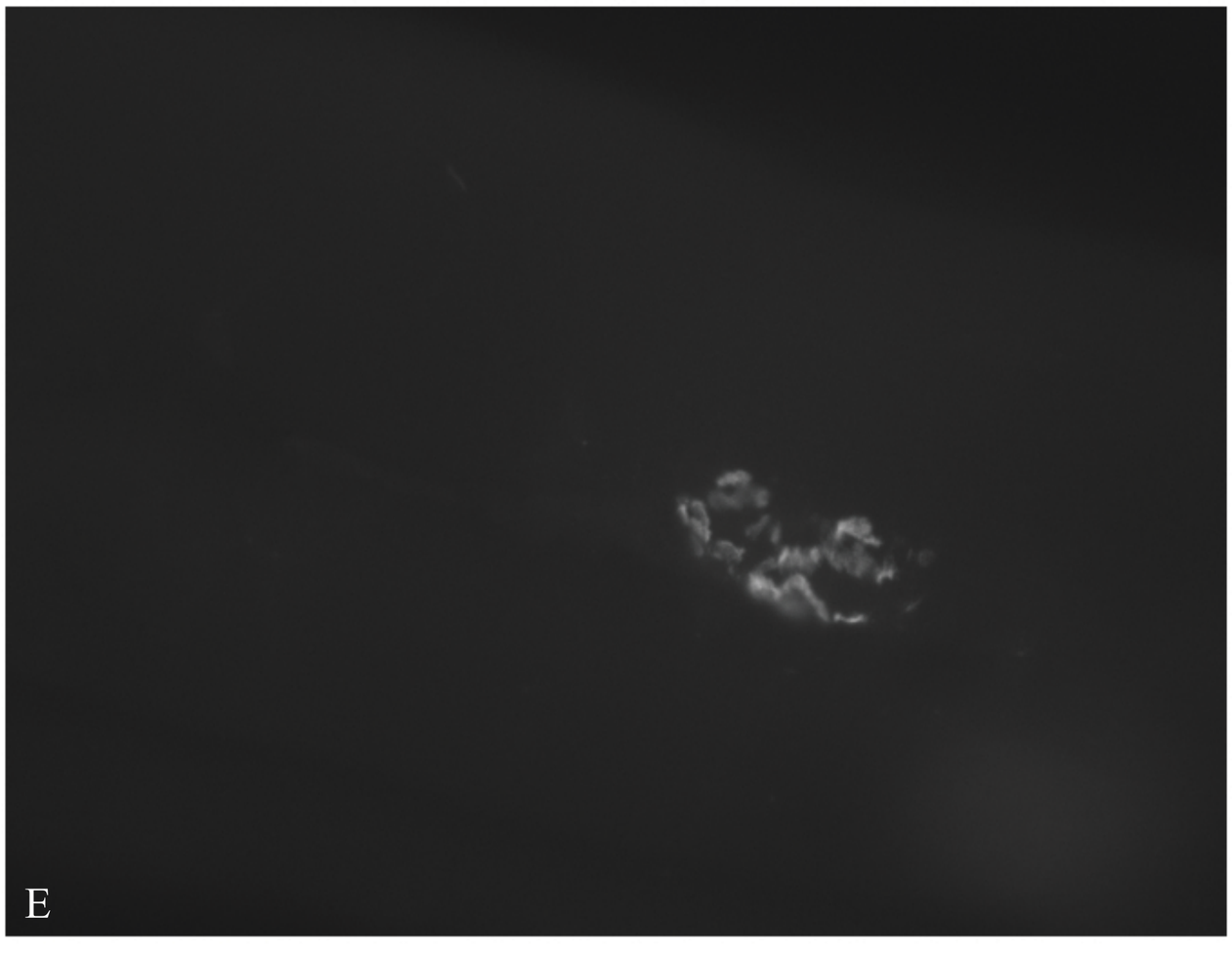
E

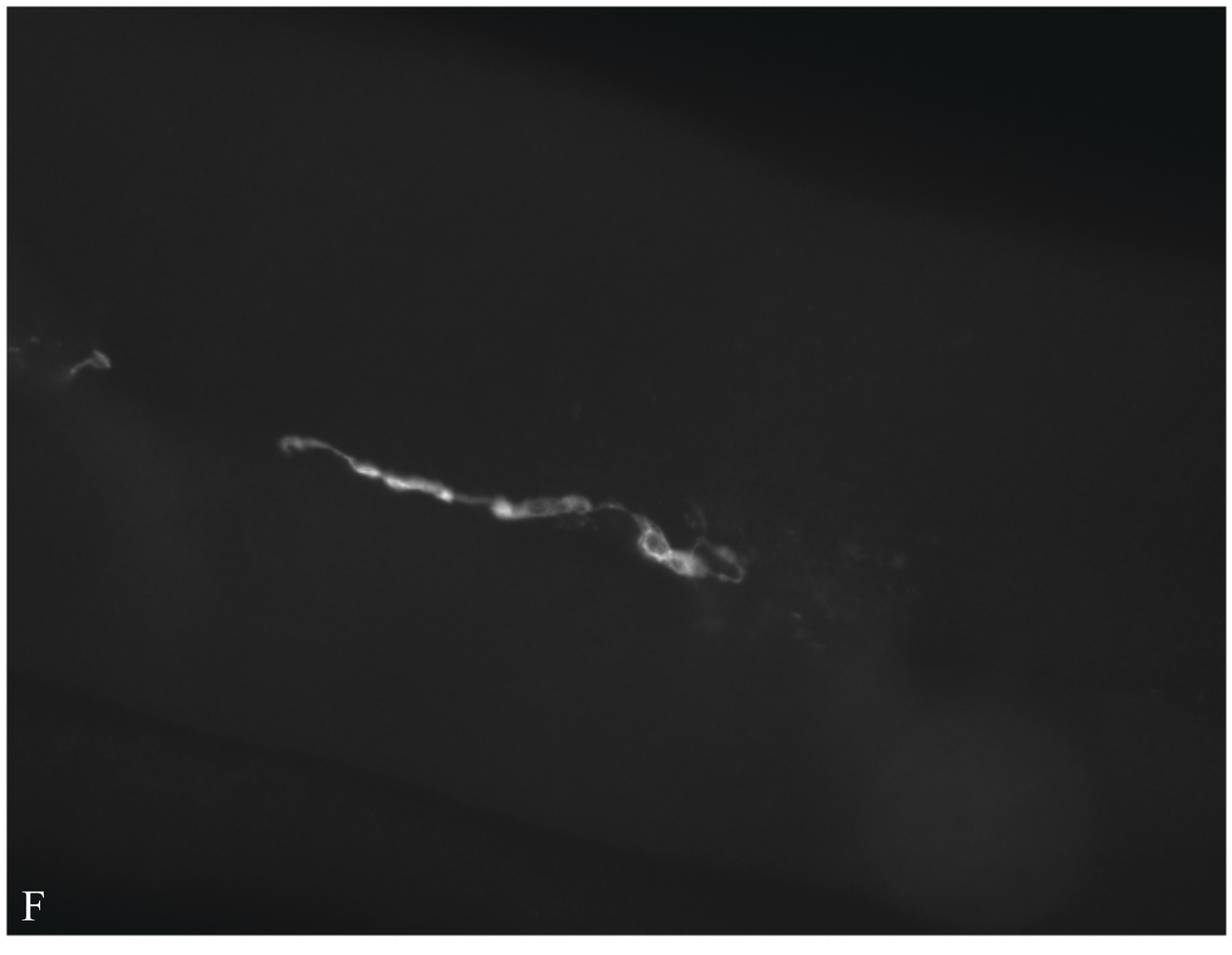
F

Figure 14: Representative images of endplates in the 43-48 day old age group. Bgt on the left, Synt on the right.
A,B): Full endplates photographed from a UCHL1+/+ mouse.
C,D): Partial endplate photographed from a 48-day-old mutant. Full endplates can be seen alongside the partial endplate (arrow).

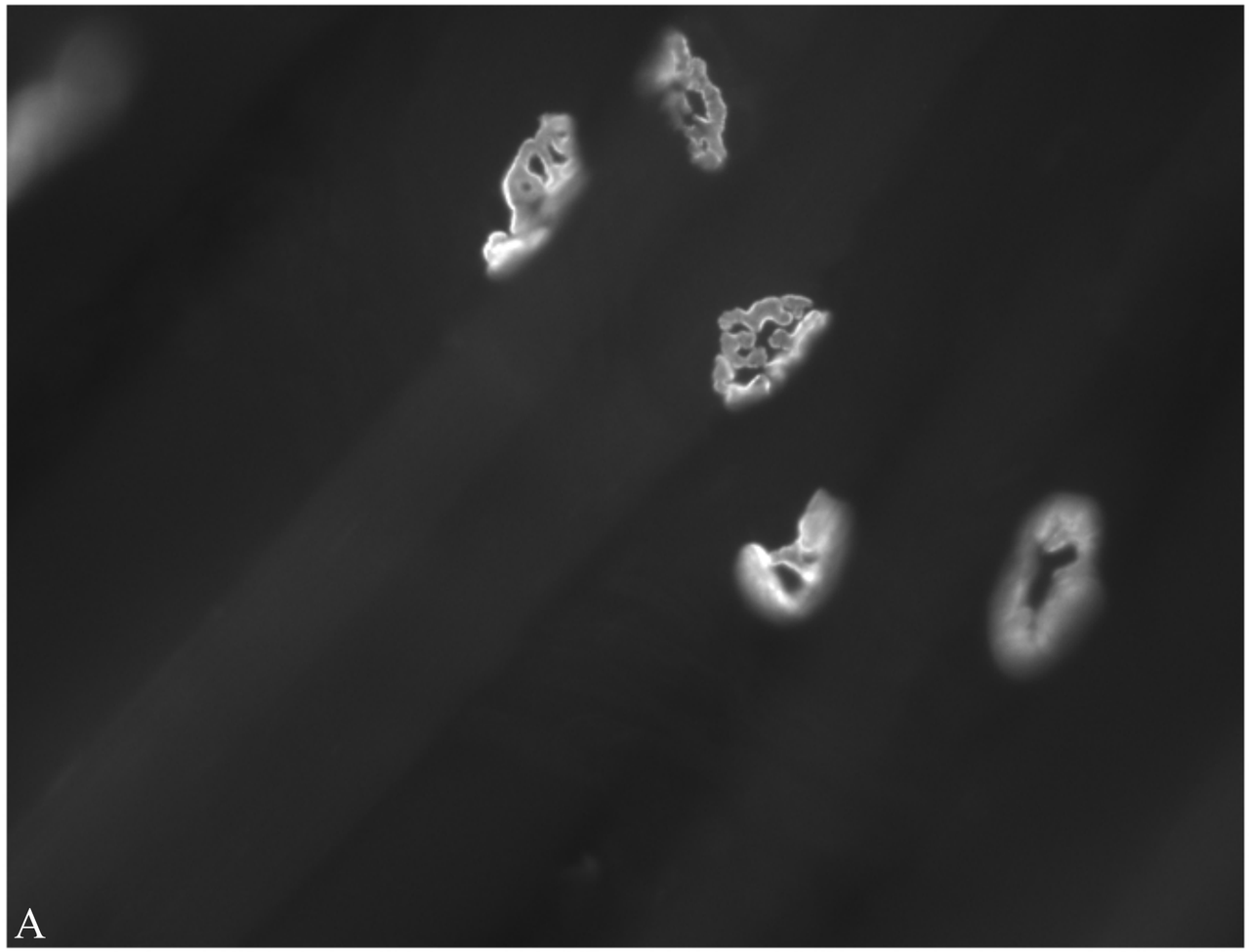
A

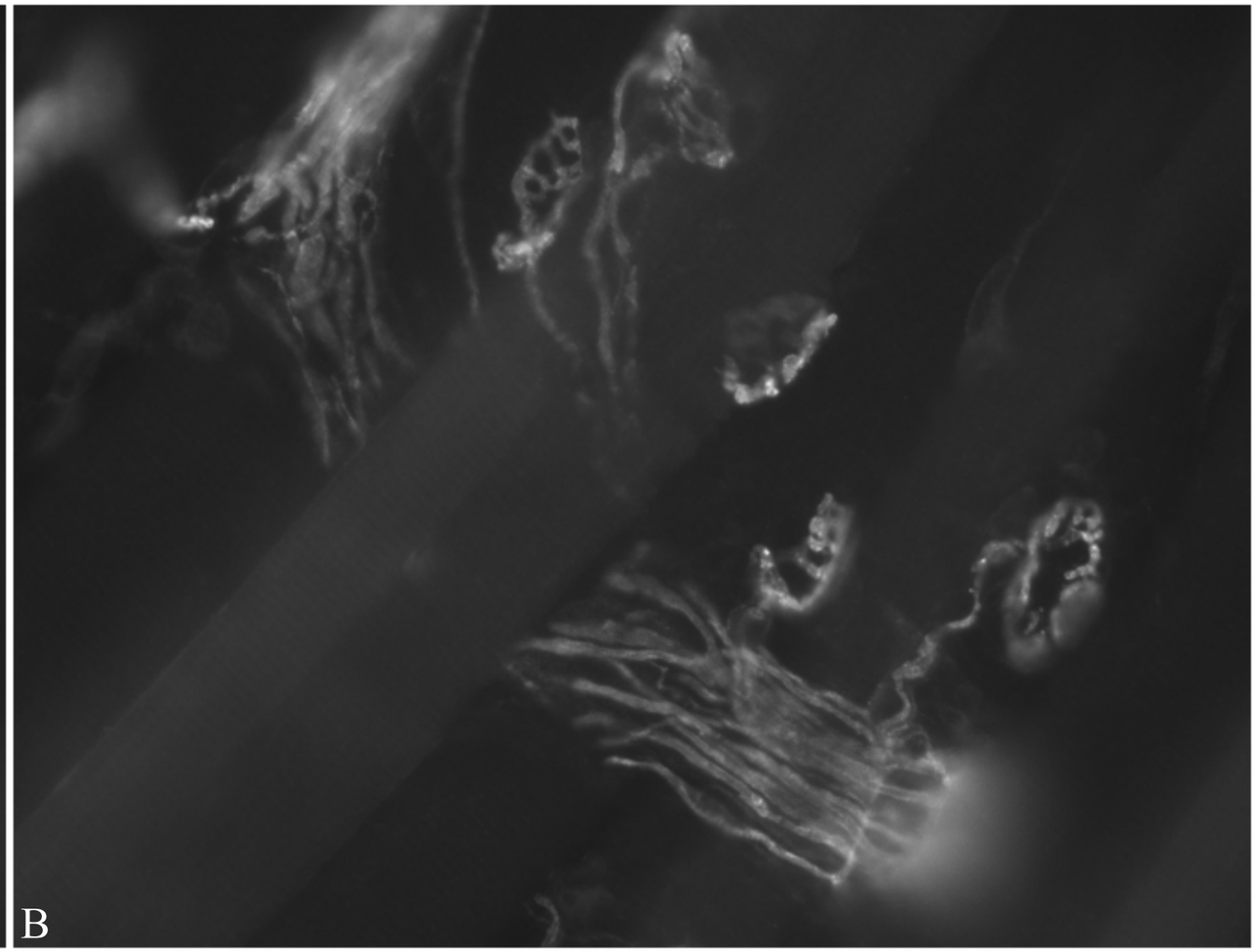
B

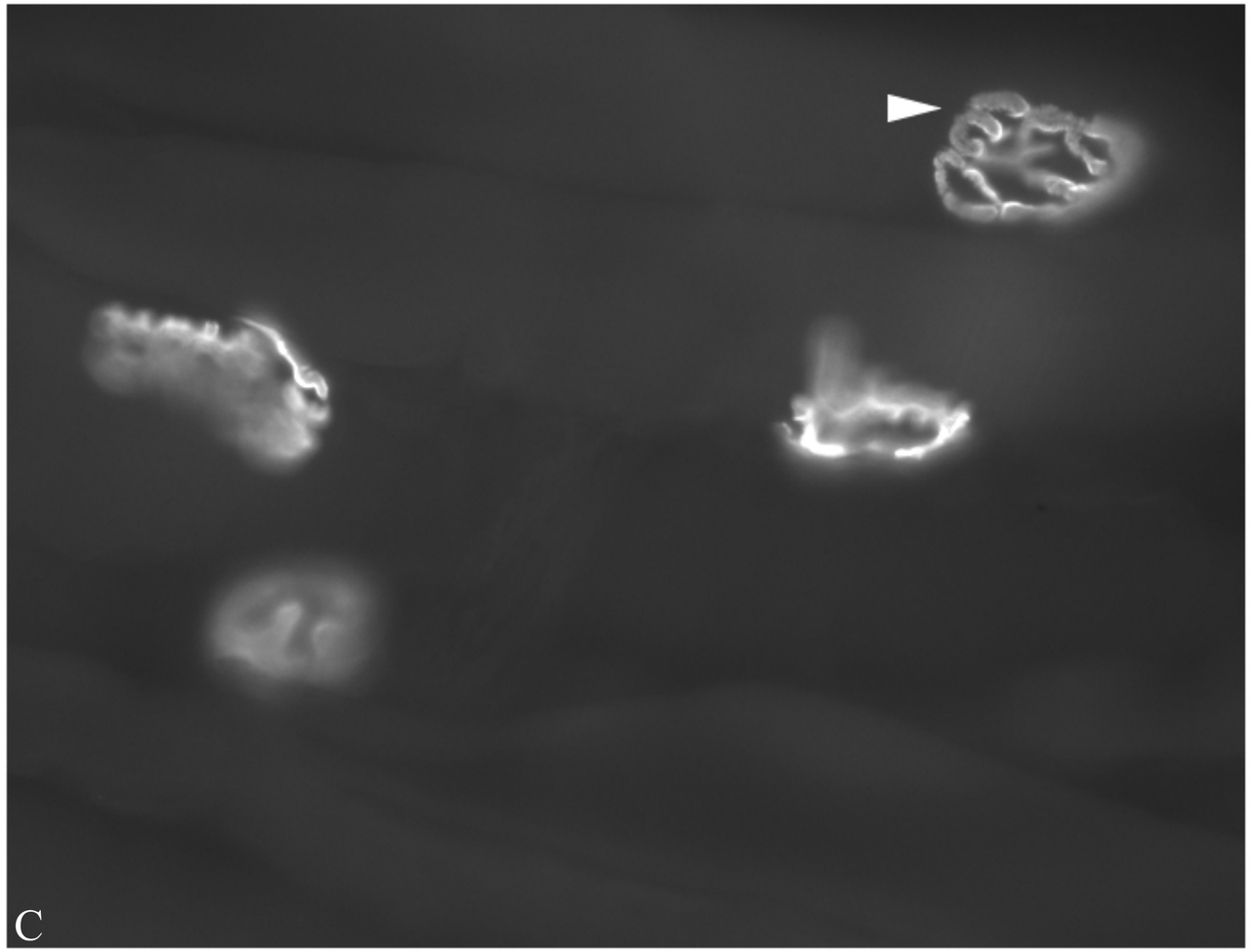
C

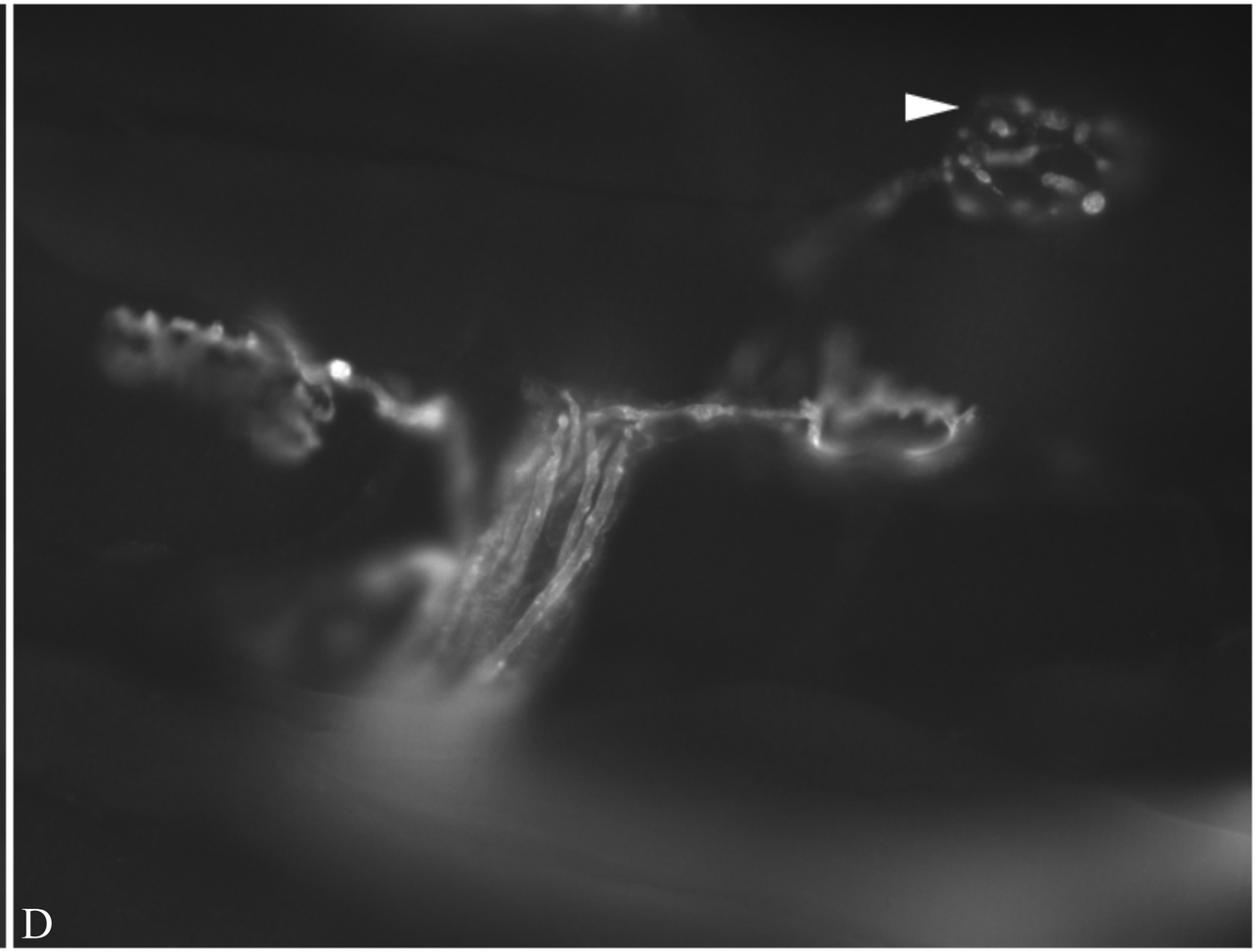
D

Figure 15: Representative images of endplates in the 63-67 day old age group. Bgt on the left, Synt on the right.
A,B): Full endplates from a UCHL1+/- mouse showing healthy colocalization.
C,D): Partial endplates from a UCHL1-/- mouse, in which the nerve is dying back. A spheroid aggregate is also visible.
E,F) Vacant endplates from a UCHL1-/- mouse.

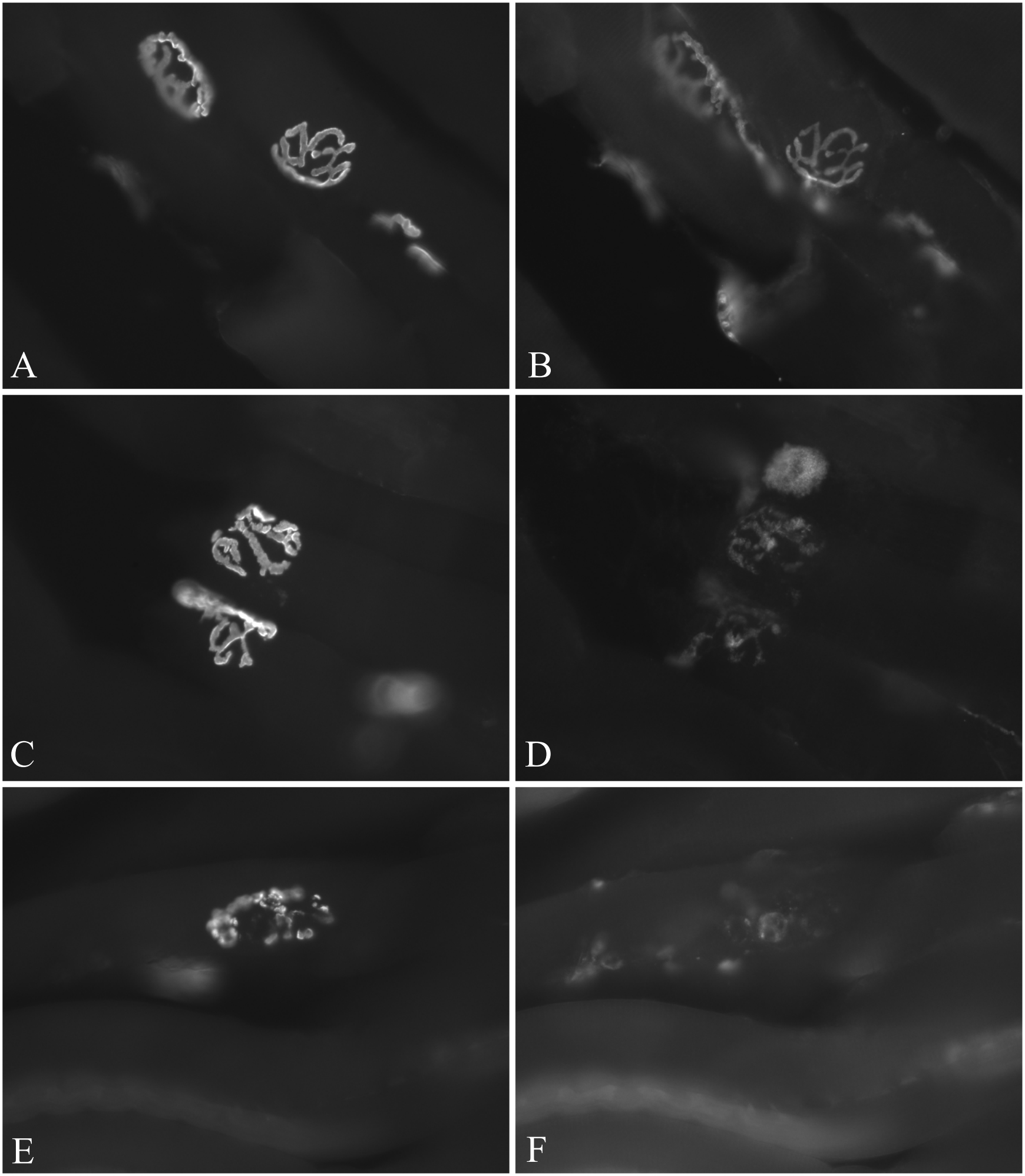
A
B
C
D
E
F

Figure 16: Representative images of endplates from the 92-99 day old age group. Bgt on the left, Synt on the right.
A,B). UCHL1+/+ endplates show healthy colocalization.
C,D): UCHL1-/- endplates. Full, partial, and vacant endplates are all visible here. Also visible are the numerous regenerating axon sprouts "overshooting" the endplate, and degenerating at their ends to produce bright spheroid aggregates.
E,F): UCHL1-/- endplates, 1 full, and 2 vacants.

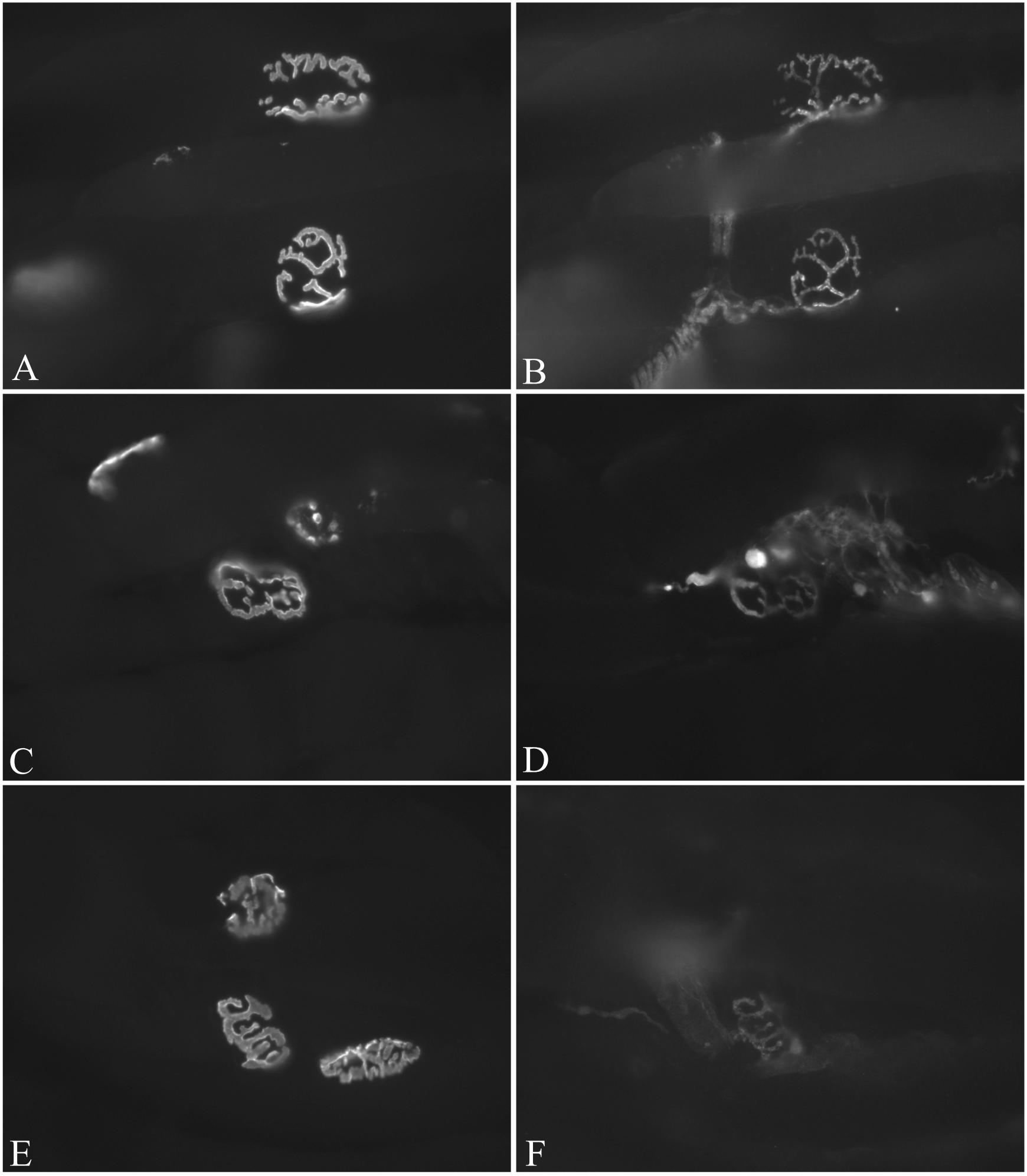
A
B
C
D
E
F

Figure 17: Representative photos of endplates of the oldest cohort.
A,B): UCHL1+/+ endplates showing perfectly healthy colocalization.
C,D): UCHL1-/- endplates showing partial innervation.
E,F). UCHL1-/- endplates showing total vacancy. Most mutant endplates in this age group looked like this.

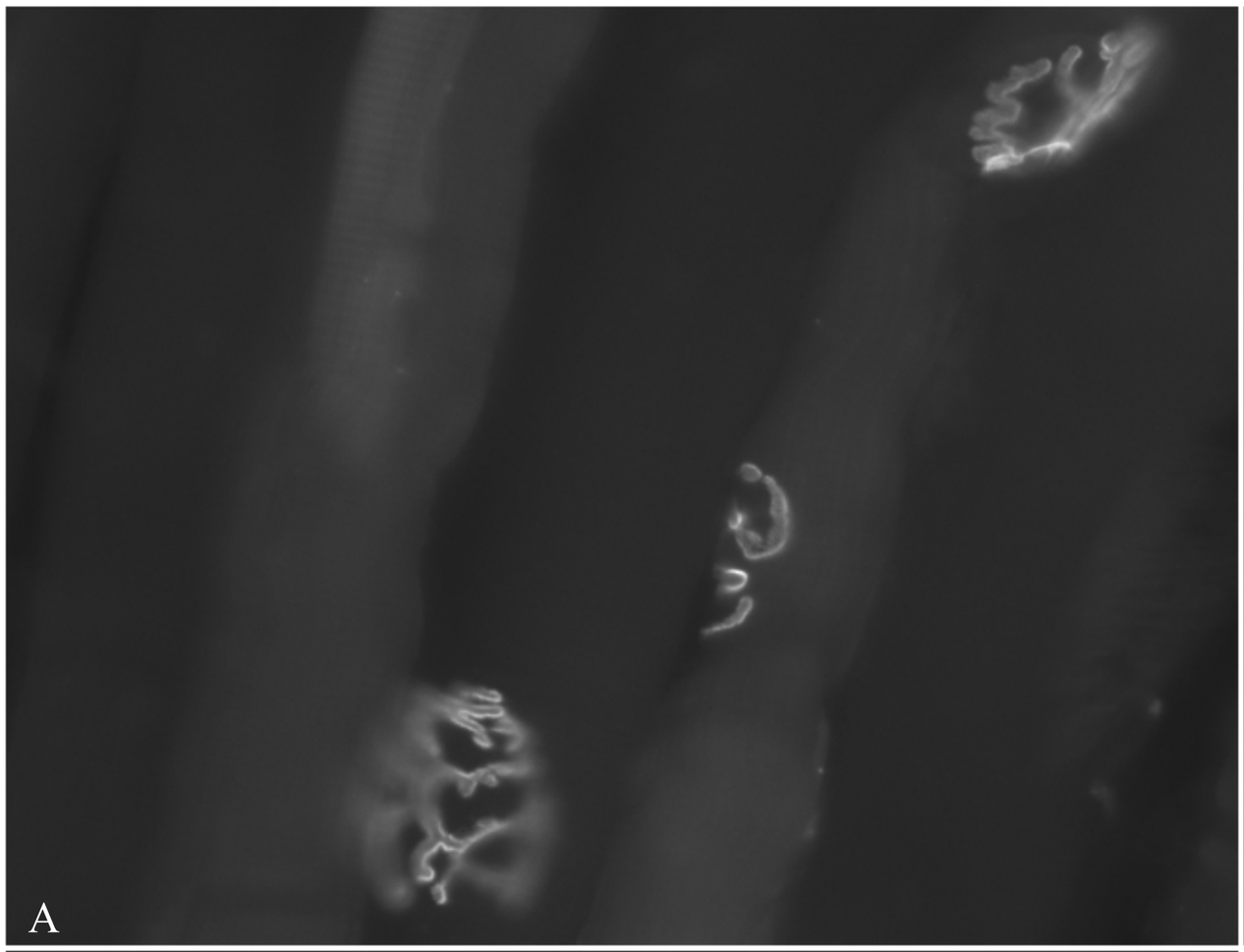
A

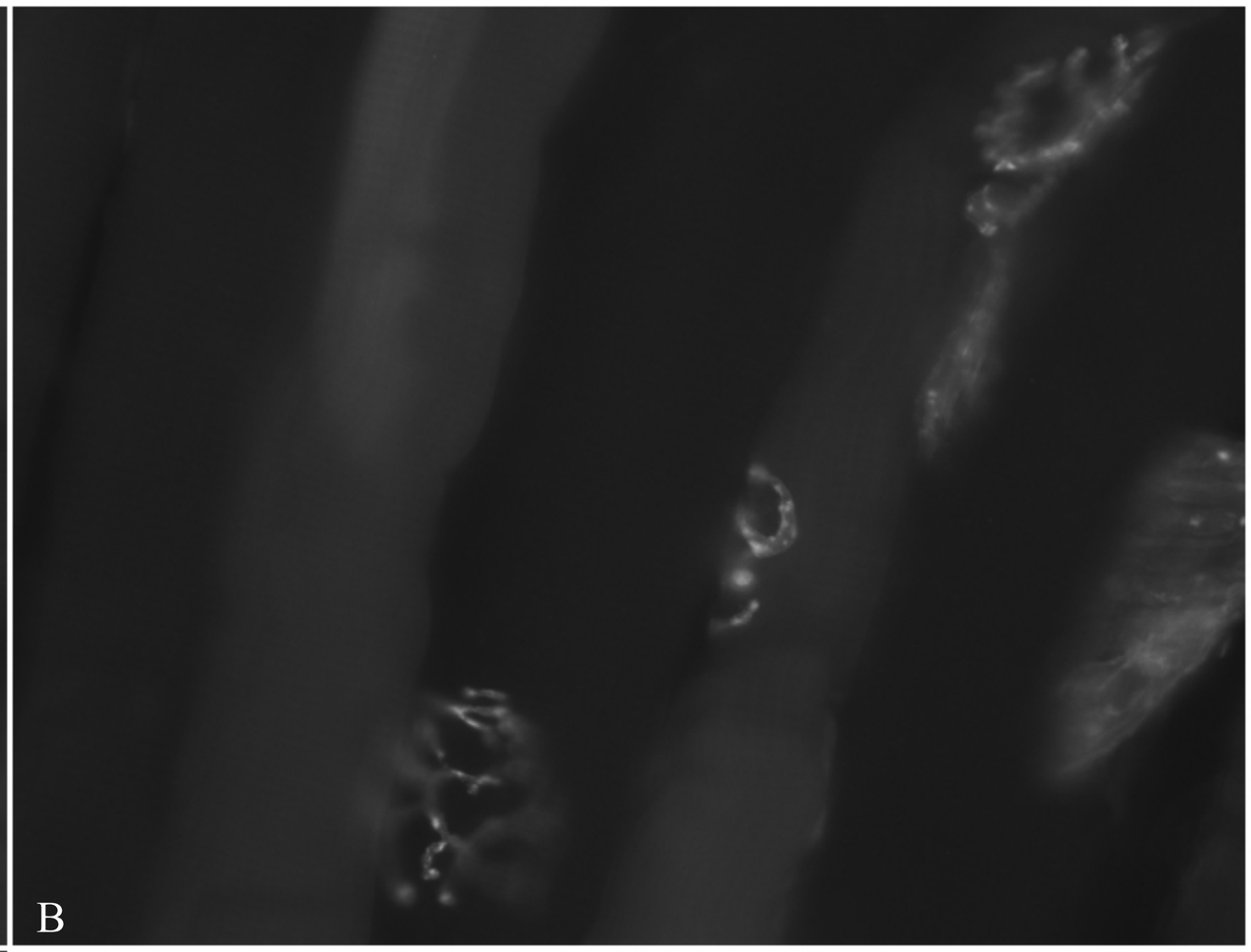
B

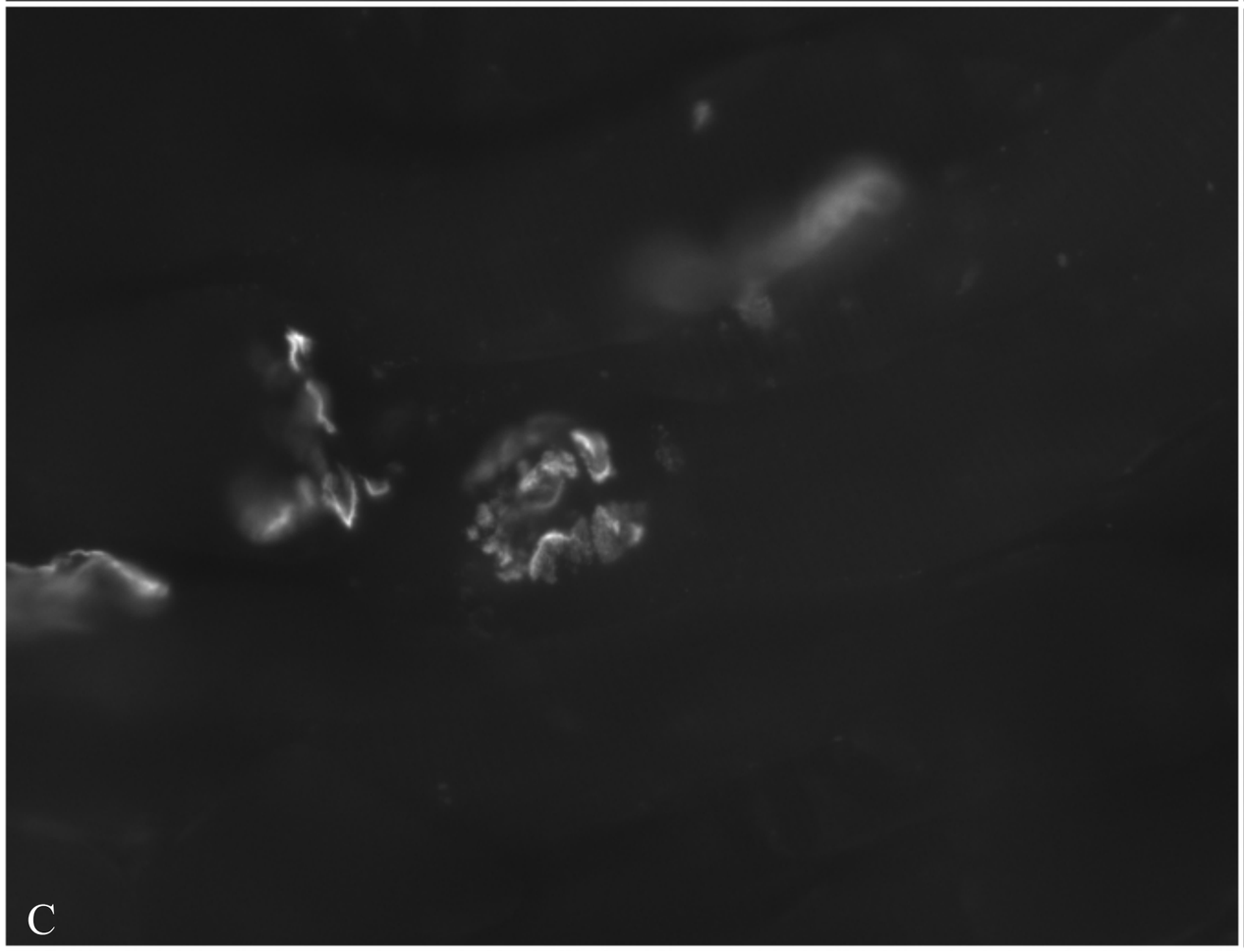
C

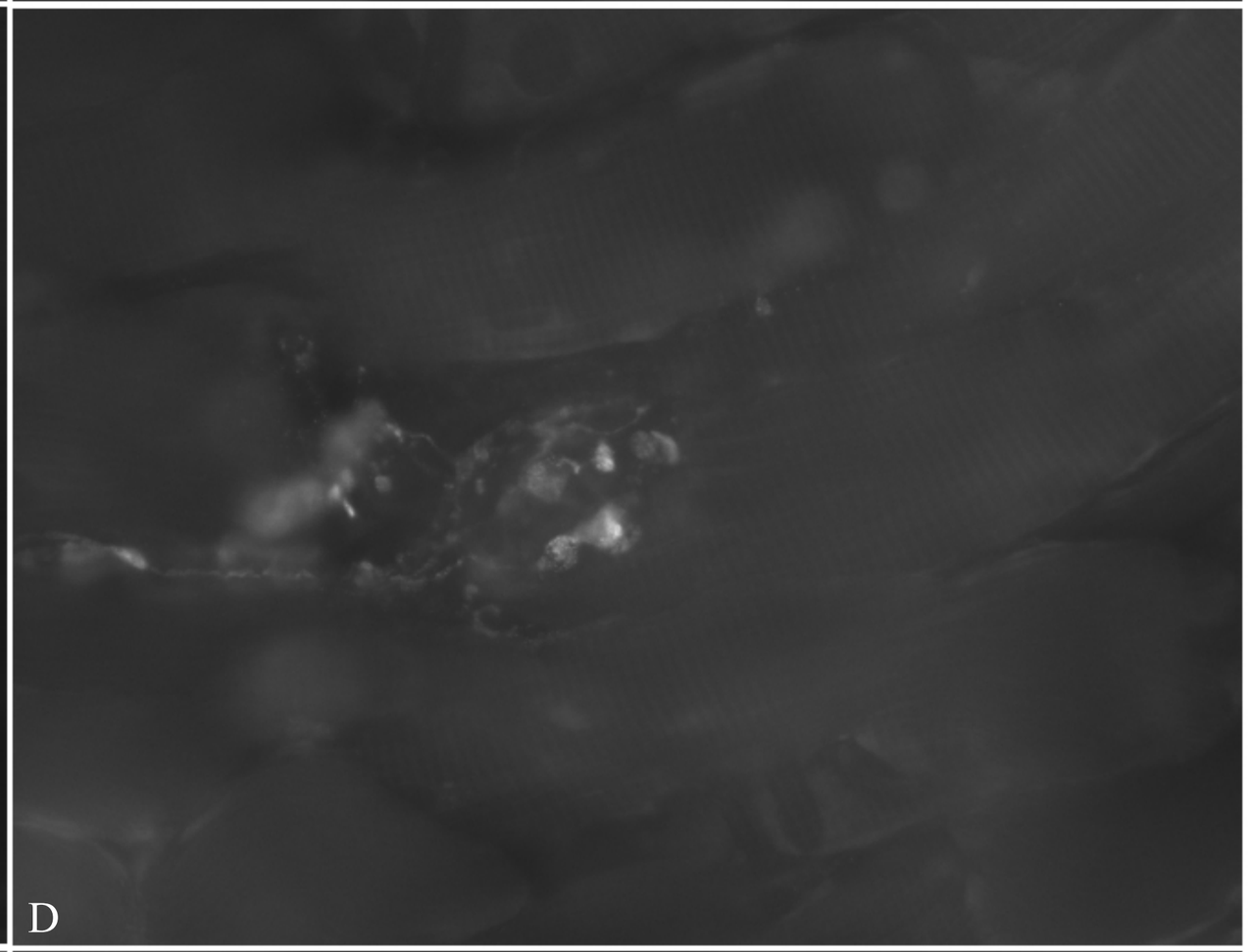
D

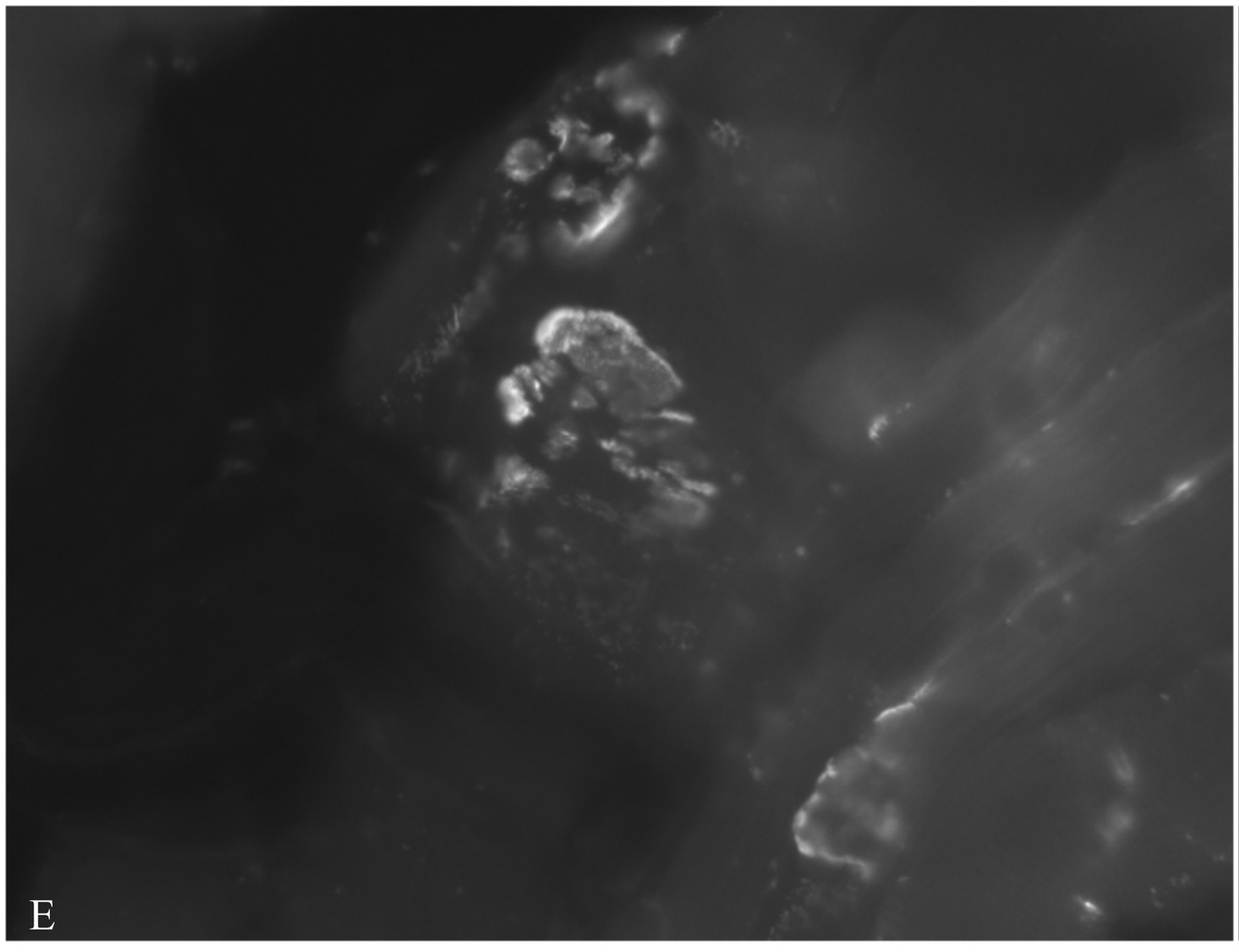
E

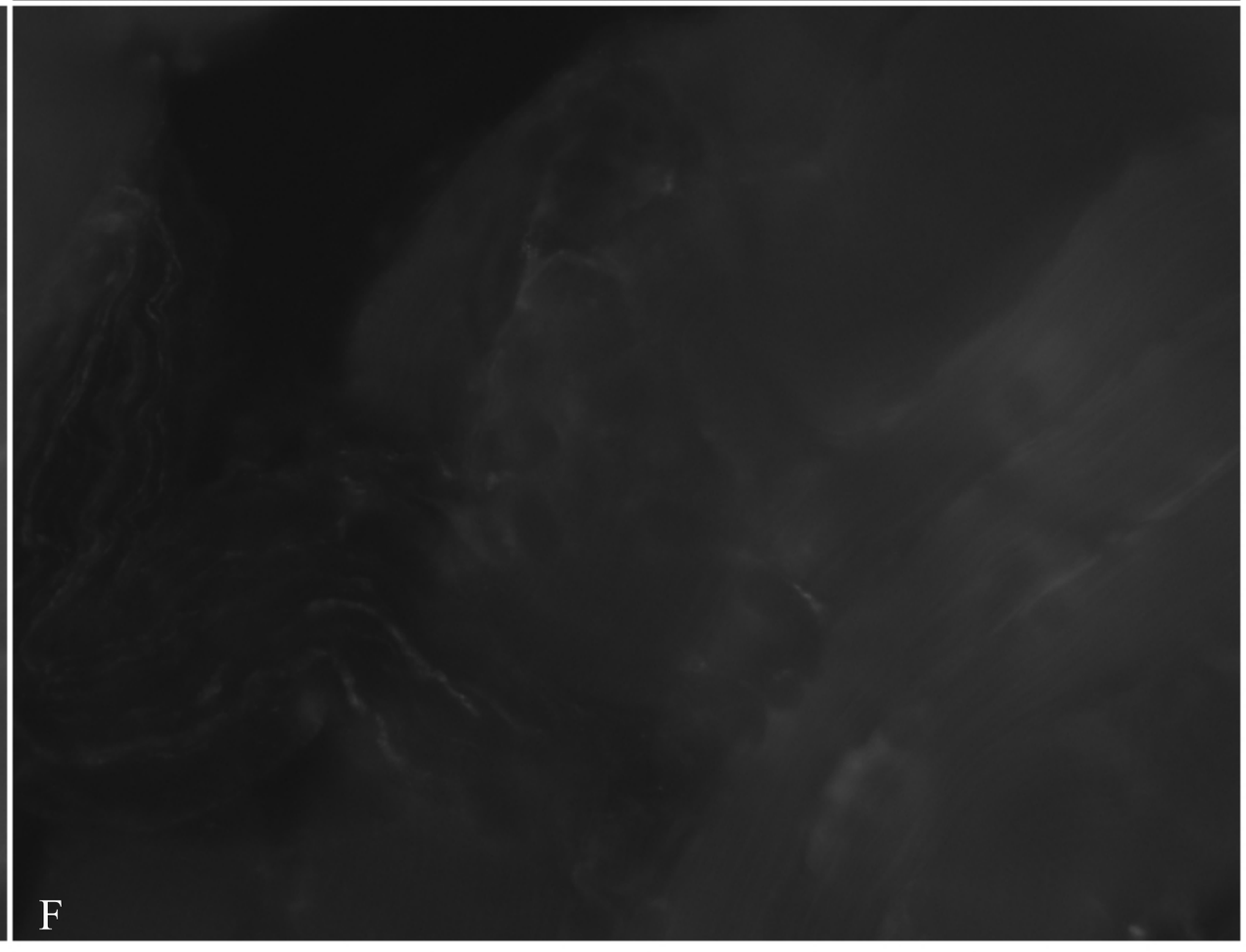
F

Figure 18: Graph summarizing the total number of fully innervated endplates counted in all age groups. Gray bars are UCHL1+/+ and +/- group, and black bars represent the mutants.

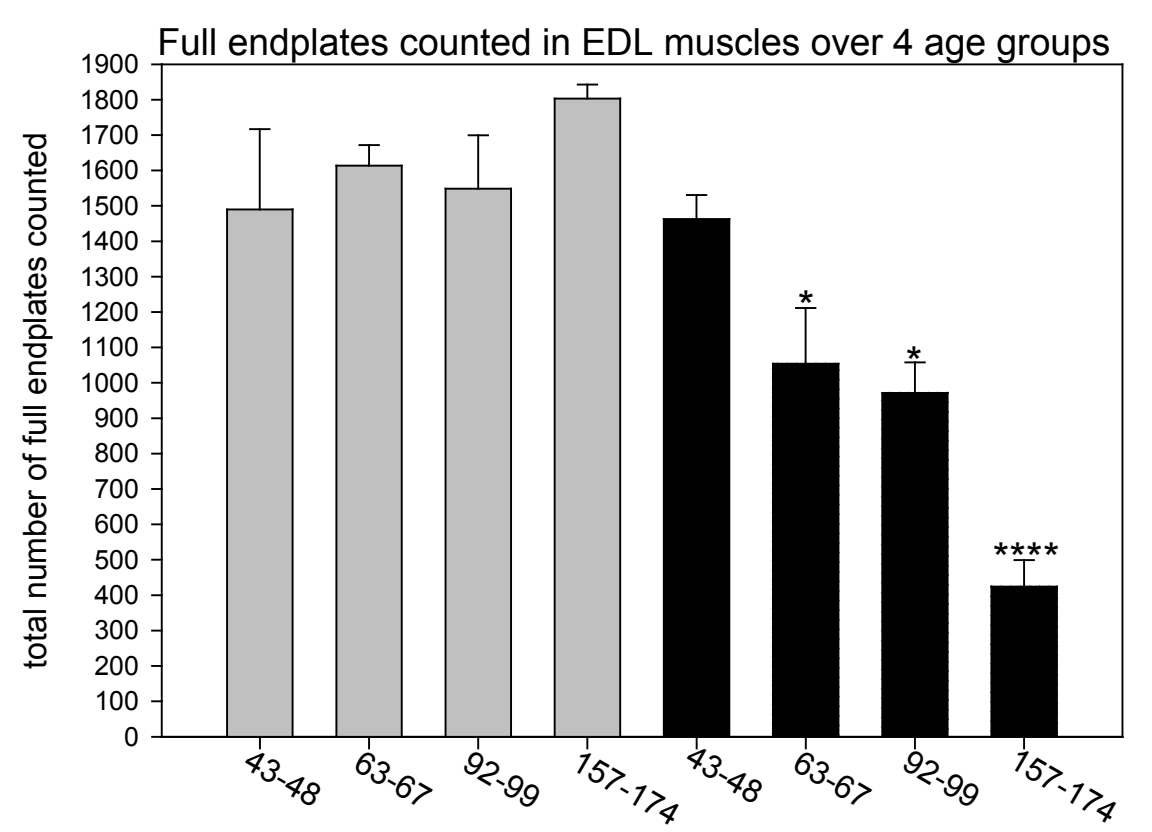
Full endplates counted in EDL muscles over 4 age groups
total number of full endplates counted
1900
1800
1700
1600
1500
1400
1300
1200
1100
1000
900
800
700
600
500
400
300
200
100
0
*
*
****
43-48
63-67
92-99
157-174
43-48
63-67
92-99
157-174

Figure 19: Graph summarizing the total number of partially innervated endplates counted in all age groups. Gray bars are healthy, black bars are mutants.

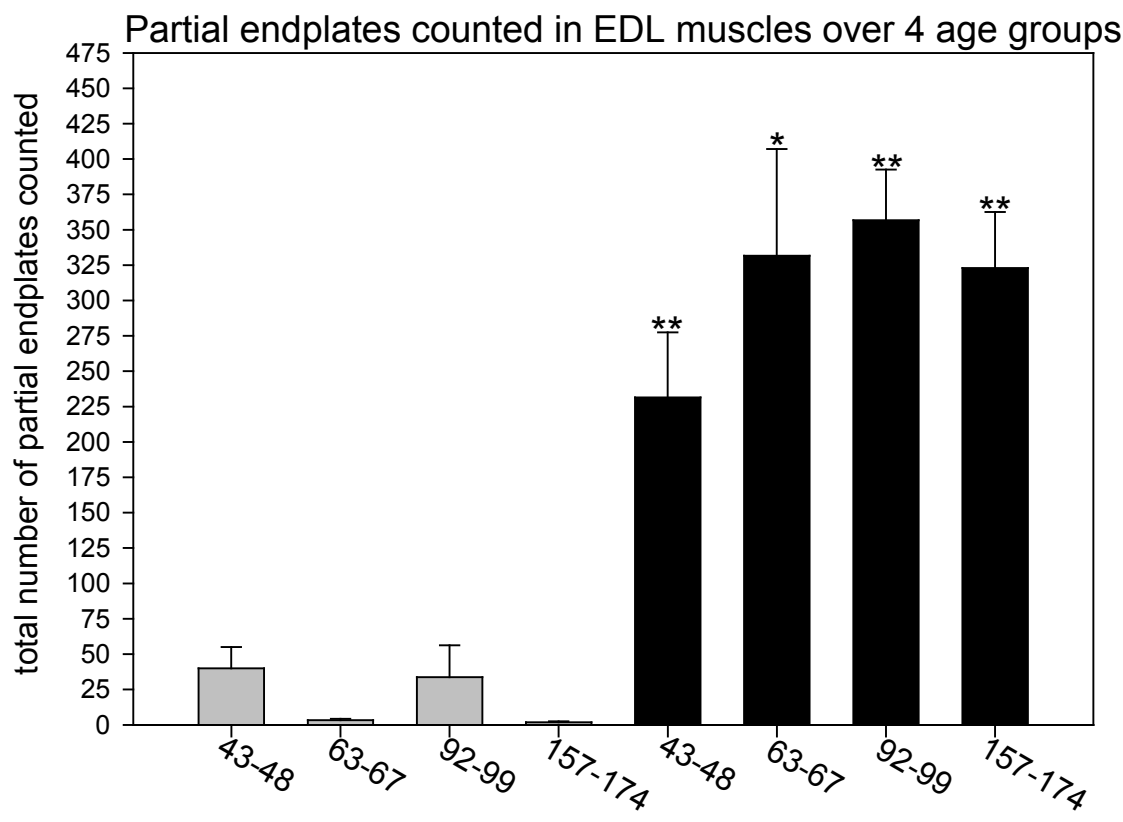
Partial endplates counted in EDL muscles over 4 age groups
total number of partial endplates counted
475
450
425
400
375
350
325
300
275
250
225
200
175
150
125
100
75
50
25
0
**
*
**
**
43-48
63-67
92-99
157-174
43-48
63-67
92-99
157-174

Figure 20: Graph summarizing the total number of vacant endplates counted in all age groups. Gray bars are healthy, black bars are mutants.

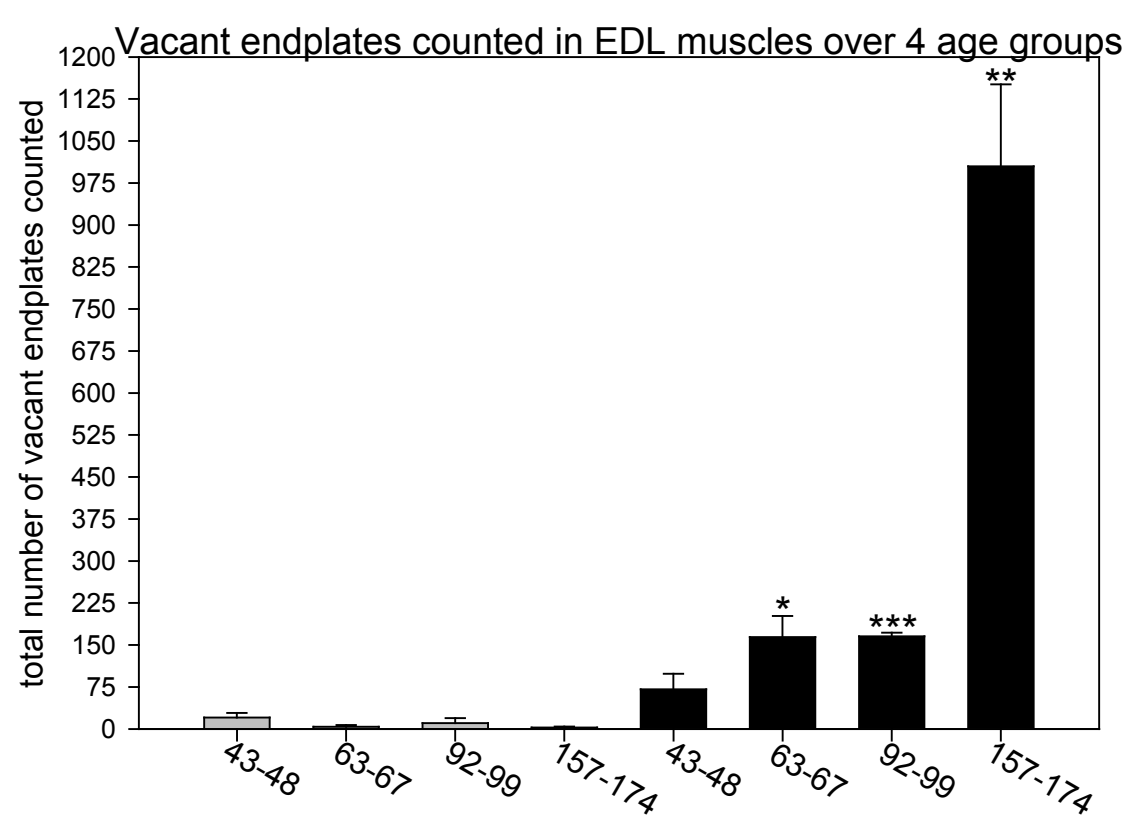
Vacant endplates counted in EDL muscles over 4 age groups
total number of vacant endplates counted
1200
1125
1050
975
900
825
750
675
600
525
450
375
300
225
150
75
0
**
*
***
43-48
63-67
92-99
157-174
43-48
63-67
92-99
157-174

Figure 21: UCHL1-/- mice show degeneration of their endplates as early as 43 days of age.
A): UCHL1+/+ healthy spindle.
B): UCHL1-/- spindle, exhibiting several abnormalities. Spheroid-like aggregates reacting strongly with the syntaxin antibody are visible, and loss of fine structure in the afferent coils is also apparent.

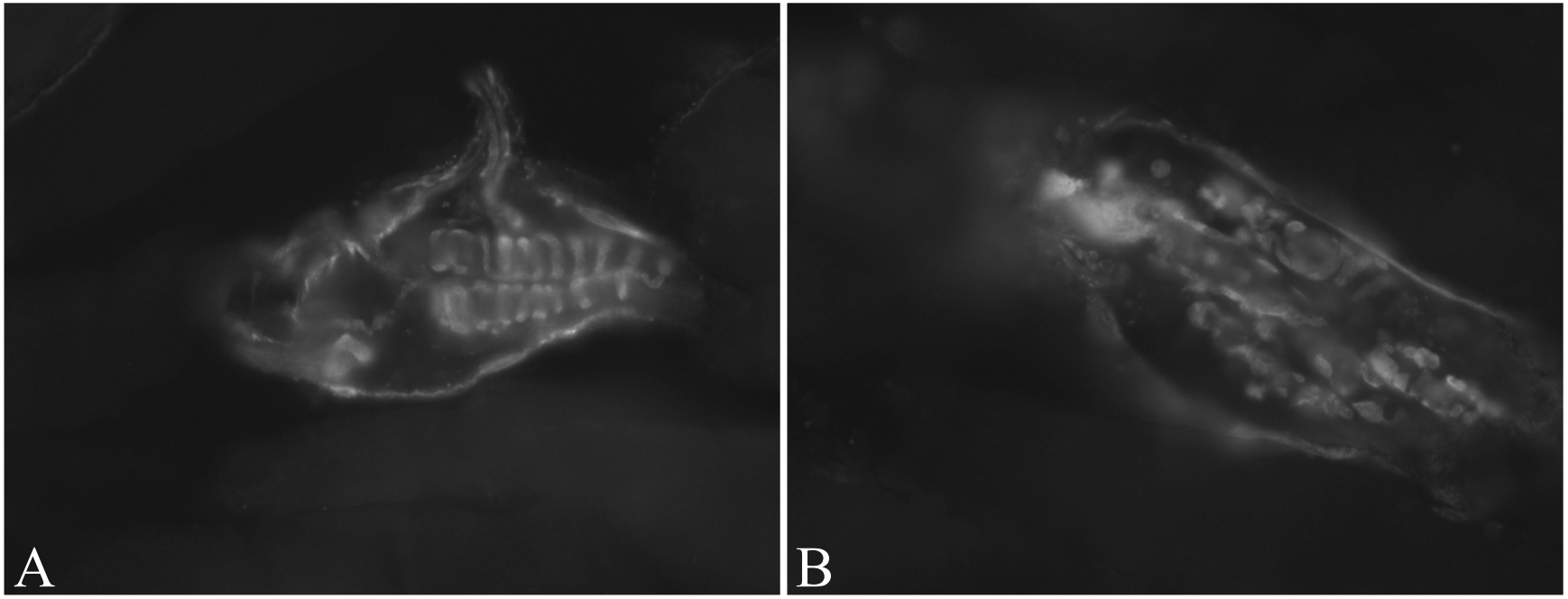
A
B

Figure 22: Representative photos of UCHL1 healthy and mutant spindles in the 63-67 day old cohort.
A-C) healthy UCHL1+/+ and +/- spindles
D,E) Photographs of the same mutant spindle showing regenerating axon sprouts (D), and spheroid aggregates (E). (D) also shows afferent coils running into each other.
F): mutant spindle showing “faded” staining.

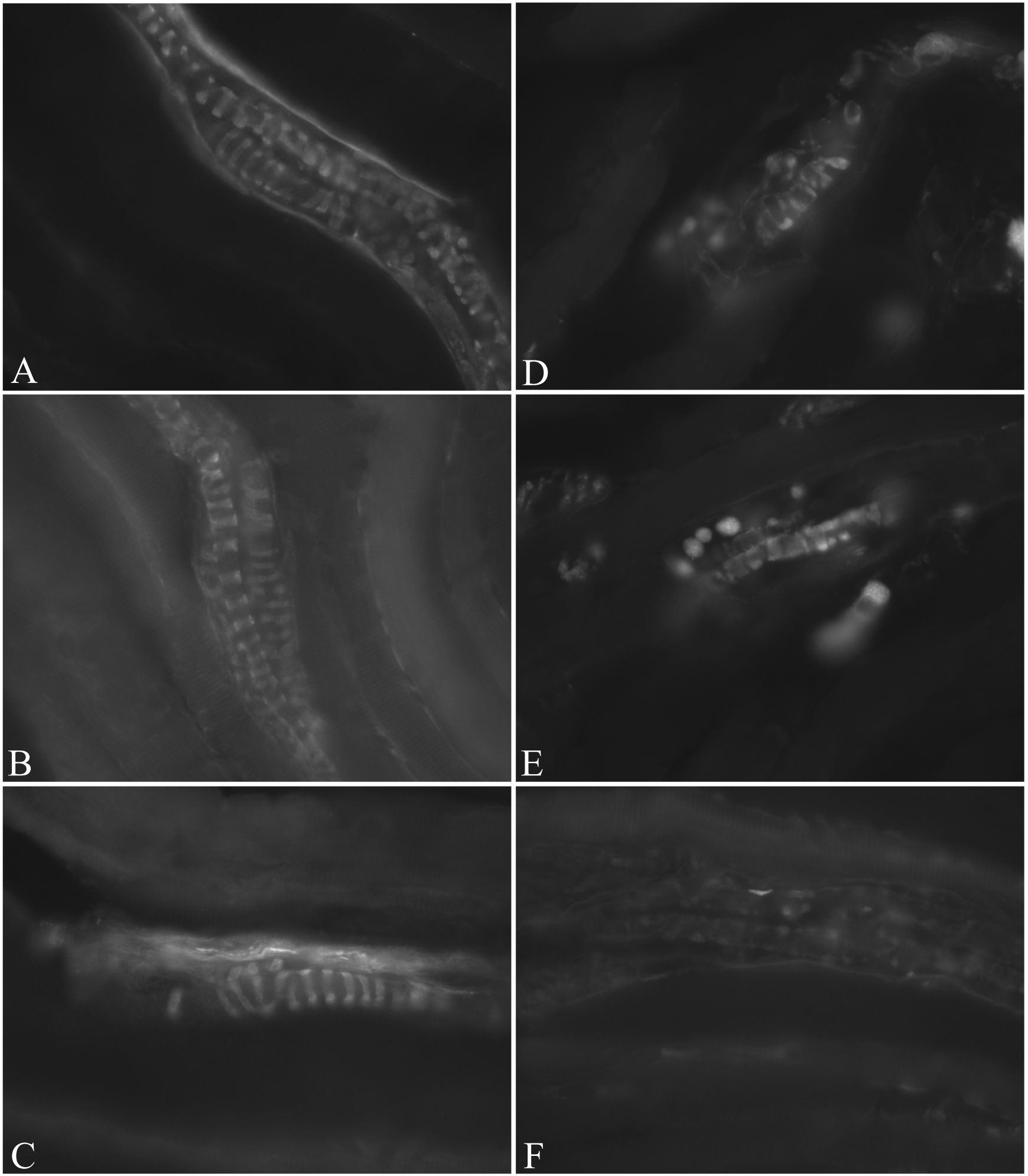
A
D
B
E
C
F

Figure 23: Representative images of mutant and healthy spindles in the 92-99 day old cohort.
A-C) Healthy spindles showing nice tight Ia afferent coils.
D-F) Mutant spindles. Regenerating axons can be seen in (D) and (E), along with prominent spheroid aggregates. (F) shows a spindle with only a small portion of afferent coil left.

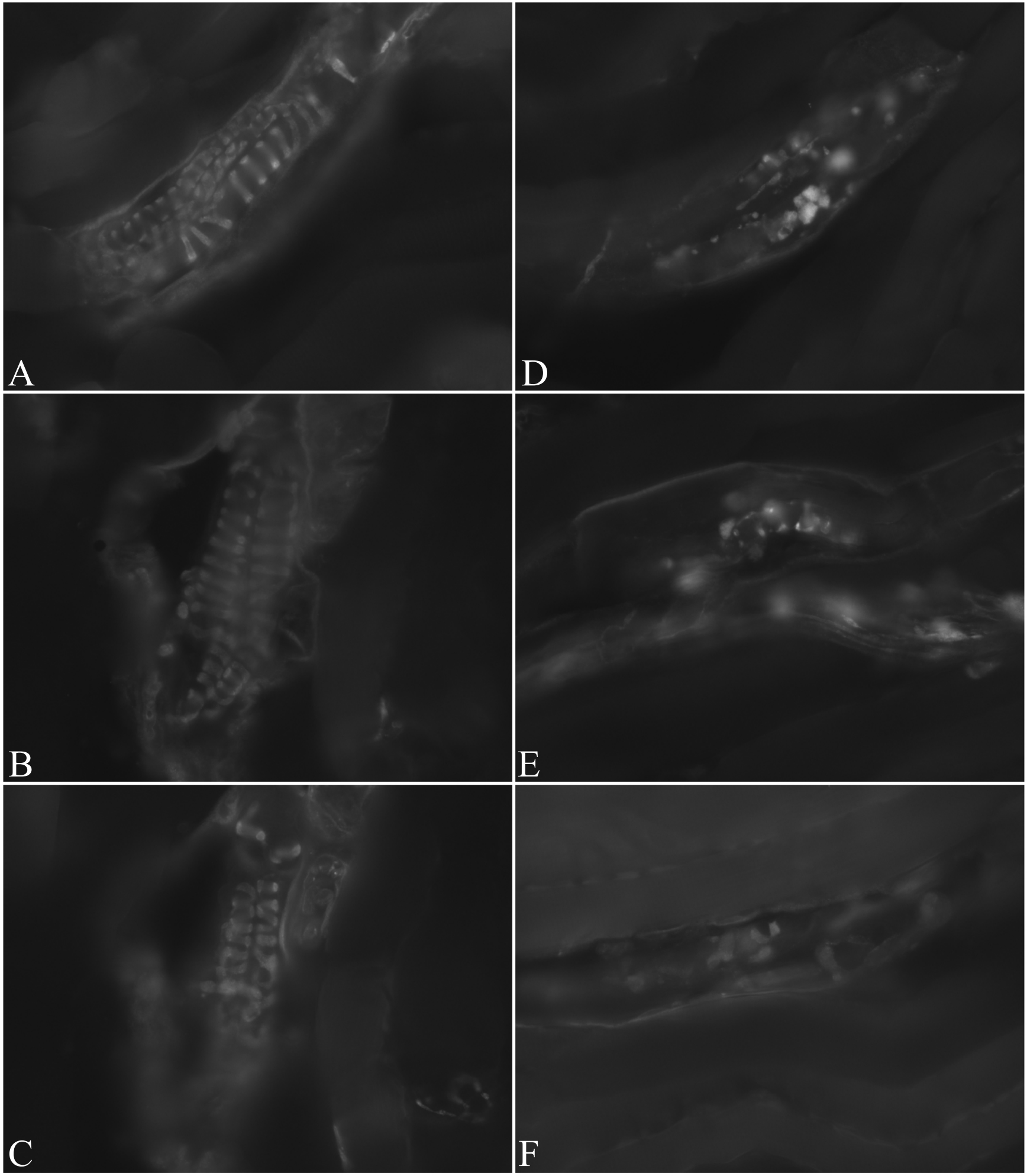
A
D
B
E
C
F

Figure 24: Representative images of spindles in the oldest age cohort.
A-C): healthy coils of UCHL1+/+ and +/- mice
D,E): photos of the same mutant spindle, showing 2 of the abnormalities mentioned- afferent coils running into each other (D, arrowhead), and a small thin axon visible along the length of the otherwise completely denervated chain fiber (E, arrowhead).
F): a completely denervated spindle.

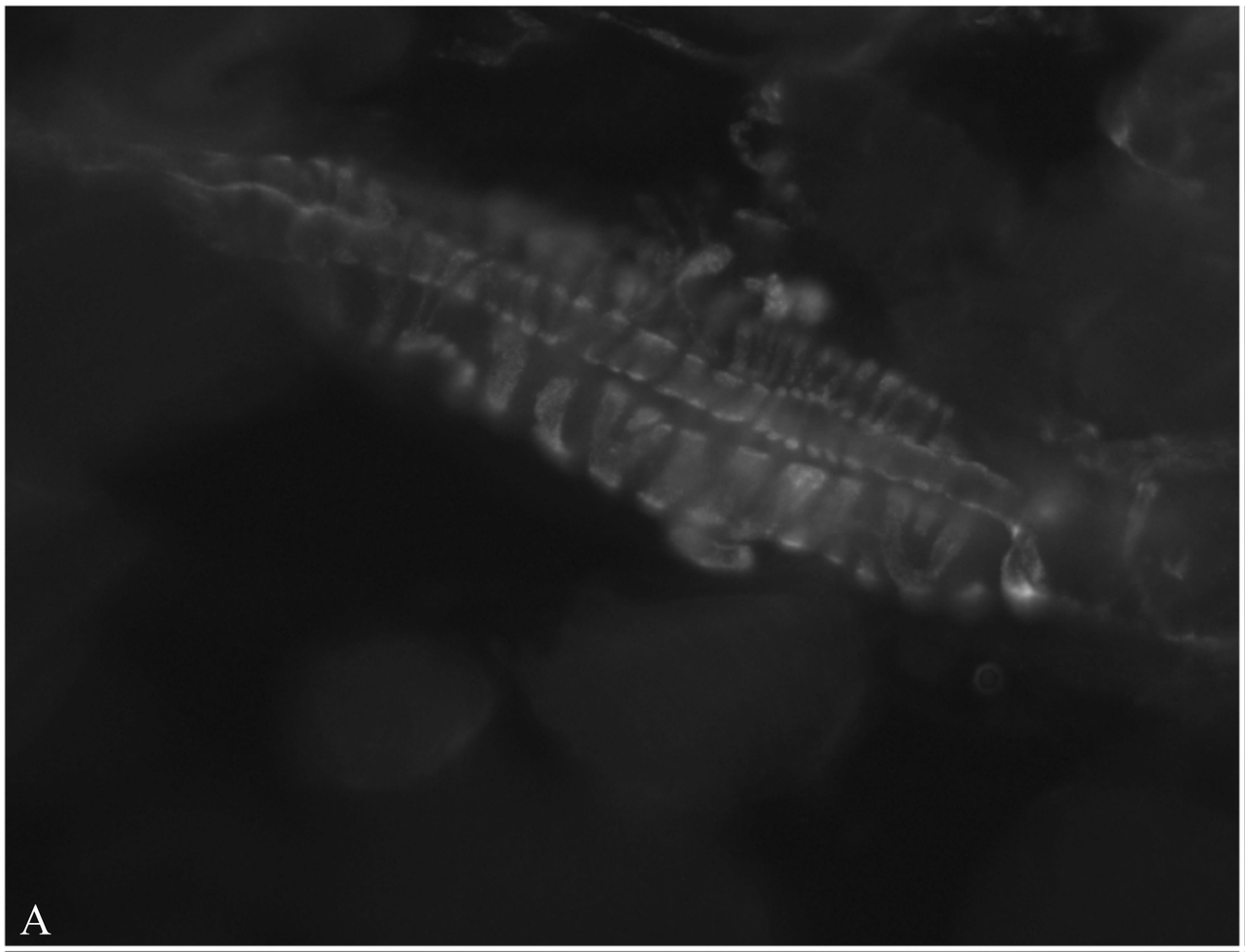
A

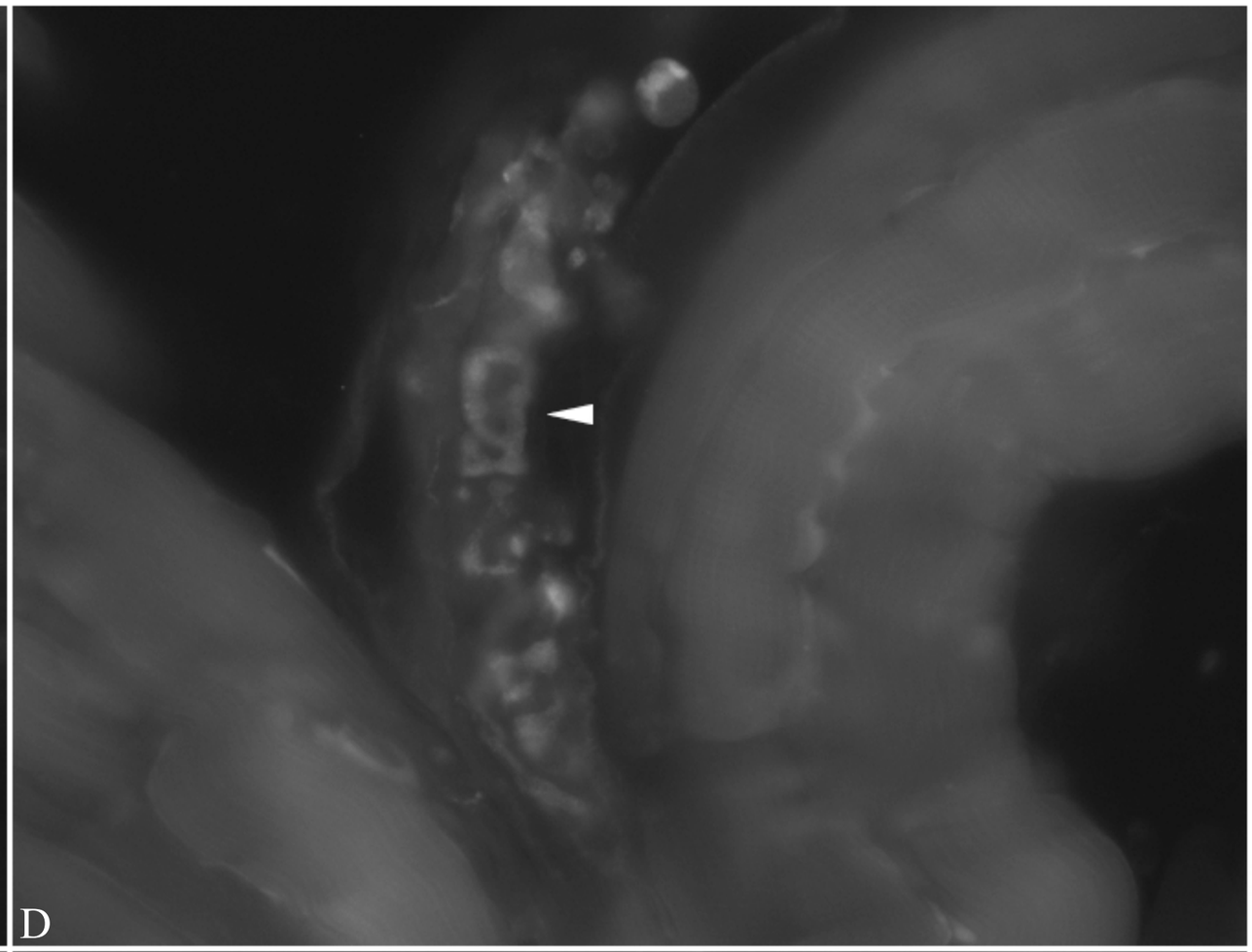
D

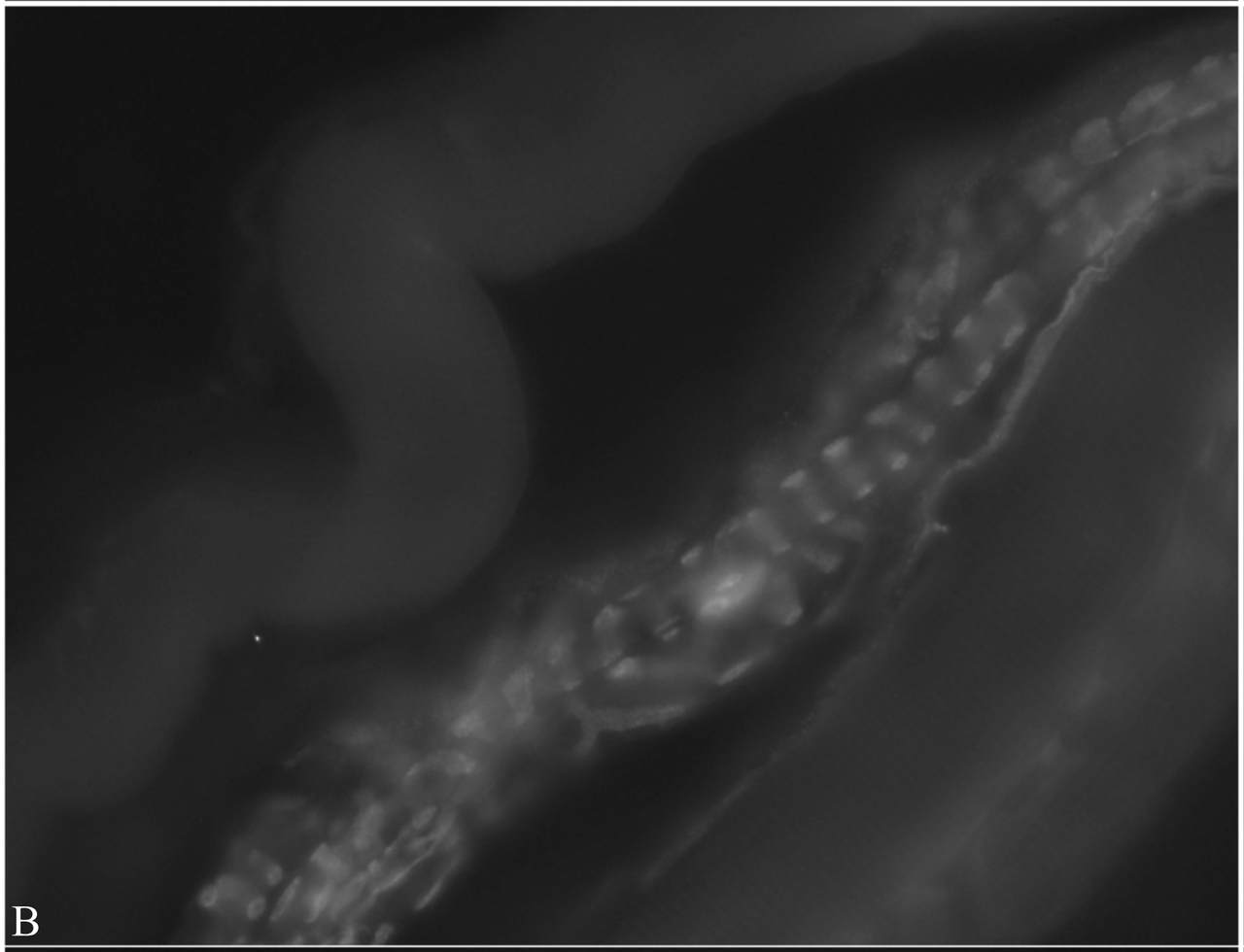
B

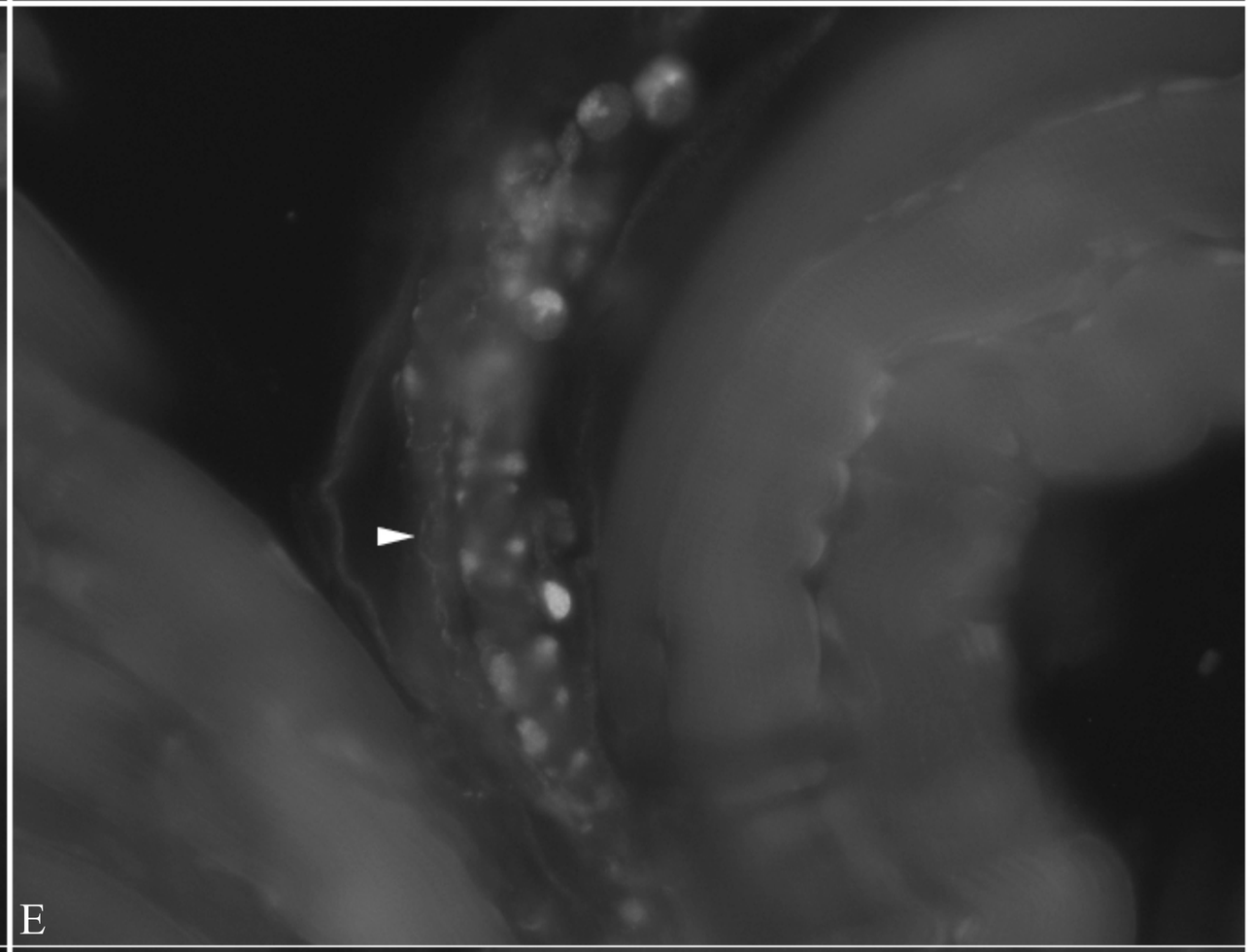
E

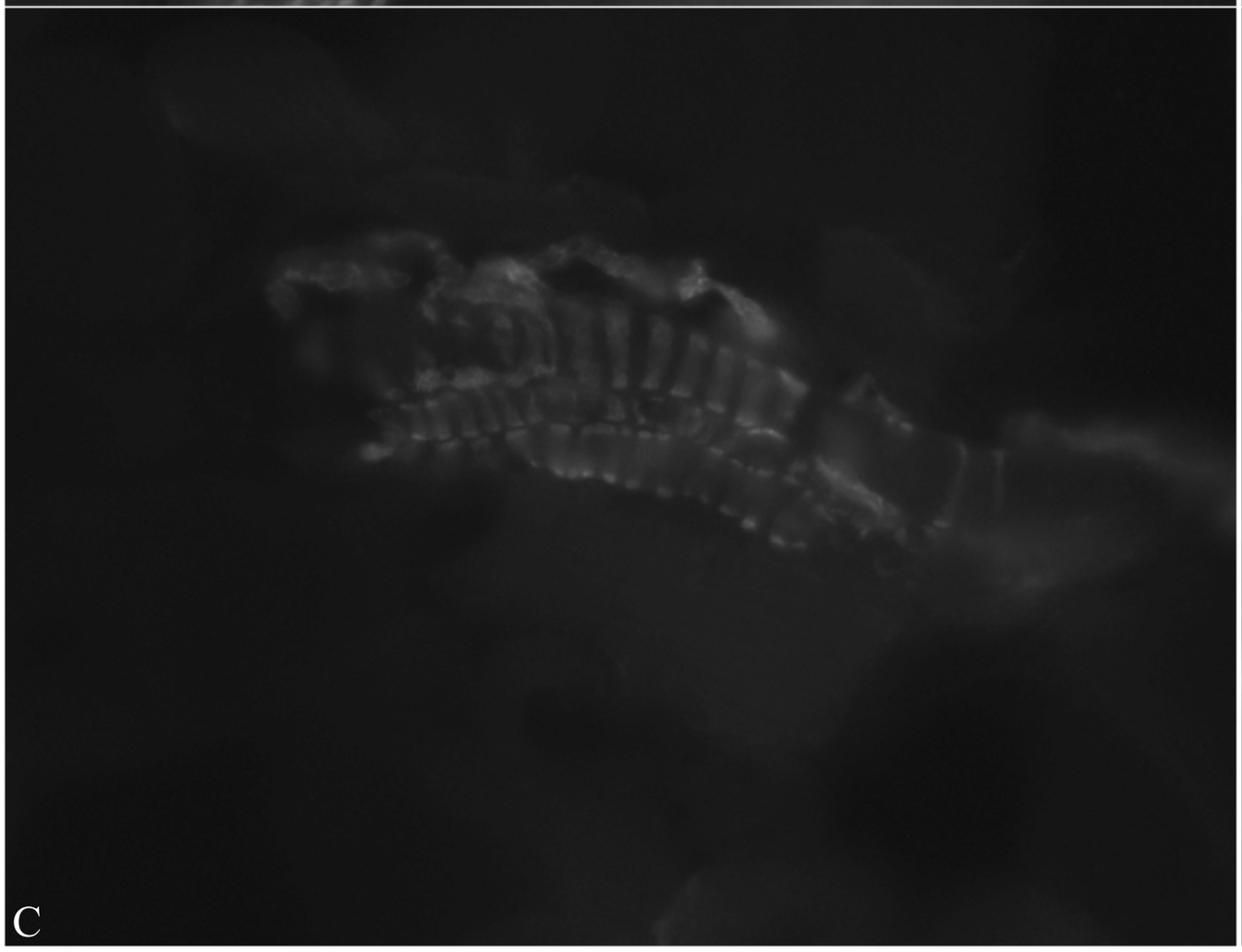
C

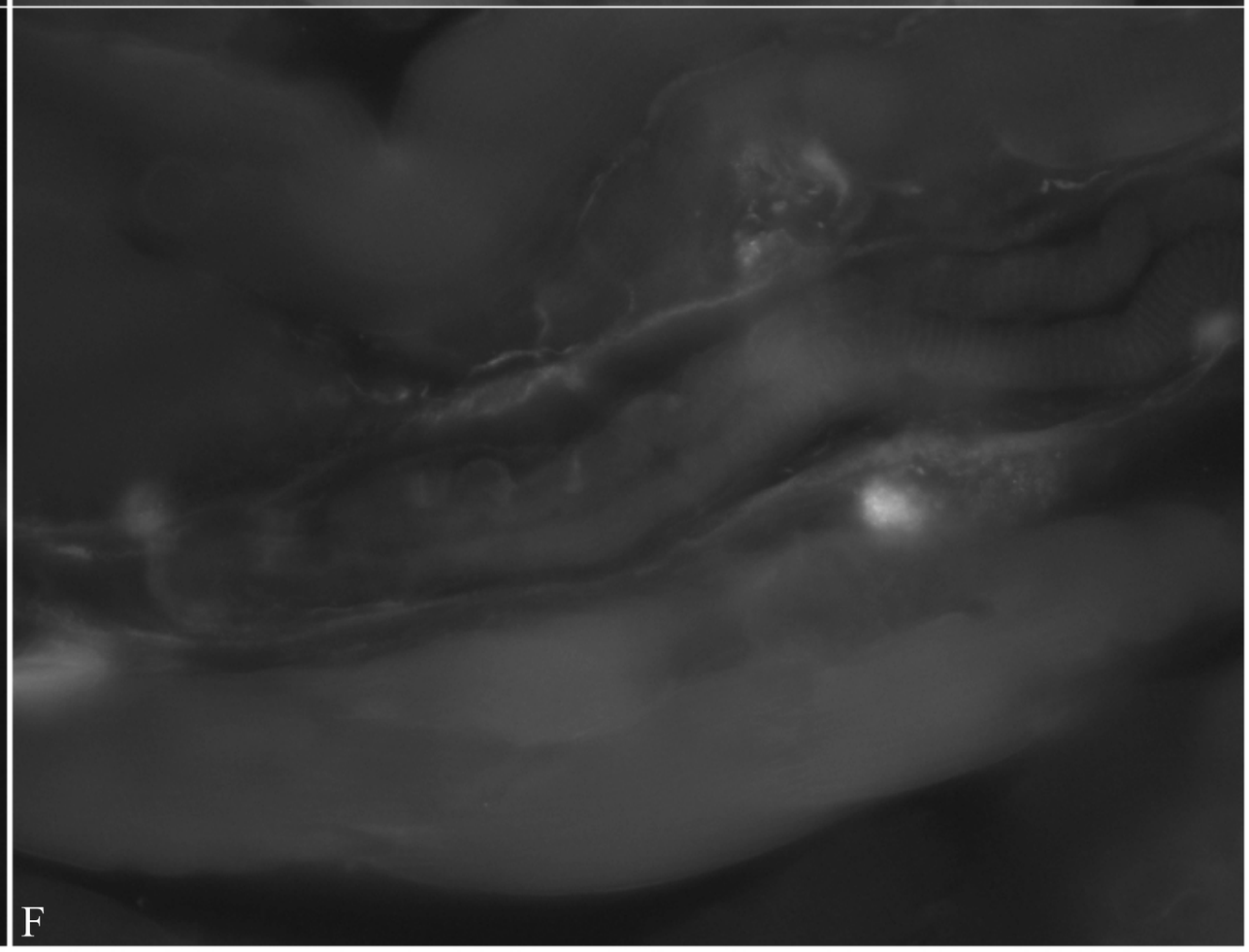
F